Comparative Characterization of Four Significant UD Strength Failure Criteria (SFC) with focusing a direct use of Friction Values, use of 'Strength' $R_{\perp\perp}$ and 'Proportional Loading'

Ralf Cuntze, Prof. Dr.-Ing. habil. VDI
Affiliation: Retired from industry, MAN-Technologie, Augsburg, Germany

Keywords: *Structural mechanics, material modelling, strength failure criteria, laminate design sheets*

Abstract:

Novel simulation-driven product development of non-cracked structural components shifts the role of physical testing to virtual testing. This requires High Fidelity concerning material models such as the design tool strength failure criterion (SFC). Usual assumption for such a material model is an ideally homogeneous (homogenized) solid material. Nowadays, reliable SFCs should be 3D-validated, because the Finite Element output presents spatial stresses that are for instance necessary to design joints.

Basic focus in design is the Strength Design Verification by designing to several Design Dimensioning Load cases using stress-based SFCs, which have the advantage that residual stresses can be relatively simply incorporated.

Often the basic task is plane loading of the envisaged laminated walls composed of transversely-isotropic UD layers. For this task the 3D-SFCs are reduced to the necessary 2D-SFC versions. At present, wall design modifications can be directly numerically investigated by the code-implemented Classical Laminate Theory (CLT) coupled with a distinct SFC.

The SFCs are the mathematical formulations of the UD failure envelopes and bodies. Their shapes significantly depend on the applied SFC. Four relevant SFCs will be characterized in this document: The author's SFC relatively detailed, the well-known Tsai-Wu and also Hashin in short and Puck medium. One aim here is to find these SFCs formulated in the same notation [*VDI 2014*], which simplifies any intended comparison work of a user. Clear terminology is a precondition for achieving High Fidelity design and will therefore initially provided. When modelling the different laminate stacks it is to distinguish the traditional, so-called 'Quad-stacked' laminates, $(0°, 45°, -45°, 90°)$-family (*non-stitched prepregs*) and the novel 'Double-Double-stacked' laminates composed of a semi-finished Non-Crimped-Fabric (*stitched dry layers*) product C-ply^{TM} $\{\varphi/-\psi/-\varphi/\psi\}$, [....] an angle-ply stack building block.

First-Ply-Failure (FPF) envelopes are searched by the SFCs, which means determination of 'Onset-of-damage' and includes both Inter Fiber Failure (IFF) and Fiber Failure (FF). Last Ply Failure (LPF) usually requires a non-linear analysis, which can be used to save a design.

Standard 3D SFCs employ the so-called cohesive (shear) strength $R_{\perp\perp}$ and regard it as a technical strength and not as a strength quantity. The mystery behind is tried to be unlocked in this investigation by deep numerical computations. Because most of the published applications are 2D-ones the employed SFCs do not require $R_{\perp\perp}$ and its determination by tests is not presented.

Results: (1) Detailed comparison of the characteristics of the four SFCs. (2) Investigation of the Cohesive shear strength $R_{\perp\perp}$ and its relation to Puck's Action plane resistance $R^A_{\perp\perp}$. (3) Cuntze's novel introduction of directly using friction values $\mu(a)$ in his SFCs instead of fictitious friction parameters a making the application more engineering-like. (4) The novel derivation of a Mohr envelope $\tau_{nt}(\sigma_n)$ with visualization of $\Theta_{fp}(\sigma_n)$ derived from a measured fracture curve $\sigma_3(\sigma_2)$.

1 Introduction 3
1.1 Motivation 3
1.2 Basics for UD-SFC formulations 4
1.3 Terminology, Specific Terms, Glossar 5
1.4 Test Data Mapping and Presentation of a Design Verification with Safety Concept 8
1.5 'Quad'-Laminates and Double-Double (DD) Laminates Lay-ups 9
2 Choice of a UD Strength Fracture Criteria Set considering 'Modal' and 'Global' SFCs 10
3 Cuntze's Failure Mode Concept-based SFCs, modal FF1, FF2, IFF1, IFF2, IFF3 12
3.1 Material Symmetry and 'Generic' Number 12
3.2 Basic Features 13
3.3 Cuntze's FMC-based Set of Modal SFCs 14
4 Tsai-Wu, global SFC 19
5 Hashin, modal SFCs, FF1, FF2, IFF1, IFF2 22
6 Puck's Action Plane IFF SFCs, modal FF1, FF2, global IFF discriminating 3 IFFs domains 23
6.1 Puck's Mohr-based IFF model and his 3D-SFCs 23
6.2 Puck's 2D IFF-SFCs 26
6.3 IFF-similarities and differences Cuntze-Puck 27
7 Unlocking the Mystery about the $\tau_{23}^{failure}$ - caused $\bar{R}_{\perp\perp}$ and $\bar{R}_{\perp\perp}{}^{A} \neq \bar{R}_{\perp\perp}$? 28
7.1 Linear Mohr-Coulomb curve $\tau_{nt}(\sigma_n)$, based on IFF2 mode 28
7.2 Action Plane Resistance $\bar{R}_{\perp\perp}{}^{A}$ and so-called Cohesive shear Strength $\bar{R}_{\perp\perp}$ 30
7.3 Non-linear Mohr-Coulomb curve, Pre-view for Annex 1 31
8 SFC-Application and Material Data Input 32
8.1 Comments on SFC Validity Limits 32
8.2 Enabling an Automatic Insertion of 3D stress states into the FMC-based SFCs 32
8.3 Test Data Set 33
9 Conclusions and Findings 36
Annex 1 Derivation of $\tau_{nt}(\sigma_n)$ and of $\Theta_{fp}(\sigma_n)$ from a mapped test fracture curve $\sigma_3(\sigma_2)$ 41
Annex 2 Replacing fictitious Model Parameters $a_{\perp\perp}, a_{\perp\parallel}$ by measurable Friction Values μ 47
Annex 3 Proportional Loading Concept marking the In-plane-Difference of *Eff* to |*F*| 51
Annex 4: Influence of Compression Stress States on Compressive Strength Capacity (IFF2) 54

1 Introduction

1.1 Motivation

Nature teaches that anisotropy is of advantage to maximize structural performance. It is therefore no wonder that many people have tried to create the necessary design tools, including strength failure criteria for the design of anisotropic laminated walls, composed of fiber materials. A basic task in structural component development is the Static Design. This involves Design Dimensioning and finally Design Verification of the chosen design.
In the general development of structural parts the application of 3D-validated SFCs is one essential pre-condition for achieving the required fidelity for the user. This includes a Yield Failure Condition for non-linear analysis of the ductile material and for design verification at the limit state 'Onset-of-Yield'. It further includes conditions to verify that 'Onset-of-Fracture' does not occur, in the case of both brittle and ductile behavior. For the here envisaged brittle UD materials the 'Onset-of Fracture' limit has been termed by Tsai 'First Ply Failure (FPF) and includes FF and IFF.

The variety of new materials in engineering needs much knowledge about the failure state in order to enable verification of the designed structural component. And this much more since lightweight design requires a higher exertion of the material and thereby contributes to sustainable engineering.

Design Verification demands for reliable reserve factors *RF* and these - beside a reliable structural analysis - demand for reliable SFCs. Such a SFC is the mathematical formulation $F = 1$ of a failure curve or of a failure surface (body). Generally required are a yield condition and fracture strength conditions. The *yield* SFC usually describes just one mode, i.e. for isotropic materials the classical 'Mises' describes shear yielding SY. *Fracture* SFCs usually must describe two independent fracture modes, shear fracture SF and normal fracture NF in the simple isotropic case. For the here focused transversely-isotropic UD material a so-called material-inherent 'generic' number 5 for fracture seems to be given [*Cun23*]. This means for UD 3 Inter Fiber failure (IFF) and 2 Fiber Failure (FF) modes and further 5 strengths are faced only.
Brittle transversely-isotropic UD material is the focus here, which means a set of 5 Strength (*fracture*) Failure Criteria (SFC) should be provided regarding material symmetry.

Principally, in order to avoid either to be too conservative or too un-conservative, a separation is required of the always needed 'analysis of the average structural behavior' in Design Dimensioning (*using average properties and average stress-strain curves*) in order to obtain optimum structural information (= 50% expectation value) from the mandatory single Design Verification analysis of the final design, where statistically minimum values for strength and minimum, mean or maximum values for the task-demanded other properties are applied as Design Values. There it is to demonstrate that 'A relevant Limit State is not met yet'. The paper at hand focuses mapping of the curves of test data by the SFCs. In these formulations each strength is an average strength consequently indicated by a bar over $\bar{R}$.

Design verification with respect to Static Strength is performed here on material level by assessing stresses in the critical location of undisturbed, uniform material areas.

1.2 Basics for UD-SFC formulations

Desired as models are 'homogeneous' solids, however, reality is much more complicate. Practically, all materials are composites. One distinguishes two structural composite types: Material Composites and Composite Materials. A structural material usually is the model on the considered scale of a homogenized complex solid that became 'smeared' to usually obtain an engineering-like macro-model. A Material Composite is structural-mechanically a composite 'construction of different materials' whereas a Composite Material is a combination of constituent materials, different in composition (constituents retain their identities in the composite). Usually a Composite Material can be modelled as smeared material.

For achieving an accurate designing it is to note at first:

* Whereas modelling is performed with average properties and average stress-strain curves, in the verification of the chosen final laminate design - task-required - upper or lower or average properties are to insert in the analysis, like $\bar{R}$. For average strength properties in model validation the bar over is applied. No bar over means general use of a strength property or the statistically-reduced one for design verification.
* The present stress-based design verification in Aerospace i.e. requires stress-based SFCs and as input A- or B-*Strength* Design Allowables *R*. A strain-based SFC design verification as precondition for certification, would firstly need authority-permission including authority-accepted strain-based SFCs coupled to *Strain* Design Allowables (*also statistically reduced*), which are not available as official values in material data sheets.

Physics combined with experience make to consider specific aspects:

* If a material element can be homogenized to an ideal crystal (= frictionless), material symmetry requires for the isotropic and the transversely-isotropic UD material a distinct minimum number of properties. This is witnessed by tests.
* A real solid material model is represented by a description of the ideal crystal + a description of its friction behavior. Mohr-Coulomb asks for the real crystal another physical parameter, namely the inherent material friction value μ with one value for isotropic and two values for UD materials.
* Unfortunately SFCs often employ just strengths. This is physically not accurate: Mohr-Coulomb acts in the case of compressed brittle materials! The computed *RF* may not be on the safe side.
* Invariants are a combination of stresses – powered or not powered – the value of which does not change when altering the coordinate system CoS. This attribute is used when looking for an optimum formulation of a usually desired scalar SFC.
* Considering Material symmetry: There seems to exist a 'generic' number for material families, namely 2 for isotropic and 5 for transversely-isotropic materials
* Direct use of the measurable, physically clear friction value μ in the SFC formulation instead of using fictitious friction model parameter is now possible [*Cun22, Annex2*]. This matches to the engineer's thinking in physical properties. A good guess for isotropic and UD materials is $\mu = 0.2$.
* The existence of twofold and threefold failure effects must be considered, see ***Fig.1-1***

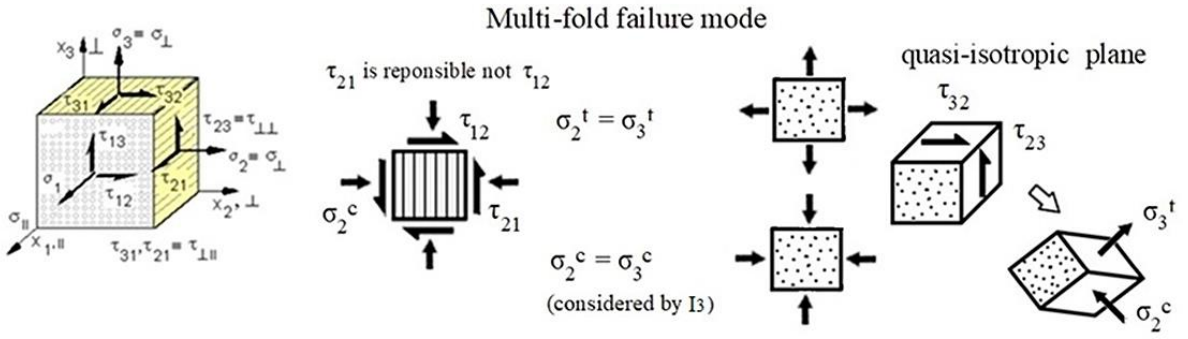

Fig.1-1: Consideration of multi-fold failures

* A usual SFC just describes a 1-fold occurring failure mode or mechanism! A multi-fold occurrence of a failure with its joint probabilistic effects must be additionally considered in the SFC formulas of each SFC theory. For UD-SFCs it is valid if $\sigma_2 = \sigma_3$: $R_{\perp}^{tt} < R_{\perp}^{t}$, $R_{\perp}^{c} > R_{\perp}^{c}$. (*"Which of the popular SFCs takes care of this effect?")*

There are UD-layer- and fabric layer-based semi-finished products which – again - require a very different modeling that affords a right lay-up description. This must be and will be sufficiently presented.

1.3 Terminology, Specific Terms, Glossar

Descriptions of Semi-finished UD Products: to lower the communication barriers [*Cun19*]

Modeling the variety of laminates is a challenge. In this context, essential for the interpretation of the failures faced after testing with potential property reduction, is the knowledge about the lay-up of the envisaged laminate, because crimped fabrics and non-crimped NCF-materials behave differently. It is further extremely necessary to provide the material-modeling design engineer and his colleague in production (*for his Ply Book*) with a clear, distinguishing description of UD-lay-ups, of NonCrimpFabrics NCFs (*stitched multi-UD-layer*) and of Fabric layers (*crimped*). Due to unclear descriptions the author unfortunately could often not use during his design work life valuable test results of fiber-reinforced materials. As editor of the VDI guideline 2014 the author makes the following proposal for a clear optical designation in order to enable a realistic material modelling:

The description of a UD-lamina-composed laminate follows the well-known lay-up denotation [0/90/90/0] = $[0/90]_S$, and an angle-ply laminate is denoted $[45/-45]_S$ with index $_S$ for symmetric (*targeting coupling reduction in [K]).* Analogously follows for a symmetrically stacked woven fabric $\left[\begin{smallmatrix}0\\90\end{smallmatrix}\right]$ (*plain weave, which is symmetric in itself*)**.** One can distinguish the various types by a square bracket [ ] and a wavy bracket { } which optically help here to distinguish NCF **{**stitched UD-stacks**}** from those woven fabrics where one practically cannot mechanically separate the single woven layers within one fabric layer as in the case of *plain weave* binding.

* Single UD-layers-*deposited* stack $[0/90]_S = [0/90/90/0]$-lay-up, prepreg

* Semi-finished product, *stitched* NCF: $\{0/90\} + \{90/0\}$ symmetrically stacked, dry deliverable 'building blocks' : $\{0/45/-45/90\}$, *novel* C-ply^{TM} $\{\varphi/-\psi/-\varphi/\psi\}$, Double-Double $\{75/-75/-15/15\}_r$ with r as repetition.

Glossar with terms for a better common understanding:

Action plane: plane where the action plane stresses work, running parallel to the fibers

Action plane resistance [*Puck*]: "*The resistance of an action plane is the maximum resistance, with which the action plane can resist its own fracture caused by a uniaxial* $\sigma_{\perp}^{t}$ *-stress, a pure* $\tau_{\perp\perp}$ *- or a* $\tau_{\perp\parallel}$ *-stress"*

Analysis: Computation that uses fixed model parameters (*e.g. Design Verification of the final design*)

Cohesive strength of brittle materials: originally the maximum tensile stress σ^{t} (≡ separation strength R^{t}) of bonding between surfaces or of tensile stressed particles building a material. However, in rock and soil mechanics cohesive strength is 'differently' defined as the inherent shear strength $R^{\tau} = \tau_{nt}$ of a plane, where the normal compressive Mohr stress $\sigma_{n}^{c} = 0$ on the about $\Theta_{fp}° \approx 70°$ inclined fracture plane and whereby the cohesive strength value R^{τ} is extrapolated from compression point-associated quantities. → *Difference* between the terms in the technical disciplines, (in contrast to a one mode-linked technical uni-axial strength *R*, the cohesive strength R^{τ} (isotropic material) $\rightarrow R_{\perp\perp}$ (transversely-isotropic UD) is located in the transition zone between two activated modes NF and SF!)

Delamination: separation of material layers within a laminate or also in a textile reinforced concrete (may be local or may cover a large area of the laminate)

Design Load: maximum amount of loading a load-carrying system is to be designed to. (Examples are design limit load *DLL*, design yield load *DYL* or here for brittle materials design ultimate load $DUL = j_{ult} \cdot DLL$

Double-Double laminates: Two angle-plies of different fiber angles form a four-ply sub-laminate

(Strength) Failure Condition: Condition on which a failure becomes effective, meaning $F = 1$ for one limit state. Mathematical formulation of the failure surface that takes the form $F = 1 = 100\ \%$. *(1) Most often meant is a strength failure condition SFC. Aim of a Failure Condition is to assess multi-axial states of stresses by just utilizing the uniaxial strength values, which are always mandatory in design. Usual SFC describe just a 1-fold occurring failure mode or mechanism! (2) A multi-fold occurrence of a compressive concrete failure (i.e.* $f_{c,}^{cc}$*) with its joint probabilistic effects must be additionally considered in the formulas. In other words, the accumulation of two damaging portions works and must be considered)*

(Strength) Failure Criterion (SFC): Distinctive feature defined as a condition for one of the 3 states, taking the form $F > 1$, $F = 1$, $F < 1$

Failure function *F* : mathematical formulation of the failure event by $F = 1$

Failure Index *FI***:** Originally just value of the failure function used with polymer composites which fits to *Eff* only in cases where the considered stress terms are linear (mathematically homogeneous) in the SFC*). (Nowadays it corresponds to the material stressing effort Eff*

Failure Mode Concept (FMC)**:** invariant, failure mode-based general concept to generate strength failure conditions for single failure modes. It is a 'modal' formulation in contrast to 'global' concepts where all failure modes are mathematically linked and a concept for materials that can be homogenized (smeared). Applicability of a SFC ends if homogenization as pre-requisite of modeling is violated

First-Ply-Failure (FPF): First Inter-Fiber-Failure IFF in a lamina of the laminate capturing FF and IFF. First-FPF envelopes depict 'Onset-of-damage'

Fracture plane resistance: resistance, which an action plane opposes to its failure as a result of a single stress ((σ_n, τ_n)) acting on it. SF is shear fracture and NF Normal Fracture.

Invariant: Combination of stresses or strains. Its value does not change when altering the coordinate system. The stresses in the invariants may be powered (exponents may 2, 3 or 4) or not powered. Invariants are advantageous when formulating the usually desired scalar failure conditions. Such material-associated invariants are given for isotropic, transversely-isotropic and orthotropic materials.

'Generic' number: Witnessed material symmetry knowledge seems to tell: There might exist a 'generic' (*term was chosen by the author*) material inherent number for material families,, namely 2 for isotropic and 5 for transversely-isotropic materials

HMH = Huber-v.Mises-Hencky: often shortly termed 'Mises'

Homogeneous: Descriptive term for a material of uniform composition throughout

Hypothesis: Physical conception of the failure processes

Lamina: Designation of the single UD ply as computational element of the laminate, used as laminate subset or building block for modelling. It might capture several equal physical layers (plies) or fractions thereof

Laminate: designation of a complete lay-up or stack of several laminas (laminas) which are bonded together

Last-Ply-Failure (LPF): LPF usually requires a non-linear analysis, which can be used to save a design

Layer, ply: Physical element from winding, tape-laying process etc.

Limit State function (Grenzzustandsfunktion): $G = F - 1$, beyond which a structural element is to be assumed to become unfit for its purpose

Mapping of a course of test data: average test data fit resulting in a statistical 'mean curve'. (requires average strength values which are marked by the statistical 'bar over' $\bar{R}$)

Material Stressing Effort $\sigma = R \cdot Eff$ (not material utilization in the usual sense of manufacture waste minimization): artificial term, generated in the UD World Wide Failure Exercises in order to get an English term for the meaningful German term Werkstoffanstrengung. The SCF is stress-based and not strain –based. In the linear case it is directly valid $f_{Res} = RF = 1/Eff$. (in his book Puck originally used the term effort ε and further exposure). $Eff_{max} = 100\% = 1$

Macro-mechanics: here is an approach in which the layers are considered homogeneous, size range of mm

Margin of Safety *MoS*: $MoS = RF - 1$

Micro-mechanics: here, an approach in the filament size range of µm

Model: Theoretical conception of a real process

PAN-CF: Precursor PolyAcrylNitril-based CF (*base CF type*); PAN-UHM-CF: higher graphitized PAN-CF

Pitch-CF: highest graphitized CF with maximum Young's modulus and pitch precursor

Properties: 'Agreed' values to achieve a common and comparable design basis. Must be provided with average value and coefficient of variation cov

Reserve Factor *RF*: load-defined value $RF_{ult} = final\ failure\ load\ /\ design\ ultimate\ load\ DUL$

(material Reserve factor f_{Res}: $f_{Res} = strength\ design\ allowable\ R\ /\ stress\ at\ design\ load\ DUL$

'Quad laminates: (0°, 45°,-45°, 90°) sub-laminate family as laminate building block in aerospace

Simulation: Process, that consists of several analysis loops and lasts until the system is imitated in the Design Dimensioning process. Model parameters are adjusted hereby to the 'real world' parameter set.

Strength: Maximum uni-axial technical stress or failure stress, which is termed Resistance *R* (one mode). Strength values in general and the strength design allowables are not marked by a 'bar over' but by *R*

Stress component: Term, that exactly should read stress tensor component or very simple just stress (*only a shear stress, like later the transversal shear stress $\tau_{\perp\perp}$, can be composed of a tensile shear stress component jointly acting with a compressive shear stress component. The stress component with the larger failure danger due to the respective mode SFC will basically determine the fracture plane angle*)

Subscripts: For the shear stresses τ, in accordance with international usage, the first subscript indicates the direction of the plane normal with respect to the plane upon which the shear stress is acting. The 2nd subscript indicates the direction of the shear force from the stress under consideration

Superscripts: Stress σ or stress τ which indicate the failure causing stress of normal fracture NF or shear SF

Transversely-isotropic material (UD, uni-directional): material model assumption, where the plane 2-3 is quasi-isotropic and due to that UD is termed transversely-isotropic

Validation of a model (from validus = strong): 'qualification' of a created model by well mapping physical test results with the derived model (here material failure model)

(design) Verification (from Latin, veritas facere): fulfillment of a design requirement data set (for a deformation, a frequency, design load, etc)

Notes on designations: As a consequence to isotropic materials (European standardization) the letter R (≡ f: in construction) has to be used for strength. US notations for UD material with letters X (*direction 1,* ∥) and Y (*direction 2,* ⊥) confuse with the structural axes' descriptions X and Y. R_m := 'resistance maximale' (French) = tensile fracture strength (superscript ^{t} is usually skipped because in mechanical engineering design runs in the tensile domain, which is opposite to civil engineering, where fiber reinforcement is coming up viewing carbon concrete), R is a strength. Composites are most often brittle and only slightly porous! In the following Table, on basis of investigations of the VDI-2014 Working Group and on investigations for the formerly planned novel ESA Materials Handbook, Cuntze proposed internationally not confusing terms for strengths and physical properties. These self-explaining symbolic designations read

Property type	**UD quantities**	**'generic' number**
fracture strength properties	$\{R\} = (R_{\|\|}^t, R_{\|\|}^c, R_{\perp}^t, R_{\perp}^c, R_{\perp\|\|})^{\mathrm{T}}$,	5
+ friction properties	$\mu_{\perp\|\|}$, $\mu_{\perp\perp}$	2
elasticity properties	$\{E\} = (\mathrm{E}_{\|\|}, E_{\perp}, G_{\|\|\perp}, \nu_{\perp\|\|}, \nu_{\perp\perp})$	5
hygrothermal properties	$\{\alpha\} = \mathrm{CTE}\,(\alpha_{\|\|}^T, \alpha_{\perp}^T)$; $\mathrm{CME}\,(\alpha_{\|\|}^M, \alpha_{\perp}^M)$	2 ; 2

1.4 Test Data Mapping and Presentation of a Design Verification with Safety Concept

Validation of the SFC model is obtained, if the courses of test data points are well mapped. This delivers an average strength set compiled exemplarily as in $\{\bar{R}\} = (1378,\ 950,\ 40,\ 125,\ 97)^T$ MPa. If shear or compression occurs a typical friction value μ is required on top. *Validation* of UD lamina-material SFCs models can be only achieved by 2D- test results together with 3D-lamina test results. Any laminate test case serves for the *verification* of the laminate design.

Before going into details – for general understanding - the engineering task "*Design Verification of the finally chosen laminate stack"* is depicted in *Fig.1-2*. In order to perform this, the average strength values $\{\bar{R}\}$ are statistically reduced to the *strength* Design Allowables ('A- or B-values', {*R*}). This shrinks the failure envelope obtained during mapping. The verification of the design requires a load-defined *Reserve Factor RF* ≥ 1.00 or a positive Margin of Safety MoS = RF – 1, respectively. If the structural problem is linear elastic then the load-defined *RF* equals the stress level-linked *material reserve factor* f_{RF} . In order to keep the generally accepted failure probability of about $p_f \approx 10^{-8}$ experience-based design Factors of Safety, *FoS j*, given in Standards, are to apply in Design Dimensioning. The very simple example below shows the *RF*-calculation as the

basic task in design which determines every procedure when generating design tools such as SFCs and analyses in the upcoming chapters.

Asssumption: Linear analysis permitted, design FoS $j_{ult} = 1.25$

* Design loading (action): $\{\sigma\}_{design} = \{\sigma\} \cdot j_{ult}$

* 2D-stress state: $\{\sigma\}_{design} = (\sigma_1, \sigma_2, \sigma_3, \tau_{23}, \tau_{31}, \tau_{21})^T \cdot j_{ult} = (0,\ -75,\ 0,\ 0,\ 0,\ 52)^T$ MPa

* Residual stresses: 0 $\left(effect\ vanishes\ with\ increasing\ micro-cracking\right)$

* Strengths (resistance) : $\{\bar{R}\} = (1378,\ 950,\ 40,\ 125,\ 97)^T$ MPa average from mesurement

statistically reduced $\{R\} = (R_{||}^t, R_{||}^c, R_{\perp}^t, R_{\perp}^c, R_{\perp||})^T = (1050,\ 725,\ 32,\ 112,\ 79)^T$ MPa

* Friction values : $\mu_{\perp||} = 0.3,\ (\mu_{\perp\perp} = 0.35)$, Mode interaction exponent: $m = 2.7$

$$\left\{Eff^{\,\text{mode}}\right\} = \left(Eff^{\,||\sigma},\ Eff^{\,||\tau},\ Eff^{\,\perp\sigma},\ Eff^{\,\perp\tau},\ Eff^{\,\perp||}\right)^T = \left(0.88,\ 0,\ 0,\ 0.21,\ 0.20\right)^T$$

$$Eff^{\,m} = (Eff^{\,||\sigma})^m + (Eff^{\,||\tau})^m + (Eff^{\,\perp\sigma})^m + (Eff^{\,\perp\tau})^m + (Eff^{\,\perp||})^m = 100\%\ .$$

The results above deliver the following material reserve factors $f_{RF} \rightarrow RF$

* $Eff^{\,\perp\sigma} = \dfrac{\sigma_2 - |\sigma_2|}{2 \cdot \bar{R}_{\perp}^t} = 0, \quad Eff^{\,\perp\tau} = \dfrac{-\sigma_2 + |\sigma_2|}{2 \cdot \bar{R}_{\perp}^c} = 0.60, \quad Eff^{\,\perp||} = \dfrac{|\tau_{21}|}{\bar{R}_{\perp||} - \mu_{\perp||} \cdot \sigma_2} = 0.51$

$$Eff = [(Eff^{\,\perp\sigma})^m + (Eff^{\,\perp\tau})^m + (Eff^{\,\perp||})^m]^{1/m} = 0.72.$$

$\Rightarrow \quad f_{RF} = 1 / Eff = 1.39 \rightarrow$ RF = f_{RF} (if linearity permitted) $\rightarrow$ MoS = $RF - 1 = 0.39 > 0$!

Fig.1-2: 2D Example of the Design Verification of a critical UD lamina in a distinct wall design

Here, the result reads: The certification–relevant load-defined Reserve Factor *RF* corresponds in the given linear case to the material reserve factor f_{RF}, the value of which is 1.39 > 1. From this follows: *The laminate wall design is verified*!

1.5 'Quad'-Laminates and Double-Double (DD) Laminates Lay-ups

Usual design objects are laminated walls. Here, the designer finds a novel building-block for laminate design. After the so-called 'Quad-laminates' (*standard laminates with 0°, 90°, 45°, -45° fiber orientations)* Tsai investigated a novel semi-finished product, termed C^{TR}-Ply, and created the promising 'Double-Double laminate (see [*Kap22*] and [*Cun22*]. In the latter document the not simply to perform transfer of Tsai's notation on stresses and strengths has been executed and is now compatible to the German Standard VDI 2014. Tsai's idea is to create *"Laminate parameter plots for in-plane loading could replace the well-known carpet plots, and all laminates can be portrayed on one plot. It is helpful to assess what laminates can and cannot do and which one is the best as decision support?"*. (This investigation has been started, [*Kap23*]).

Whereas the 'Quad' family is well known the novel 'DD' family has to be presented.

Double-Double (DD) means a sub-laminate of two angle-plies or two Doubles, respectively: Two angle-plies of different fiber angles form a four-ply sub-laminate. It is a multi-ply semi-fished product identified by the brackets {..} to discriminate it from [..] for the UD-layer prepreg stacks. DD is automatically balanced, needs no ten-percent-rule, no stacking sequence. Practical homogenization makes mid-plane symmetry unnecessary. Of-course, stitching of the C-ply harms the UD material, however this is captured in the material tests determining the material design

values in test data evaluation. By-the-way, the use of C-ply™ makes minimum coupling in the laminate stiffness matrix [K] possible.

In strength analysis the repeated double angle-ply sub-laminate and the full laminate can be modelled ply-wise as $\{\varphi / -\varphi / \psi / -\psi\}$ in each sub-laminate stack. ($\pm\varphi$, $\pm\psi$) *corresponds to the* ω*-angle in net-theory* $\pm\omega_1, \pm\omega_2$*, where* $\alpha_1 = \omega_1$, $\alpha_2 = -\omega_1$, $\alpha_3 = \omega_2$, $\alpha_4 = -\omega_2$.)

2 Choice of a UD Strength Fracture Criteria Set considering 'Modal' and 'Global' SFCs

Present SFCs can be basically separated into two groups, global and modal SFC ones. *Fig.2-1* presents the main differences between them (*The author chose the term "Global" as a 'play on words' to "modal" and to being self-explaining*). Global SFCs describe the full failure surface by one single mathematical equation. This means that for instance a change of the UD *tensile* strength $\bar{R}_{\perp}^{t}$ affects the failure curve in the *compression* domain, where no physical impact can be! Hence, the computed Reserve Factor may not be on the safe side in this domain.

However, Modal SFCs need an interaction of the failure modes. This is performed by a probabilistic approach (series failure system) in the transition zone of neighboring modes.

The following table depicts the advantages and disadvantages of global and modal SFCs.

Table 2-1: Pros (+, for) and Cons (-, contra) of 'Global' and 'Modal' SFCs

Global SFCs like Tsai-Wu, Drucker-Prager (*applied in construction*)

(+) Describe the full failure surface by one single mathematical equation ('single-value criterion')

(-) Usual global SFCs do not capture a multi-fold acting failure mode, i.e. $\sigma_I = \sigma_{II}$ or $\sigma_2 = \sigma_3$ or a 3-fold acting failure mode under σ_{hyd} with tension or compression

(-) Re-calculation: In the case of a test data change in a distinct mode domain re-calculation of model parameters is mandatory. Any change in one of the 'forcibly married' modes requires a new global mapping which also changes the failure curve in a physically independent failure domain, see *Fig.2-2*. In consequence, the material reserve factor has to be determined again

(-) The determination of *RF* for multi-axial stress states seems to be questionable for the generally in civil engineering. applied well-known isotropic Drucker-Prager model (*conical failure body).*

Modal SFCs like Mises, Hashin, Puck, Cuntze

The 'Mises' (HMH) yield failure condition was the model of the author. It is a modal SFC that captures just one failure mode. Later, Hashin with his 4 modes supported the author's modal thinking.

(+) Describes each failure mode-associated part of the full failure surface by a single equation. Therefore, modal SFCs are more physically-based than global SFCs

(+) A change within one mode just hits this mode, *see Fig.2-2*. The *RF* is just to re-determine in the affected failure mode domain!

(+) Equivalent stresses σ_{eq} are always determinable for isotropic UD materials

(+) Cuntze's SFCs capture multi-fold occurring failure modes by an additional term

(+) Cuntze's SFCs directly use the well to estimate friction value μ

(- , +) Cuntze FMC-based set affords an interaction of the SFCs to capture all activated failure modes. This delivers information about the mode's design-driving size via Eff^{mode}. Practically, there is no more numerical effort

(+) By using the interaction equation $Eff\,(Eff^{modes}) = 1$ the modal SFC-set formally becomes a quasi-global SFC but without the bottlenecks of a global SFC.

Fig.2-2 visualizes for a distinct global SFC, used in a German guideline, how dramatically a change of the tensile strength $\bar{R}_{\perp}^{t}$ affects the failure curve in the compression domain, although no physical impact can be! Considering the shortcomings of Global UD SFCs, my friend John Hart-Smith, cited in [*Har93*]:

"It is scientifically incorrect to employ polynomial interaction failure models **(**'global' ones**),**
if the mechanism of failure changes?"

In this context: Often, SFCs employ just strengths and no friction value. This is physically not accurate, since Mohr-Coulomb always acts in the case of compressed brittle materials! Then, an undesired consequence in Design Verification is: The computed *Reserve Factor RF* may be not on the safe side!

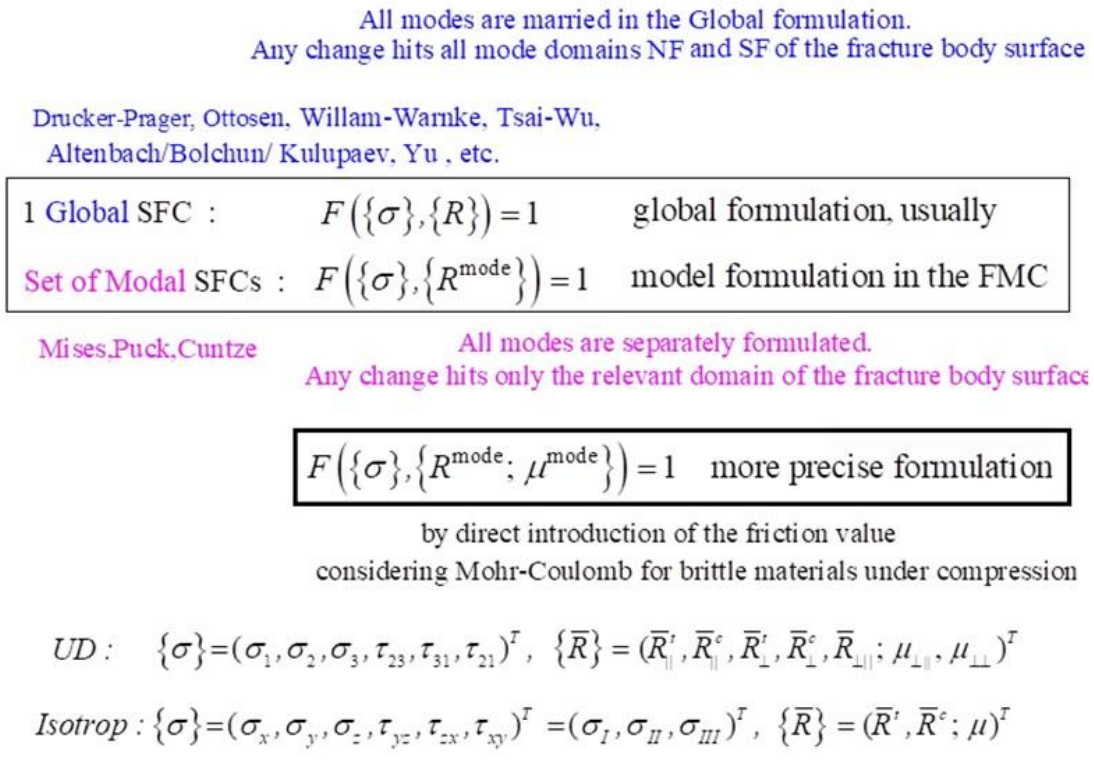

Fig.2-1: 'Global' and 'Modal' SFCs.

Some well-known SFCs shall be displayed in *Chapter 3*, which captures 3D-stressed laminates. This is performed by using the same notation to simpler allow a comparison of the different SFC-contents, and is helpful for decision making when choosing a SFC.

The author's FMC-based SFC set shall be presented in more detail at first, the other SFCs are presented in the following chapter.

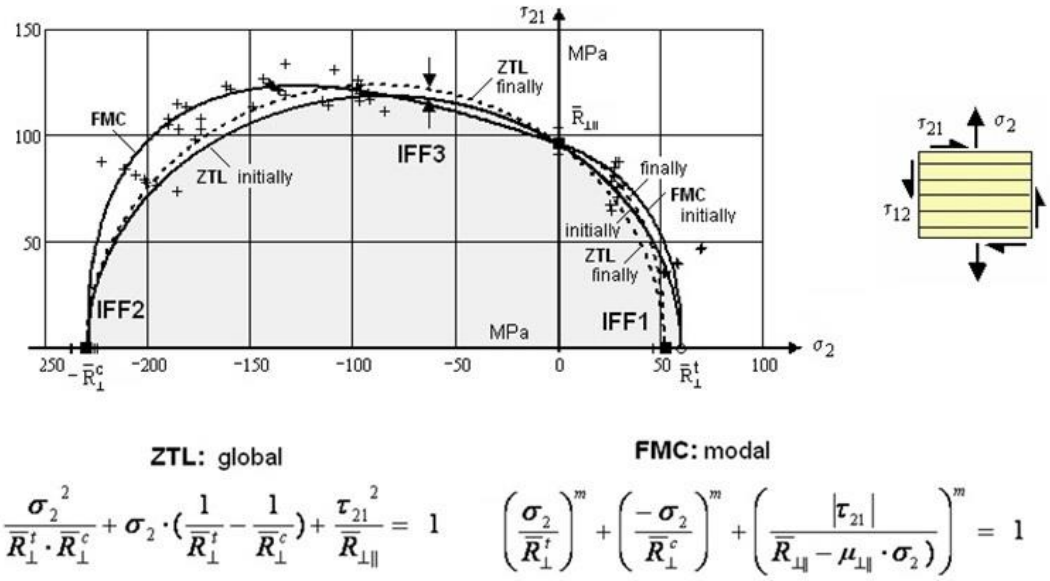

$$\frac{\sigma_2^2}{\bar{R}_\perp^t \cdot \bar{R}_\perp^c} + \sigma_2 \cdot \left(\frac{1}{\bar{R}_\perp^t} - \frac{1}{\bar{R}_\perp^c}\right) + \frac{\tau_{21}^2}{\bar{R}_{\perp\|}} = 1 \qquad \left(\frac{\sigma_2}{\bar{R}_\perp^t}\right)^m + \left(\frac{-\sigma_2}{\bar{R}_\perp^c}\right)^m + \left(\frac{|\tau_{21}|}{\bar{R}_{\perp\|} - \mu_{\perp\|} \cdot \sigma_2}\right)^m = 1$$

Fig.2-2: Effect of global modelling, ZTL-SFC, *still used in the HSB*

3 Cuntze's Failure Mode Concept-based SFCs, modal FF1, FF2, IFF1, IFF2, IFF3

$$\{\sigma\} = (\sigma_1, \sigma_2, \sigma_3, \tau_{23}, \tau_{31}, \tau_{21})^T, \quad \{\bar{R}\} = (\bar{R}_\|^t, \bar{R}_\|^c, \bar{R}_\perp^t, \bar{R}_\perp^c, \bar{R}_{\perp\|})^T \quad \text{5 strengths, mandatory,}$$

$$\text{Failure Function: } F\left(\{\sigma\}, \{\bar{R}\}, \mu \text{ directly}\right) = 1$$

History: Cuntze's invariant-based thinking followed at first Mises (*invariant* J_2) on isotropic materials and later he gladly grasped Hashin's Hypothesis 2 on UD materials and the UD invariants.

3.1 Material Symmetry and 'Generic' Number

Under the design-simplifying presumption "Homogeneity is a permitted assessment for the material concerned", and regarding the respective material tensors, it follows from material symmetry that the number of strengths equals the number of elasticity properties!
Fracture morphology gives further evidence: Each strength property corresponds to a distinct strength failure mode and to a distinct strength failure type, to Normal Fracture (NF) or to Shear Fracture (SF). This means, a characteristic number of quantities is fixed: 2 for isotropic material and 5 for the transversely-isotropic UD lamina (≡ lamellas in civil engineering). Hence, the applicability of material sym*metry involves that in general just a minimum number of properties needs to be measured* (cost + time benefits) which is helpful when setting up strength test programs, beneficial when regarding material modelling and for the required amount of testing.

Witnessed material symmetry knowledge seems to tell: There might exist a 'generic' (*term was chosen by the author*) material inherent number for:

Transversely-Isotropic Material: number 5 for the these basically brittle materials

- 5 e*lastic 'constants', 5 strengths, 5 strength failure modes fracture* (NFs with SFs)
- *2 physical parameters such as the coefficient of thermal expansion CTE, the coefficient of moisture expansion CME, and the friction value μ, etc.) (CTE, CME,* $\mu_{\perp\perp}$, $\mu_{\perp\|}$ *etc.).*

3.2 Basic Features

The basic features of the FMC, derived about 1995, are: see [*Cun04 through Cun17*]

- Each failure mode represents 1 independent failure mechanism and thereby represents 1 piece of the complete failure surface.
- A failure mechanism at the lower micro-scopic mode level shall be considered in the applied desired macro-scopic SFC
- Each failure mechanism or mode is governed by 1 basic strength *R*, only (*witnessed!*)
- Each failure mode can be represented by 1 SFC. Therefore, equivalent stresses can be computed for each mode. This is of advantage when deriving S-N curves and generating Haigh diagrams in fatigue with minimum test effort in order to relatively effortless obtain Constant Fatigue Life curves, see [*Cun22, and 23*] for lifetime estimation. Modal SFCs lead to a *clear* mode strength-associated equivalent stress
- Of course, a modal FMC-approach requires an interaction in all the mode transition zones reading

$$Eff = \sqrt[m]{(Eff^{\text{mode 1}})^m + (Eff^{\text{mode 2}})^m + ...} = 1 = 100\% \quad for \quad \text{Onset-of-Failure .}$$

It employs the so-called 'material stressing effort' (*artificial term, generated in the WWFE in order to get an English term for the meaningful German term Werkstoffanstrengung*). analogous to 'Mises'

$$Eff^{\text{yield mode}} = \sigma_{eq}^{\text{Mises}} / R_{0.2} \quad \rightarrow \quad Eff^{\text{fracture mode}} = \sigma_{eq}^{\text{fracture mode}} / R \ ,$$

with a mode interaction exponent *m,* also termed rounding-off exponent, the size of which is high in case of low scatter and vice versa. The value of *m* is obtained by curve fitting of test data in the transition zone of the interacting modes. General FRP mapping experience delivered that *2.5 < m < 3*. A lower value chosen for the interaction exponent is more on the safe RF side or more 'design verification conservative'. For CFRP *m* = 2.6 is recommended from mapping experience. From engineering reasons the interaction exponent *m* is chosen the same in all transition zones of adjacent mode domains. Using the interaction equation in the mode transition zones is leading again to a pseudo-global failure curve or surface. In other words, a '*single surface failure description*' is achieved again, such as with Tsai/Wu but without the shortcomings of the global SFCs.
Above interaction of adjacent failure modes is modelled by the 'series failure system'. That permits to formulate the total material stressing effort *Eff* generated by all activated failure modes as 'accumulation' of Eff^{modes} ≡ sum of the single mode failure danger proportions. *Eff* = 100% = 1 represents the mathematical description of the complete surface of the failure body! In practice, i.e. in thin UD laminas, at maximum, 3 modes of the 5 modes (*2 FF + 3 IFF*) will physically interact. Considering 3D-loaded thick laminas embedded in laminates, there, all 3 IFF modes might interact.

In order to only use experimentally derivable material quantities, the author directly introduced in his 3D-SFCs for the compression domain, the internal material friction μ as a SFC model parameter. Friction is a well-known physical property in engineering. However, one does not yet find a direct use of μ in the textbooks and codes! Why using Mohr's friction angle $\varphi_{friction}$ if μ ($\varphi_{friction}$) is directly applicable? The direct introduction of the measurable friction value is possible for the modal shear fracture SFCs. This possibility was achieved after the performance of an effortful transition of the

SFC formulated in structural stresses into a Mohr stresses formulated one *(at first in Chapter 6 of Cun22; here in Annex2*).

3.3 Cuntze's FMC-based Set of Modal SFCs

Of interest is not only the interaction of the fracture surface portions in a *mixed failure domain* or transition zone of adjacent failure modes, respectively, but failure in a *multi-fold failure domain* (superscript ^{MfFD}) such as in the (σ_2^t, σ_3^t)-domain. There the associated mode material stressing effort acts twofold. It activates failure in two orthogonal directions which may be considered by adding a multi-fold failure term, proposed in [*13*] for isotropic materials. It can be applied as well to brittle UD-material in the quasi-isotropic transversal plane $\sigma_2(\sigma_3)$. Invariants from [*Boe85*] are employed. These read ($\sigma_1 = V_f \cdot \sigma_{1f}$)

$$I_1 = \sigma_1, \quad I_2 = \sigma_2 + \sigma_3, \quad I_3 = \tau_{31}^2 + \tau_{21}^2, \quad I_4 = (\sigma_2 - \sigma_3)^2 + 4 \cdot \tau_{23}^2 \text{ (Boehler, applied)}$$

$$I_5 = (\sigma_2 - \sigma_3) \cdot (\tau_{31}^2 - \tau_{21}^2) - 4\tau_{23}\tau_{31}\tau_{21}. \qquad I_4 = \tau_{23}^2 - \sigma_2 \cdot \sigma_3 \text{ (Hashin).}$$

The 2nd term in I_5 can be deleted because on one side this combination is very seldom of importance, and on the other side can be made zero if a transformation in the quasi-isotropic plane is accomplished. This is recommended and can be performed by

$$\{\sigma\}_{\text{lamina}} = (\sigma_1, \sigma_2, \sigma_3, \tau_{23}, \tau_{31}, \tau_{21})^T \rightarrow \sigma_1, \sigma_2^{pr}, \sigma_3^{pr}, 0, \tau_{31}^{pr}, \tau_{21}^{pr})^T, \text{ for further use}$$

$$\text{simplifiable to} \quad \Rightarrow \quad \{\sigma\}_{\text{lamina}} = (\sigma_1, \sigma_2, \sigma_3, 0, \tau_{31}, \tau_{21})^T.$$

In the quasi-isotropic UD domain the transformation into the two principal stresses is performed by

$$\sigma_2^{pr} = 0.5 \cdot (\sigma_2 + \sigma_3) + \sqrt{(0.5 \cdot (\sigma_2 - \sigma_3))^2 + \tau_{23}^2}, \quad \tan(2\varphi) = 2\tau_{23} / (\sigma_2 - \sigma_3),$$

$$\sigma_3^{pr} = 0.5 \cdot (\sigma_2 + \sigma_3) - \sqrt{(0.5 \cdot (\sigma_2 - \sigma_3))^2 + \tau_{23}^2}, \quad \varphi = \varphi° \cdot \pi / 180°.$$

Table 3-1 collects the FMC-derived 5 SFC formulations. Therein, the used invariants have been inserted into the stress formulations.

From friction parameters *b* to friction values μ : The structural stresses-formulated UD-fracture curve $\sigma_2(\sigma_3)$ could be transferred into a Mohr-Coulomb one obtaining $\tau_{nt}(\sigma_n)$, *(at first in Cun22; here in Annex1*). ***1***]. This novel, mathematically pretty effortful transformation enabled the author to link the fictitious friction parameters *b* of the respective SFCs via a determined fracture angle with the measurable physical friction value μ, see also [*VDI97*]. The author's FF1- and FF2-formulations for instance take care, that transversal equi-biaxial compression might cause FF1. The two FF formulations correspond to a maximum stress SFC, however the strain formulation FF1 captures micro-mechanical failure of the constituent fiber under bi-axial compressive stressing.

The invariants in the originally invariant-formulated failure functions *F* are replaced by the associated stresses and then *Eff* is inserted and for the *Eff* s resolved.

Table 3-1 'Dense' UD materials: Cuntze's 3D SFC formulations for FF1, FF2 and IFF1, IFF2, IFF3

FF1: $Eff^{\|\sigma} = \breve{\sigma}_1 / \bar{R}_{\|}^{t} = \sigma_{eq}^{\|\sigma} / \bar{R}_{\|}^{t}$ with $\breve{\sigma}_1 \cong \varepsilon_1^t \cdot E_{\|}$ (matrix neglected)

FF2: $Eff^{\|\tau} = -\breve{\sigma}_1 / \bar{R}_{\|}^{c} = +\sigma_{eq}^{\|\tau} / \bar{R}_{\|}^{c}$ with $\breve{\sigma}_1 \cong \varepsilon_1^c \cdot E_{\|}$

IFF1: $Eff^{\perp\sigma} = [(\sigma_2 + \sigma_3) + \sqrt{\sigma_2^{\,2} - 2\sigma_2 \cdot \sigma_3 + \sigma_3^{\,2} + 4\tau_{23}^{\,2}}\,] / 2\bar{R}_{\perp}^{t} = \sigma_{eq}^{\perp\sigma} / \bar{R}_{\perp}^{t}$

IFF2: $Eff^{\perp\tau} = [a_{\perp\perp} \cdot (\sigma_2 + \sigma_3) + b_{\perp\perp} \sqrt{\sigma_2^{\,2} - 2\sigma_2\sigma_3 + \sigma_3^{\,2} + 4\tau_{23}^{\,2}}\,] / \bar{R}_{\perp}^{c} = \sigma_{eq}^{\perp\tau} / \bar{R}_{\perp}^{c}$

IFF3: $Eff^{\perp\|} = \{[a_{\perp\|} \cdot I_{23-5} + (\sqrt{a_{\perp\|}^{\,2} \cdot I_{23-5}^{\,2} + 4 \cdot \bar{R}_{\perp\|}^{\,2} \cdot (\tau_{31}^2 + \tau_{21}^2)^2}\,] / (2 \cdot \bar{R}_{\perp\|}^{\,3})\}^{0.5} = \sigma_{eq}^{\perp\|} / \bar{R}_{\perp\|}$

$\left\{\sigma_{eq}^{\text{mode}}\right\} = \left(\sigma_{eq}^{\|\sigma},\ \sigma_{eq}^{\|\tau},\ \sigma_{eq}^{\perp\sigma},\ \sigma_{eq}^{\perp\tau},\ \sigma_{eq}^{\|\perp}\right)^T$, $I_{23-5} = 2\sigma_2 \cdot \tau_{21}^2 + 2\sigma_3 \cdot \tau_{31}^2 + 4\tau_{23}\tau_{31}\tau_{21}$

Inserting the compressive strength point $(0,\ -\bar{R}_{\perp}^{c}) \rightarrow a_{\perp\perp} \cong \mu_{\perp\perp} / (1 - \mu_{\perp\perp})$, $b_{\perp\perp} = a_{\perp\perp} + 1$

from a measured fracture angle $\rightarrow \mu_{\perp\perp} = \cos(2 \cdot \theta_{fp}^{c}\,° \cdot \pi / 180)$, for $51° \rightarrow \mu_{\perp\perp} \cong 0.18$.

$a_{\perp\|} = 2 \cdot \mu_{\perp\|}$. Typical friction value ranges: $0 < \mu_{\perp\|} < 0.25$, $0 < \mu_{\perp\perp} < 0.2$.

The interaction equation - thinking principal stresses, which makes τ_{23} zero without leaving a general use - reads in the **2D** version (*absolute values are used to bypass senseless negative Effs*):

$$\{\sigma\} = (\sigma_1, \sigma_2, \tau_{12})^{\mathrm{T}}, \quad \{\bar{R}\} = (0,0,\bar{R}_{\perp}^{t}, \bar{R}_{\perp}^{c}, \bar{R}_{\perp\|})^T, \ \mu_{\perp\|}.$$

$$Eff = [(Eff^{\|\sigma})^m + (Eff^{\|\tau})^m + (Eff^{\perp\sigma})^m + (Eff^{\perp\|})^m + (Eff^{\perp\tau})^m]^{m-1} \text{ with the mode portions}$$

$$Eff^{\|\sigma} = \frac{(\sigma_1 + |\sigma_1|)}{2 \cdot R_{\|}^{t}},\ Eff^{\|\tau} = \frac{(-\sigma_1 + |\sigma_1|)}{2 \cdot R_{\|}^{c}},\ Eff^{\perp\sigma} = \frac{\sigma_2 - |\sigma_2|^*}{2 \cdot \bar{R}_{\perp}^{t}},\ Eff^{\perp\tau} = \frac{-\sigma_2 + |\sigma_2|}{2 \cdot \bar{R}_{\perp}^{c}},\ Eff^{\perp\|} = \frac{|\tau_{21}|}{\bar{R}_{\perp\|} - \mu_{\perp\|} \cdot \sigma_2}.$$

If micromechanical failure from bi-axial compression is included, then failure occurs without any σ_1., which is captured by

This is captured by: $Eff^{\|\sigma} = \frac{(\varepsilon_1 + |\varepsilon_1|) \cdot E_{\|}}{2 \cdot R_{\|}^{t}}$, $Eff^{\|\tau} = \frac{(-\varepsilon_1 + |\varepsilon_1|) \cdot E_{\|}}{2 \cdot R_{\|}^{c}}$ with ε_1 from FEA.

Due to successful comparison with the 3D-reduced SCF (*suffix 3 to drop*) the shear failure $Eff^{\perp\|}$ could be further simplified. The interaction exponent is taken *m* = 2.6. By above formulation physical senseless negative *Effs* are by-passed.

Above equation includes all mode material stressing efforts and each of them represents a portion of load-carrying capacity of the material. In practice in thin laminas, at maximum, 3 modes of the 5 modes will physically interact. The superscripts shall indicate the failure active σ- or τ-stress. Considering 3D-loaded thick laminas, there, all 3 IFF modes might interact.

Usually, the value of *m* is obtained by curve fitting of test data in the interaction zone. FRP mapping experience delivered that 2.5 < m < 3, at least for CFRP. The mode interaction exponent m is also termed rounding-off exponent, the size of which is high in case of low scatter and vice versa. A lower value chosen for the interaction exponent is more on the safe side. From engineering reasons the interaction exponent m is chosen the same in the transition zones of adjacent domains.

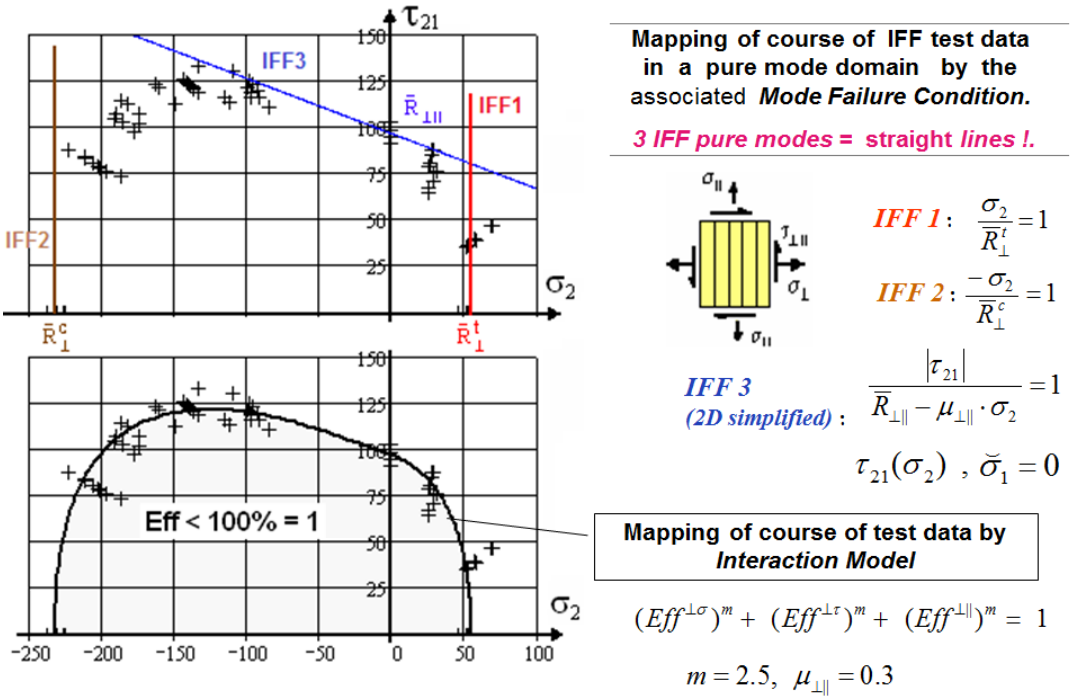

Fig.3-1: Visualization of the IFF interaction of a UD-material [Cun06]

Viewing SFCs, be careful with conclusions reported in literature (personal experience):

Unfortunately, SFC model variations in the literature - created by another author - are published under the name of an originator, i.e. the author in the following case *[A Strength tensor based Failure Criterion with Stress Interactions, P.V. Osswald and T.A. Osswald. Polymer Composites 2018, 2826-2833]*. Therein, the author faced several peaks of insolence**:** *(1) The 'Osswald-Cuntze SFC' - poorly rated by the Osswalds - is not even depicted in their publication! And, unfortunately, the cited investigated WWFE-I test cases suffer from correctness as the author knows and discussed in his WWFE-I-contribution. (2) " .. ... with a certain manipulation of tensile and compressive stresses (What is really meant, remains open. (3) Statement of the Osswalds:"Cuntze's model did not include other stress-interactions, and therefore does not predict well the failure surface in the σ_{11}-σ_{22} plane". The Cuntze model captures all stress interactions! Did they not understand Cuntze's model? And, did they not look at the well mapped WWFE-II test case, depicted here in Fig.4-2, proving the theoretical model by tests?*

Fig.3-2 depicts the fracture failure body of UD materials. The upper picture contains the failure body of the plane 2D stress state and the lower picture the body of the 3D stress state. These look the same and are the same. Only some years ago the author sorted out *"If one replaces the lamina stresses by the associate equivalent mode stresses then the (surface of the) 2D-failure body simply becomes the (surface of the) general 3D-failure body".*

Necessary hint, regarding a citation in WWFE-II [*Kad13*] on the author's SFC set:

*"For his set of 5 modal UD failure criteria Cuntze needs **75 parameters".*** This fully mixes up apples and oranges". (I can never believe that you Sam formulated this! Unfortunately you are the main author).

*No, necessary are just **7 measurable model parameters** (5 strengths + 2 friction values) and **1** chosen **interaction exponent m**, a value derived from more than 25 years of mapping experience with isotropic, transversely-isotropic and orthotropic materials. A small value of m =2.5 is on the safe side, because it smoothens the transition zone between two modes harsher, which means a more*

inside rounding. One might value this as a 'Damage to reputation' because respected colleagues like Christensen have taken the value 75 for contra-argumentation.

In this context it is to note: Failure envelopes are not just an empirical fit through uniaxial tensile and compressive strength points as it was still assumed in the WWFE-I and –II, further! Friction is acting.

Of interest is not only the interaction of the fracture surface parts in the discussed mixed failure domains or interaction zones of adjacent failure modes, respectively, but additive failure danger is faced in a multi-fold failure domain (*superscript MfFD, see again Fig.1-1*). There the associated mode stress effort acts twofold. It activates failure in two directions which is considered by adding a multi-fold failure term, proposed in [*Awa78*] for isotropic materials, $\sigma_{II}(\sigma_{III})$. It can be applied to brittle UD material in the transversal, quasi-isotropic plane as well, $\sigma_2(\sigma_3)$.

Before presenting the UD-SFCs some pre-requisites are to check to really achieve a *reliable design process* before applying the SFCs. This is valid for test specimens, as well:

- Good fiber placement and alignment, and uniform distribution
- '*Fabrication signatures'* such as fabrication-induced fiber waviness and wrinkles are small and do not vary in the test specimens
- If applicable, residual stresses from the curing cycle are to be computed for the difference '*stress free temperature to room temperature 22°C'* as an effective temperature difference. Considering curing stresses or moisture stresses, the specimens are most often assumed to be well conditioned
- The stress-strain curves are average curves in design dimensioning, which is also the type one needs for test data mapping in order to obtain the best estimation, 50%.

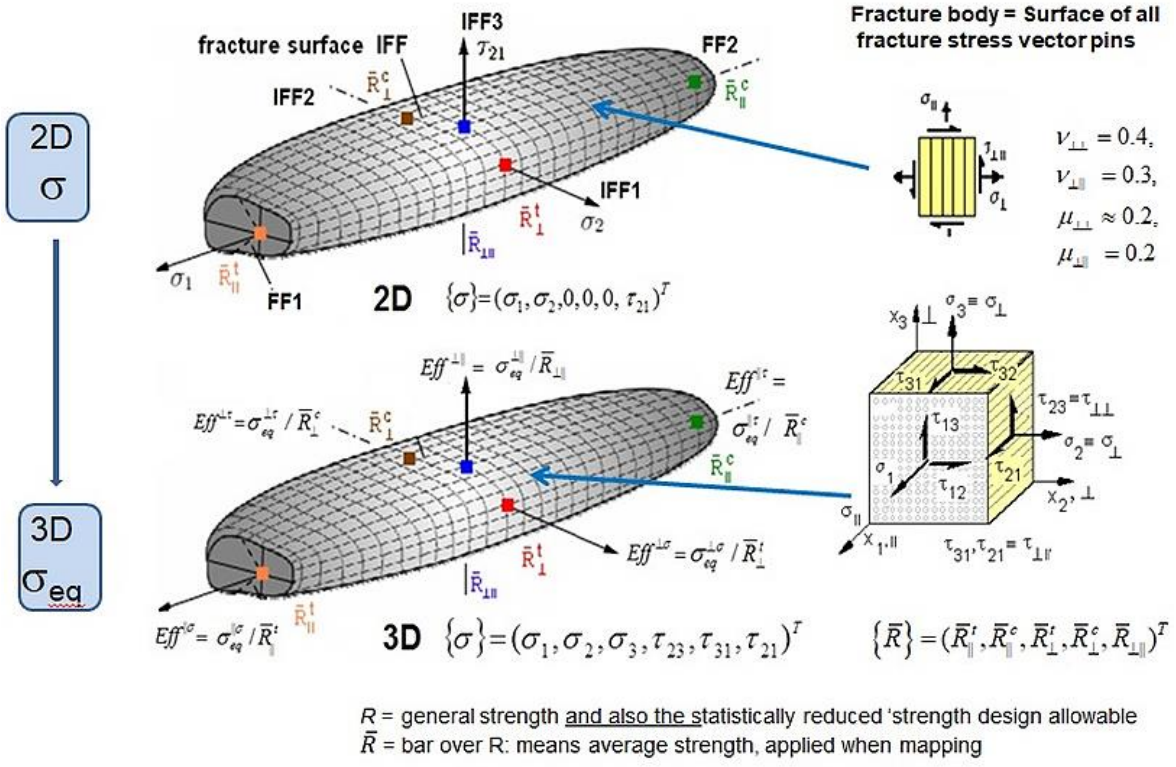

Fig.3-2: From a 2D- to a 3D-failure body by just replacing stresses by equivalent stresses

Delamination:

Delamination within a laminate may occur in tensile-shear cases and compression-shear cases (*remember the so-called wedge failure of Puck with its inclined fracture plane* [9]). Considering such a delamination a 3D stress state is to be regarded. This is especially the case if bends in the structure are stretched or compressed which generates stresses across the wall thickness. These stresses are activated by the delamination-critical stresses including inter-laminar stresses (index $_3$):

$$\{\sigma\}_{\text{lamina}} = (0, \sigma_2, \sigma_3, \tau_{23}, \tau_{31}, \tau_{21})^T \quad .$$

Delamination is a failure in the 'structure' laminate, and at its edges it is termed edge effect. Within the laminate it can be predicted by the application of the inter-laminar stresses-associated 3D-SFCs. At the edges it is - due to the stress singularity – a task of fracture mechanics tools using a cohesive zone model.

These Delamination SFCs are just a *subset* of the 5 SFCs above. They are intentionally given here in a separate manner because other researchers present special delamination conditions. With regard to the 3D nature of the IFF conditions, both, IFF1 ($F_{\perp}^{\sigma}$ *transverse tensile failure; inter-laminar stresses* $\sigma_3^t, \tau_{32}, \tau_{31}$ *may cause cracking)* and IFF2 ($F_{\perp}^{\tau}$ *wedge failure; intra-laminar stresses such as* σ_2^c, τ_{21} *cause cracking and may initiate a local 3D state of stress, including* σ_3) can also serve as conditions for the assessment of *'onset of delamination'* which practically is a *laminate* failure type. One or two modes will be the design driving ones in the critical local material location of a composite lay-up. These are activated by the delamination-critical stress state $\{\sigma\}_{\text{lamina}} = (0, \sigma_2, \sigma_3, \tau_{23}, \tau_{31}, \tau_{21})^T$, which includes all inter-laminar stresses. Introducing the two relevant combinations of the delamination-active stress state above delivers:

Tension/shear stressing

$$(Eff^{\perp\sigma})^m + (Eff^{\perp\parallel})^m = 1 \text{ with } \{\sigma\}_{\text{lamina}} = (0, \sigma_2^t, \sigma_3^t, \tau_{23}, \tau_{31}, \tau_{21})^T$$

Compression-shear stressing

$$(Eff^{\perp\tau})^m + (Eff^{\perp\parallel})^m = 1 \text{ with } \{\sigma\}_{\text{lamina}} = (0, \sigma_2^c, \sigma_3^t, \tau_{23}, \tau_{31}, \tau_{21})^T \quad .$$

Eventually *Fig.3-3* presents an IFF curve for a GFRP and a CFRP material. Test rig for the tube test specimen was the still mentioned test specimen-dedicated Tension-Compression/Torsion test machine.

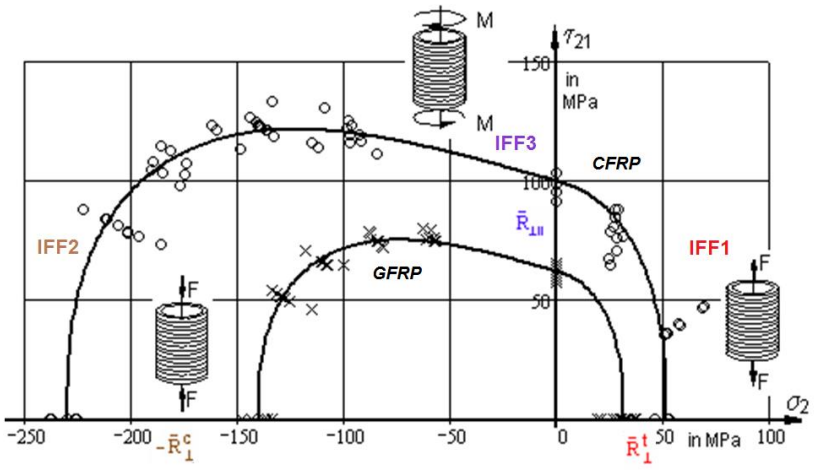

Fig.3-3, IFF test results: 2 GFRP, 1 CFRP test series (from MAN Technologie research project on Puck's IFF criterion, [Cun97], m =2.7 Fig. E-glass / LY556, HT976, DY070; CFRP: T300 / LY556, HT976

Lessons Learned from mapping experience with the WWFE Test Cases:

"*SFCs models may still have shortcomings and these shortcomings can only be reduced by using test data that represent real experimental 2D and 3D evidence. Test the provided test results, analyze your analysis, it might be cruder than you think. Always use information to improve an investigation. At least one third of the WWFE Test Cases was questionable up to not applicable for model validation*!" They could only provide the WWFE-contributors with available published test results taking the possible short comings regarding test inaccuracies and test data evaluation into account.

Now, some short presentations of three well-known SFCs are given to remind that different SFCs map a course of failure test data differently and may lead to a different prediction of 'Onset-of-Fracture Failure'.

The applied strengths in the formulas are strictly marked by a bar over $\bar{R}$
in order to mark that ' model validation is here the subject'.

4 Tsai-Wu, global SFC

$$\{\sigma\} = (\sigma_1, \sigma_2, \sigma_3, \tau_{23}, \tau_{31}, \tau_{21})^{\mathrm{T}}, \quad \{\bar{R}\} = (\bar{R}_{\parallel}^{t}, \bar{R}_{\parallel}^{c}, \bar{R}_{\perp}^{t}, \bar{R}_{\perp}^{c}, \bar{R}_{\perp\parallel};\ \bar{R}_{\perp\perp})^{\mathrm{T}} = (\mathrm{X}, X', Y, Y', S;\ \mathrm{S}_{23})^{\mathrm{T}}$$

$$F\left(\{\sigma\}, \{\bar{R}\}\right) = 1, \quad 6 \text{ strengths principally}$$

A general anisotropic tensor polynomial expression of Zakharov and Goldenblat-Kopnov with the parameters F_i, F_{ij} as strength model parameters was the basis of the Tsai-Wu SFC

$$\sum_{i=1}^{6}\left(F_i \cdot \sigma_i\right) + \sum_{j=1}^{6}\sum_{i=1}^{6}\left(F_{ij} \cdot \sigma_i \cdot \sigma_j\right) = 1.$$

From this tensorial formulation Tsai-Wu used the linear and quadratic terms, see *Table 4-1*:

*Table 4-1: Tsai-Wu **3D SFC** [Tsa71, Tsa22]*

$$F_i \cdot \sigma_i + F_{ij} \cdot \sigma_i \cdot \sigma_j = 1 \quad \text{with} \quad (\text{i,j} = 1,2..6) \quad \text{or executed}$$

$$F_{11} \cdot \sigma_1^2 + \; F_1 \cdot \sigma_1 + 2F_{12} \cdot \sigma_1 \cdot \sigma_2 + 2F_{13} \cdot \sigma_1 \cdot \sigma_3 + F_{22} \cdot \sigma_2^2 + F_2 \cdot \sigma_2 +$$

$$+ 2F_{23} \cdot \sigma_2 \cdot \sigma_3 + F_{33} \cdot \sigma_3^2 + \; F_{33} \cdot \sigma_3^2 + F_3 \cdot \sigma_3 + F_{44} \cdot \tau_{23}^2 + F_{55} \cdot \tau_{13}^2 + F_{66} \cdot \tau_{12}^2 = 1$$

with the strength model parameters

$$F_1 = 1/\bar{R}_{\parallel}^t - 1/\bar{R}_{\parallel}^c, \;\; F_{11} = 1/(\bar{R}_{\parallel}^t \cdot \bar{R}_{\parallel}^c), \;\; F_2 = 1/\bar{R}_{\perp}^t - 1/\bar{R}_{\perp}^c, \;\; F_{22} = 1/(\bar{R}_{\perp} \cdot \bar{R}_{\perp}^c) = F_{33},$$

$$F_{13} = F_{12}, \;\; F_{55} = F_{66} = 1/\bar{R}_{\perp\parallel}^2, \;\; 2F_{23} = 2F_{22} - 1/\bar{R}_{\perp\perp}^2, \;\; F_{44} = 2 \cdot (F_{22} + F_{23})$$

and - *in order to avoid an open failure surface* - the so-called interaction term

$$F_{12} = \bar{F}_{12} \cdot \sqrt{F_{11} \cdot F_{22}} \quad \text{with} \quad -1 \le \bar{F}_{12} \le 1\,; \quad \text{usually it is applied } F_{12} = -\,0.5.$$

In *Fig.4-1* the general types of stress of a UD-composite element causing FF and IFF. Shown are the inclined (oblique) planes in which brittle fracture occurs.

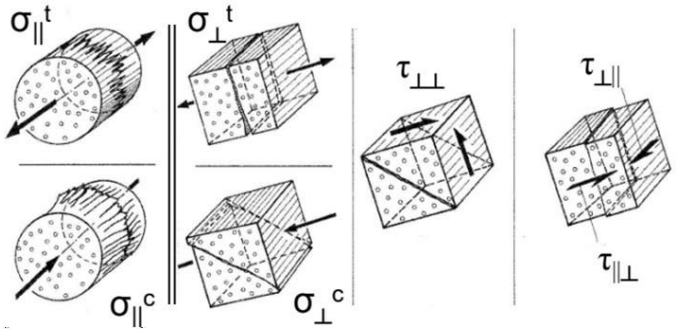

Fig. 4-1: The 6 stresses acting at a UD material element [Lut6, Puck]

The inter-laminar (3D) strength quantity $\bar{R}_{\perp\perp}$ (see §4.4) is the result of the formalistic evaluation of the polynomial model. How it is to determine is not presented. For 2D-applications it is not necessary and thus the problem is not given. The FMC does not need this quantity but just the 5 physically necessary measurable strengths.

A. Puck turned out that - after skillfully collecting the F_{ij}-terms - the above tensor polynomial is also a stress invariant-based formulation.

Questions: *Value for F_{12} ? What about the determination of $\bar{R}_{\perp\perp}$ to be used in 3D applications?*

Some months ago Steve informed me about: "*Prof. Shuguang Li was most helpful to explain the conditions for the interaction term F_{12} in the failure criterion*". And: *We are happy to have Shuguang Li in Chapter 9 to show that -1/2 is in fact the correct value for the interaction term if it is assumed that the failure envelope is a paraboloid (with very large resistance to tri-axial compression, the same assumption made for the von Mises criterion for isotropic materials). It is important to have removed one critical uncertainty of the Tsai-Wu criterion", see there* Chapter 9:" *Fully Rationalized Tsai-Wu Failure Criterion for Transversely Isotropic Materials"*. Tsai's Book *Double-Double*. 2022.

Above 3D formulation reduces to the following **2D SFC**, which captures interaction,

$$F_{11}\cdot\sigma_1^2 + \;\; F_1\cdot\sigma_1 + 2\frac{F_{12}}{\sqrt{\bar{R}_{\parallel}^{\,t}\cdot\bar{R}_{\parallel}^{\,c}\cdot\bar{R}_{\perp}^{\,t}\cdot\bar{R}_{\perp}^{\,c}}}\cdot\sigma_1\cdot\sigma_2 + +F_{22}\cdot\sigma_2^2 + F_2\cdot\sigma_2 + F_{66}\cdot\tau_{12}^2 = 1.$$

Some special comments on the interpolative 'global' SFC of Tsai-Wu:

(1) The formulation is mathematically elegant

(2) For $F_{12} \neq 0$ the predicted bi-axial failure stress values are higher than the strengths $R_{\parallel}^{c}, R_{\perp}^{c}$ in the (σ_1^c, σ_2^c) domain

(3) Prediction of a non-feasible domain in quadrant III of Fig.4-2, whereas the modal versions of Puck and the FMC-based one of Cuntze map)

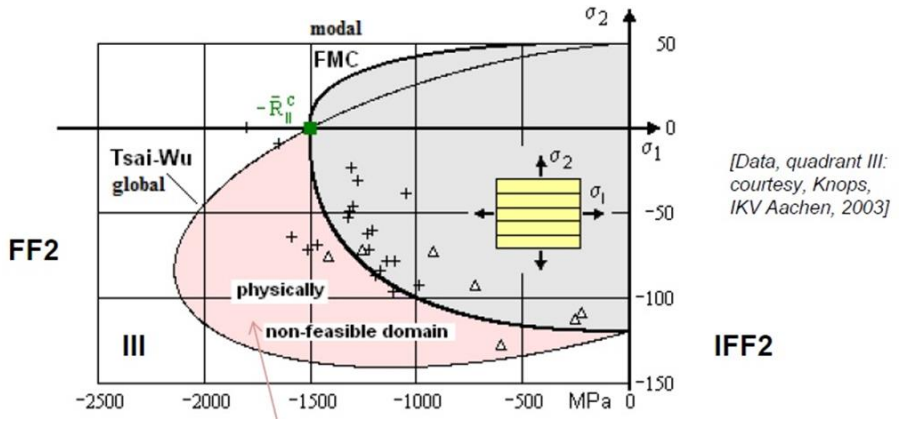

Fig.4-2, WWFE-II: Mapping of $\sigma_2(\sigma_1)$ test data (test results: M. Knops, IKV Aachen, [Kno3, Kno07]

(4) Treatment of (σ_2, τ_{21}) like (σ_2, τ_{31}), which is not accurate but model inevitably

(5) Cannot map for instance the $(\sigma_2^{\,c}, \tau_{21})$-humb in *Fig.3-3*, because the material inherent internal friction cannot be directly considered in the global SFC. Hence, the computed Reserve Factor may not be on the safe side in this domain

(6) Difficult determination of the model parameters in the 3D-formulation, and especially for F_{12} in the case of Tsai-Wu. The stress interaction term $F_{12} = F_{13}$ needs additional *bi-axial* (σ_1, σ_2)-tests. The bi-axial material parameter F_{12} is 'principally' obtained bi-axial compression tests. Usually it is applied F_{12} = - 0.5. For application just strength values are necessary, but this is not sufficient!

(7) No information on the prevailing failure mode FF or IFF is received

(8) The difference of the 'old' Failure Index *FI* and the material stressing effort *Eff* is visible, when not addressing the failure envelope, where *FI* =|*F*| = *Eff* = 100% = 1. See *Annex 3*.

5 Hashin, modal SFCs, FF1, FF2, IFF1, IFF2

$\{\sigma\} = (\sigma_1, \sigma_2, \sigma_3, \tau_{23}, \tau_{31}, \tau_{21})^T$, $\{\bar{R}\} = (\bar{R}_{\parallel}^t, \bar{R}_{\parallel}^c, \bar{R}_{\perp}^t, \bar{R}_{\perp}^c, \bar{R}_{\perp\parallel}; \bar{R}_{\perp\perp})^T$; 6 strengths, principally

Hypothesis 1: $F\left(\{\sigma^A\}, \{\bar{R}^A\}, \theta_{fp}\right) = 1$, Puck's way $\Leftrightarrow$ Hypothesis 2: $F\left(\{\sigma\}, \{\bar{R}\}\right) = 1$, Cuntze's way

* Hypothesis 1, valid for Puck's Action Plane IFF formulation, see [*Has80*]:

"In the event that a failure plane under a distinct fracture angle can be identified, the failure is produced by the normal and shear stresses on that plane".

Hashin proposed a modified Mohr-Coulomb IFF approach but did not pursue this idea due to numerical difficulties (*A. Puck succeeded on this way*).

Also into this paper Hashin included an invariant-based global quadratic approach (this is *Cuntze's invariant way, below*).

* Hypothesis 2, valid for Cuntze's FMC formulation:

"*For UD-material the SFCs should be invariant under any rotation around the fiber direction*."

Based on this, Hashin used the 5 stress invariants

$I_1 = \sigma_1$, $I_2 = \sigma_2 + \sigma_3$, $I_3 = \tau_{31}^2 + \tau_{21}^2$, $I_4 = \tau_{23}^2 - \sigma_2 \cdot \sigma_3$, $I_5 = 4\tau_{23}\tau_{31}\tau_{21} - \sigma_2 \cdot \tau_{31}^2 - \sigma_3 \cdot \tau_{21}^2)$.

*Table 5-1: Hashin's four **3D SFCs***

FF1, $\sigma_1 > 0$: $\left(\frac{\sigma_1}{\bar{R}_{\parallel}^t}\right)^2 + \frac{\tau_{31}^2 + \tau_{21}^2}{\bar{R}_{\perp\parallel}^{\,2}}$; FF2, $\sigma_1 < 0$: $\left(\frac{-\sigma_1}{\bar{R}_{\parallel}^c}\right)^2 = 1$,
IFF1, $\sigma_2 + \sigma_3 > 0$: $\frac{(\sigma_2 + \sigma_3)^2}{\bar{R}_{\perp}^t} + \frac{\left(\tau_{23}^2 - \sigma_2 \cdot \sigma_3\right)}{\bar{R}_{\perp\perp}^{\,2}} + \frac{\left(\tau_{31}^2 + \tau_{21}^2\right)}{\bar{R}_{\perp\parallel}^{\,2}} = 1$,
IFF2, $\sigma_2 + \sigma_3 < 0$: $\left(\frac{\bar{R}_{\perp}^{c\,2}}{4 \cdot \bar{R}_{\perp\perp}^{\,2}} - 1\right) \cdot \frac{(\sigma_2 + \sigma_3)}{\bar{R}_{\perp}^c} + \frac{(\sigma_2 + \sigma_3)^2}{4 \cdot \bar{R}_{\perp\perp}^{\,2}} + \frac{\left(\tau_{23}^2 - \sigma_2 \cdot \sigma_3\right)}{\bar{R}_{\perp\perp}^{\,2}} + \frac{\left(\tau_{31}^2 + \tau_{21}^2\right)}{\bar{R}_{\perp\parallel}^{\,2}} = 1$,
Interlaminar failure: $\sigma_3 > 0$: $\left(\frac{\sigma_3}{R_3^t}\right)^2 = 1$; $\sigma_3 < 0$: $\left(\frac{-\sigma_3}{R_3^c}\right)^2 = 1$.

In hypothesis 2, the 3D Hashin Criteria (1980) divide the mechanisms of UD failure into the two groups FF and IFF. The invariants are replaced in the generated SFCs by its stress relationships to set up the following (*just*) 4 SFCs, wherein the strength $\bar{R}_{\perp\perp}$ is seen to equal the failure shear stress of τ_{23} (see *Conclusions*):

Ansys uses the 4 failure modes of Zvi Hashin, shear mode IFF3 is missing.

Questions: *(1) What about the determination of* $\bar{R}_{\perp\perp}$ *? (2) How does the mandatory smoothing interaction of the 4 modes to determine FPF look like?*

2D-SFC: Equations without the suffix $_3$ remain.

6 **Puck's Action Plane IFF SFCs, modal FF1, FF2, global IFF** discriminating 3 IFFs domains

$\{\sigma\} = (\sigma_1, \sigma_2, \sigma_3, \tau_{23}, \tau_{31}, \tau_{21})^{\mathrm{T}}$, $\{\bar{R}\} = (\bar{R}_{\parallel}^{t}, \bar{R}_{\parallel}^{c}, \bar{R}_{\perp}^{t}, \bar{R}_{\perp}^{c}, \bar{R}_{\perp\parallel};\ \bar{R}_{\perp\perp})^{\mathrm{T}}$ 6 strengths, principally

Applying Mohr stresses the SFC reads $F\left(\sigma_n, \tau_n, \bar{R}_{\sigma}, \bar{R}_{\tau}, \theta_{\mathrm{fp}}\right) = 1$

means using action plane stresses and $\theta = \theta_{\mathrm{fp}}$, $\tau_n = \sqrt{\tau_{nt}^{\ 2} + \tau_{n1}^{\ 2}}$

$F\left(\{\sigma^A\}, \{\bar{R}^A\}, \theta_{\mathrm{fp}}\right) = 1$ with $\{\bar{R}\} = (\bar{R}_{\parallel}^{t}, \bar{R}_{\parallel}^{c}, \bar{R}_{\perp}^{A} = \bar{R}_{\perp}^{t}, \bar{R}_{\perp\perp}^{A}, \bar{R}_{\perp\parallel}^{A} = \bar{R}_{\perp\parallel};\ \bar{R}_{\perp\perp}^{A} \neq \bar{R}_{\perp\perp})^{\mathrm{T}}$,

Two IFF fracture plane resistances directly are the associated strengths because the action plane, superscript ^{A}, corresponds to the fracture failure plane. Statement Puck: "It is to note, that the angle-dependent action plane fracture resistance $\bar{R}_{\perp\perp}^{A}$ shall not be mixed up with the 'strength' $\bar{R}_{\perp\perp}$".

History:

* As early as 1969 A. Puck recognized to separate FF from IFF (*not Hashin as is sometimes said*). Since the mid-eighties Puck from Uni Kassel, Cuntze from MAN and colleagues of the DLR-Braunschweig looked together for an improved IFF-SFC. H. Schuermann, Uni Darmstadt, found the article [*Has80*] with the Hypothesis 1 which Puck could successfully follow.
* Beside several dissertation works, Puck's IFF model was developped in a founded research project 1994 [*R. Cuntze (project leader MAN), R. Deska, B. Szelinski, R. Jeltsch-Fricker, S. Meckbach, D. Huybrechts, J. Kopp, L. Kroll, S. Gollwitzer and R. Rackwitz*] the results of which are published under *Neue Bruchkriterien und Festigkeitsnachweise für unidirektionalen Faserkunststoffverbund unter mehrachsiger Beanspruchung – Modellbildung und Experimente* . VDI Progress Reports Series 5 Vol.506, VDI-Verlag, Düsseldorf, 1997. The investigations for this book gave valuable results for Puck's book, 1996.
* Due to the still highly established Puck IFF model Cuntze invited Puck to put his SFC into the [VDI 2014] *German Guideline, Sheet 3, Development of Fibre-Reinforced Plastic Components, Analysis*. Beuth-Verlag, 2006 (*in German and English, where Cuntze was convenor, editor and co-author*).

Basic in the development of Puck's IFF-SFC was (see [*Puc96, 02, 02b*]):

Mohr's Statement for isotropic materials:

" The strengths of a material are determined by the stresses σ_n, τ_{nt} on the fracture plane" (*the fracture plane is usually inclined with respect to the action of the external stresses*)

Paul's modification of the Mohr-Coulomb Hypothesis:

" Brittle (behaving) material will fracture in either that plane where the shear stress τ_{nt} reaches a critical value which is given by the shear resistance of a fiber-parallel plane increased by a certain amount of friction, caused by the simultaneously acting compressive stress σ_n on the n-t plane, (*Fig.Wo?? 4-3*). Or, it will fracture in that plane, where the maximum principal (tensile) stress reaches the transverse tensile strength $R_{\perp}^{\ t}$ ".

Hashin [Has80]:

The modified Mohr-Coulomb IFF approach, which Hashin did not pursue due to numerical difficulties he saw at that time as obstacles for the designer (*Puck succeeded on the Hypothesis 1*).

6.1 Puck's Mohr-based IFF model and his 3D-SFCs

Concluding: Puck's so-called Action Plane IFF Conditions 1991) base on Mohr-Coulomb and Hashin. In his interaction approach for the 3 IFF modes Puck interacted the 3 Mohr stresses σ_n, τ_{nt},

τ_{n1} on the IFF fracture plane, see *Fig.6-1*. He uses simple polynomials (*parabolic or elliptic*) to formulate a so-called master fracture body in the (σ_n , τ_{nt} , τ_{n1}) space. Thereby he assumes that a compressive σ_n cannot cause fracture on its action plane and that the stress σ_1 does not have any influence on the angle of the IFF fracture plane. The stresses on the fracture plane are decisive for fracture: A tensile stress σ_n supports the fracture, while in contrast a compressive stress makes the material 'stronger'. In other words: A compressive σ_n impedes IFF which is caused by the action plane shear stresses τ_{nt} and τ_{n1}, or – in other words - cannot cause fracture on its action plane. Fracture-responsible are only those stresses which act on a common action plane.

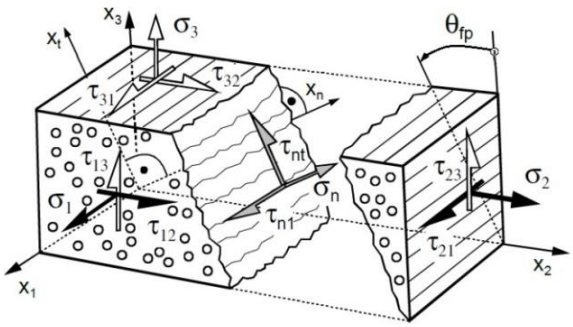

Fig.6-1, UD-composite element: Lamina and action plane stresses at an inclined failure angle θ_{fp} (from [Lut05, SAMPE])

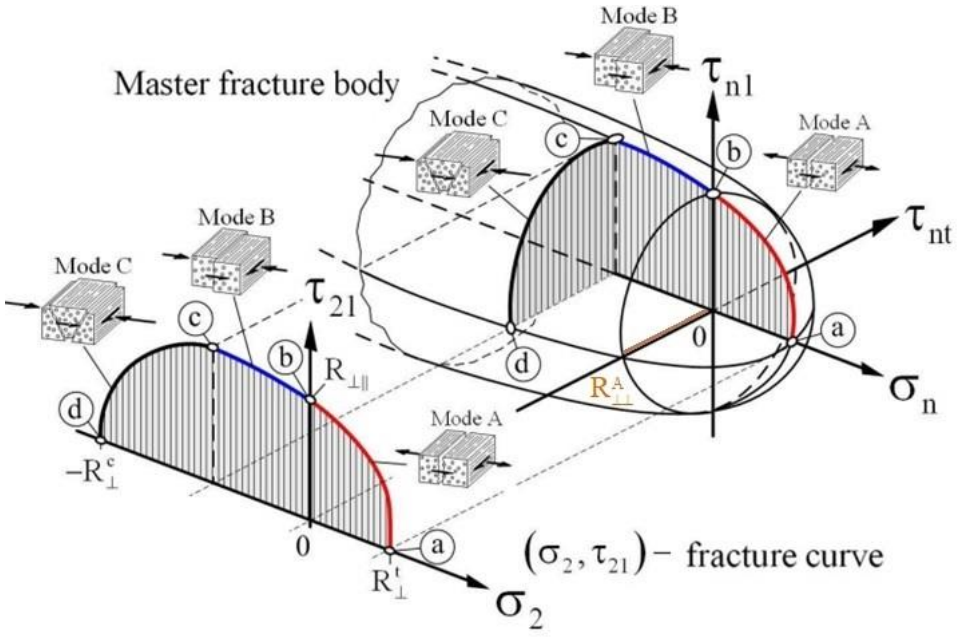

Fig.6-2: Master fracture body with Puck's IFF modes and action plane stresses (σ_n, τ_{nt}, τ_{n1}). *(left) Lamina stresses and main IFF cross section of the fracture body in lamina stresses* (σ_2, τ_{21}) *[courtesy H. Schürmann]*

The 3D Puck criteria set below identifies the many lamina failure mechanisms and quantifies the impact of each type of an IFF mode on the laminas embedded in the laminate. His 3D SFCs are collected in *Table 6-1*.

Therein, the fracture resistance R^A is defined as being that *resistance of the fiber-parallel action plane* which an action plane opposes to *its* fracture as the result of an individual uniaxial stress state by a uniaxial $\sigma_\perp^t$-stress, a pure $\tau_{\perp\perp}$-stress or a $\tau_{\perp\parallel}$-stress (*shear stress τ with its two stress components is captured*). It is to note, that the angle-dependent *action plane fracture resistance*

$\bar{R}_{\perp\perp}^{A}$ shall not be mixed up with the *strength* $\bar{R}_{\perp\perp}$! The value for $\bar{R}_{\perp\perp}^{A}$ must be calculated from the result of a transverse $\tau_{\perp\perp}$-compression test [*Puc02; Kno07*]. If fracture plane and action plane of the applied stress correspond to each other, the material strength and the fracture resistance of the action plane have the same value, see $\{\bar{R}\} = (\bar{R}_{\parallel}, \bar{R}_{\parallel\perp}^{A}, \bar{R}_{\perp}^{\tau}, \bar{R}_{\perp\parallel}^{A}, \bar{R}_{\perp}^{A}; \bar{R}_{\parallel}, \bar{R}_{\perp}^{A})$

The variables $p_{\perp\perp}^{t}$ and $p_{\perp\parallel}^{c}$ are termed inclination parameters, see <u>*Fig.6.4*</u> [*Puc02b*].

The master fracture body (σ_n, τ_{nt}, τ_{n1}) governs the strength against brittle IFF caused by any combination of stresses (σ_2, σ_3, τ_{23}, τ_{31}, τ_{21}). The body is open towards negative σ_n, because compressive σ_n cannot cause fracture on its action plane.

The usual presentation of the σ_2 (τ_{21})-IFF curve, [*Lut13*], is still depicted at the left of *Fig.3-3*.

Table 6-1: Puck's three 3D IFF SFCs with his FF1, FF2

In literature, IFF modifications of 'Puck' can be found, which usually serve for mathematical simplification.

FF1, $\sigma_1 > 0$: $\left(\frac{\sigma_1}{\bar{R}_{\parallel}^{t}}\right)^2$; FF2, $\sigma_1 < 0$: $\left(\frac{-\sigma_1}{\bar{R}_{\parallel}^{c}}\right)^2 = 1$, (maximum stress criteria)

and due to the IFF hypotheses, two different eqations are provided [*Puc* 96, *p.*118]

IFF: $\sigma_n > 0$: $\varepsilon = \left(\frac{\tau_{nt}}{\bar{R}_{\perp\perp}^{A}}\right)^2 + \left(\frac{\tau_{n\ell}}{\bar{R}_{\perp\parallel}^{A}}\right)^2 + \left(\frac{\sigma_n}{\bar{R}_{\perp}^{A}}\right)^2 = 1,$

IFF: $\sigma_n < 0$: $\varepsilon = \left(\frac{\tau_{nt}}{\bar{R}_{\perp\perp}^{A} - p_{\perp\perp}^{c} \cdot \sigma_n}\right)^2 + \left(\frac{\tau_{n\ell}}{\bar{R}_{\perp\parallel}^{A} - p_{\perp\parallel}^{c} \cdot \sigma_n}\right)^2 = 1,$ [*Puc*96, *p.*143]

$\Rightarrow$ from originally assumed 6 material strengths now down to 5 action plane resistancies which capture all 3 sub-modes IFF1, IFF2 and IFF3, reads (brackets θ_{fp} skipped).

The following transfer relationship is to apply above ($_{fp}$ = failure plane)

$$\begin{Bmatrix} \sigma_n(\theta_{fp}) \\ \tau_n(\theta_{fp}) \\ \tau_{n\ell}(\theta_{fp}) \end{Bmatrix} = \begin{bmatrix} c^2 & s^2 & 2sc & 0 & 0 \\ -sc & sc & c^2 - s^2 & 0 & 0 \\ 0 & 0 & 0 & s & c \end{bmatrix} \cdot \begin{Bmatrix} \sigma_2 \\ \sigma_3 \\ \tau_{23} \\ \tau_{31} \\ \tau_{21} \end{Bmatrix}, \quad c = \cos\theta_{fp} \text{ and } s = \sin\theta_{fp} .$$

<u>Determination of the (IFF) action plane angle</u> θ_{fp}:

This task is performed by a search process, see <u>*Fig.6-3.*</u> For -90°< θ_{fp} < 90° the maximum, angle-dependent value of $\varepsilon_{IFF}(\theta)$ is to determine, which is given for the fracture angle θ_{fp} with the suffix $_{fp}$ for the indicating the failure plane. This means in other words: Puck's so-called 'stress exposure' f_E – the equivalent quantity to Eff – is a maximum.

There is now not anymore given a problem to carry out a numerical iterative search for the fracture plane angle as part of the designer's work.

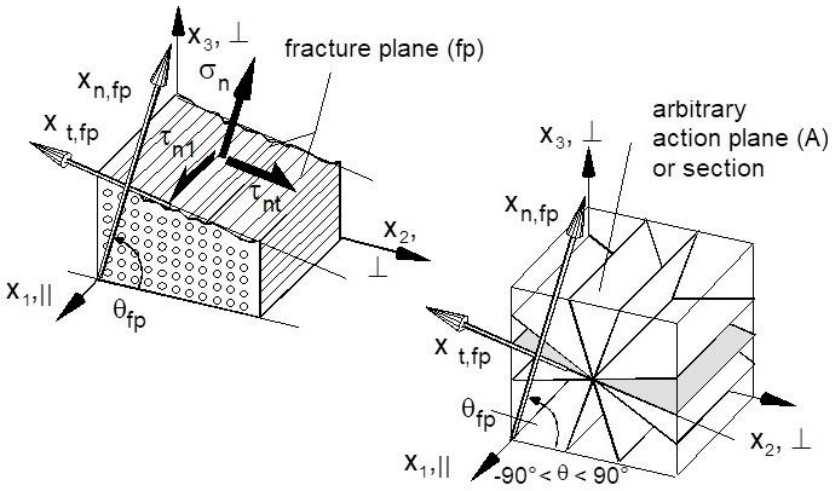

Fig. 6-3: Action plane stresses and general search of the failure plane angle [Puc96]

6.2 Puck's 2D IFF-SFCs

Fig.6-4 presents Puck's 3 IFF modes: mode A (= IFF1), mode B (≡IFF3), mode C (≡IFF2. The modes A and B lead to transversal fracture planes with $\theta_{fp} = 0$, whereas in mode C inclined planes occur $O° < \theta_{fp} < 55°$ (for CFRP).

Table 6-2: 2D-IFF [VDI2014]

Mode A (= IFF1) : $\varepsilon = \frac{1}{\bar{R}_{\perp\parallel}} \cdot \sqrt{\left(\frac{\bar{R}_{\perp\parallel}}{\bar{R}^t_{\perp}} - p^t_{\perp\parallel}\right)^2 \cdot \sigma_2^{\,2} + \tau_{21}^2} + p^t_{\perp\parallel} \cdot \sigma_2;$

Mode B (≅ IFF3) : $\varepsilon = \frac{1}{\bar{R}_{\perp\parallel}} \cdot \sqrt{p^{c\,2}_{\perp\parallel} \cdot \sigma_2^{\,2} + \tau_{21}^2} + p^c_{\perp\parallel} \cdot \sigma_2;$

Mode C (≅ IFF2) : $\varepsilon = \frac{\tau_{21}^2}{4 \cdot \left(\bar{R}_{\perp\parallel} + p^c_{\perp\parallel} \cdot \bar{R}^A_{\perp\perp}\right)^2} \cdot \frac{\bar{R}^c_{\perp}}{-\sigma_2} + \frac{-\sigma_2}{\bar{R}^c_{\perp}}$

ε is also termed f_E [*Lut*05, *VDI* 2014]

$\tau_{21}^{tp} = \bar{R}_{\perp\parallel} \cdot \sqrt{1 + 2 \cdot p^c_{\perp\perp}}$, $\sigma_2^{tp} = -\bar{R}^A_{\perp\perp}$, $\bar{R}^A_{\perp\perp} = \left[\bar{R}_{\perp\parallel} \cdot \sqrt{1 + 2 \cdot p^c_{\perp\parallel} \cdot \bar{R}^c_{\perp} / \bar{R}_{\perp\parallel}} - 1\right] / 2 \cdot p^c_{\perp\parallel}$,

* The action plane resistance $\bar{R}^A_{\perp\perp}$ depends on the chosen fracture body model such as the parabolic Mohr envelope and not just the linear Mohr approach.

* Assumption on coupling the inclination parameters: $p^c_{\perp\perp} = p^c_{\perp\parallel} \cdot \bar{R}^A_{\perp\perp} / \bar{R}_{\perp\parallel}$.

For the in-plane stress state $\tau_{21}(\sigma_2)$ which is dominant in many structural components, Puck found an analytic solution for the angle of the fracture plane [*Puc02*]:

$$\cos\theta_{fp} = \sqrt{\frac{1}{2 + 2 \cdot p^c_{\perp\perp}} \cdot \left[\left(\frac{\bar{R}^A_{\perp\perp}}{\bar{R}_{\perp\parallel}}\right)^2 \cdot \left(\frac{\tau_{21}}{\sigma_2}\right)^2 + 1\right]}.$$

Practically, 5 independent failure activing stresses are left, which would support Cuntze's 'generic' number of 5 for UD materials.

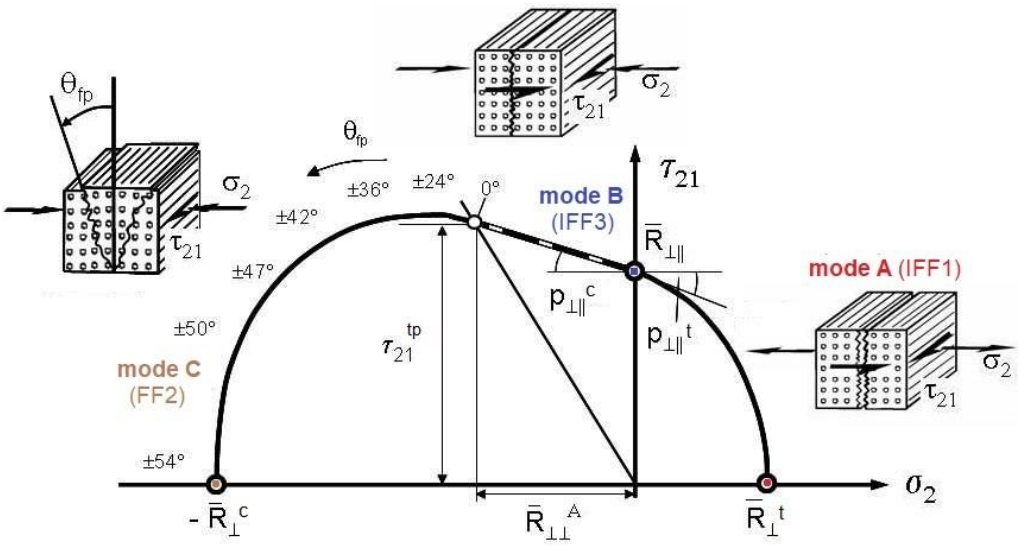

Fig. 6-4: Fracture modes of the (σ_2,τ_{21})-failure envelope; index ^{tp} marks the touchpoint between mode B and C, [Lut13, Puc96]

Interaction of IFF with the two FF

Of course, an interaction of IFF with the two FF modes is also with Puck mandatory in order to capture the combined (joint) failure danger. This procedure is documented in detail in the VDI 2014, sheet 3. Reason to do that is that experiments demonstrate micro-damage activation at the ends of broken filaments. Puck terms this 'weakening of the matrix' and uses a so-called weakening factor. Applying Cuntze's interaction equation *Eff* = 1 this is automatically performed together with an information which pure mode is design driving.

The SFC models of Puck and Cuntze are most probably those SFC models, which are best validated by 2D and 3D UD experiments.

6.3 IFF-similarities and differences Cuntze-Puck

Cuntze formulated for each pure IFF mode a criterion, namely $Eff^{\perp\sigma}$, $Eff^{\perp||}$, $Eff^{\perp\tau}$.

An *Eff*–value in a transition zone between the pure modes is to calculate by employing the interaction equation $Eff^{IFF} = [\,(Eff^{\perp\sigma})^m + (Eff^{\perp||})^m + (Eff^{\perp\tau})^m\,]^{m-1}$.

Puck formulated his Mohr-based IFF approach and thereby this formulation naturally acts like Cuntze's interaction equation, considering the IFF modes, only. The modes A, B, C are linked via the Mohr approach and therefore Puck can set fixed mode transition points, like $(\tau_{21}^{tp}, \bar{R}_{\perp\perp}^{A})$, and each mode domain can present a clear mode domain description.

Cuntze does not use different inclination angles at the shear strength point, because physically and statistically should not be a kink in the curve, practically it must be smooth. Cuntze captures smoothing in the transition zone of modes by the statistics-linked interaction exponent *m*.

Question: *What about the determination of* $\bar{R}_{\perp\perp}$ *?*

7 Unlocking the Mystery about the $\tau_{23}^{failure}$ - caused $\bar{R}_{\perp\perp}$ and $\bar{R}_{\perp\perp}{}^{A} \neq \bar{R}_{\perp\perp}$?

7.1 Linear Mohr-Coulomb curve $\tau_{nt}(\sigma_n)$, based on IFF2 mode

The full Mohr-Coulomb (M-C) shear curve $\tau_{nt}(\sigma_n)$ is the result of two commonly acting failure modes and captures the transition zone between IFF2 and IFF1. As with isotropic materials it is a bi-axial fracture stress curve. A short numerical analysis shall explain this, used are Cuntze's SFCs. With the data set $\bar{R}_{\perp}^{t} = 35\text{MPa}$, $\bar{R}_{\perp}^{c} = 104\text{MPa}$, $\mu_{\perp\perp} = 0.18$ ($\Theta_{fp}° = 51°$, $a_{\perp\perp} = 0.26$, $b_{\perp\perp} = a_{\perp\perp} + 1$) the influence exemplarily shall be quantified for $\tau_{\perp\perp} = 30\ \text{MPa}$. Replacing $\tau_{\perp\perp}$ by its components $\sigma_2 = -\sigma_3 = \tau_{\perp\perp}/\sqrt{2}$ makes the failure driving NF mode obvious through the computed two values

$$\text{IFF1: } Eff^{\perp\sigma} = [(\sigma_2 + \sigma_3) + \sqrt{\sigma_2{}^2 - 2\sigma_2 \cdot \sigma_3 + \sigma_3{}^2}]/2\bar{R}_{\perp}^{t} = 0.61,$$

$$\text{IFF2: } Eff^{\perp\tau} = [a_{\perp\perp} \cdot (\sigma_2 + \sigma_3) + b_{\perp\perp}\sqrt{\sigma_2{}^2 - 2\sigma_2\sigma_3 + \sigma_3{}^2}]/\bar{R}_{\perp}^{c} = 0.26.$$

From the resulting *Effs* is to conclude: IFF1 causes much more failure danger than the compressive mode IFF2. Therefore, in order to accurately determine $\tau_{nt}(\sigma_n)$ both the modes must be included in the derivation process of the M-C curve. In case of *brittle* materials the tensile stress component σ_2^t of $\tau_{\perp\perp}$ will be decisive for fracture due to the vector force relationship (*stresses, acting along their specific length*) $(\sqrt{2}\cdot\tau_{\perp\perp})^2 = \sigma_2^{t\,2} + \sigma_2^{c\,2} \equiv 2\cdot\sigma^2 \rightarrow \sigma = \sigma_2^t = |\sigma_3^c| = \tau_{\perp\perp}$. The stress σ_2^t impacts the resulting fracture plane angle according to its failure effort depending on the size of the *Effs*.

The necessary relationships for the derivation of the M-C curve (envelope) are collected *Table 7-1*.

Table 7-1: Relationships for the determination of the Mohr-Coulomb curve (Mohr envelope)

$$Eff^{\perp\tau} = [a_{\perp\perp}\cdot(I_2) + b_{\perp\perp}\cdot\sqrt{I_4}]/\bar{R}_{\perp}^{c} = 1 \text{ with } a_{\perp\perp} = b_{\perp\perp} - 1 \text{ after inserting } \bar{R}_{\perp}{}^{c}$$

$$= [a_{\perp\perp}\cdot(\sigma_2 + \sigma_3) + b_{\perp\perp}\cdot\sqrt{(\sigma_2 - \sigma_3)^2 + 4\tau_{23}{}^2}]/\bar{R}_{\perp}^{c} = 1$$

$$= [a_{\perp\perp}\cdot(\sigma_n + \sigma_t) + b_{\perp\perp}\cdot\sqrt{(\sigma_n - \sigma_t)^2 + 4\tau_{nt}{}^2}]/\bar{R}_{\perp}^{c} = 1 \text{ (Mohr) with}$$

$$I_2 = \sigma_n + \sigma_t = \sigma_2 + \sigma_3,\ \sigma_n - \sigma_t = C\cdot(\sigma_2 - \sigma_3) = C\cdot\eta,\ \tau_{nt} = -0.5\cdot\sqrt{1-C}\cdot\eta,\ C = \cos(2\cdot\Theta_{fp}),$$

$$\Theta_{fp} = 0.5\cdot\arccos C,\ \Theta_{fp}° = \Theta_{fp}\cdot 180°/\pi,\ c^2 = (C+1)\cdot 0.5,\ C = 2\cdot c^2 - 1$$

$$\sigma_t = s^2\cdot\sigma_2 + c^2\cdot\sigma_3,\ \sigma_n = (C+1)\cdot 0.5\cdot\sigma_2 + (1-C)\cdot 0.5\cdot\sigma_3,\ \tau_{nt} = -0.5\cdot\sqrt{1-C^2}\cdot\eta.$$

In the compression strength point $(\sigma_2 = -\bar{R}_{\perp}^{c},\ \sigma_3 = 0 \rightarrow \eta = -\bar{R}_{\perp}^{c}$ it is obtained the '*fracture angle measure*' $C \rightarrow C_{fp}{}^{c}$, $b_{\perp\perp} = 1/\left(C_{fp}{}^{c} + 1\right) \cong 1/(1-\mu_{\perp\perp})$; $a_{\perp\perp} = \mu_{\perp\perp}/(1-\mu_{\perp\perp})$ and after dissolving

$$a_{\perp\perp}\cdot(2\sigma_n + C_{fp}{}^{c}\cdot\eta) + b_{\perp\perp}\cdot\sqrt{(C_{fp}{}^{c}\cdot\eta)^2 + 4\tau_{nt}{}^2}]/\bar{R}_{\perp}^{c} = 1 \text{ the desired M-C curve reads}$$

$$\Rightarrow \tau_{nt}(\sigma_n,\ C_{fp}{}^{c}, \mu_{\perp\perp}) = \left[\sqrt{2a_{\perp\perp}\cdot\sigma_n - \bar{R}_{\perp}^{c} - C\cdot\bar{R}_{\perp}^{c}}\cdot\sqrt{2a_{\perp\perp}\cdot\sigma_n - \bar{R}_{\perp}^{c} - C\cdot\bar{R}_{\perp}^{c}}\right]/2\cdot b_{\perp\perp}.$$

This approach is an extrapolation from the compressive strength point, when estimating the so-called cohesive strength $\tau_{\perp\perp}^{failure} \equiv \bar{R}_{\perp\perp}$.

Neglecting IFF1, being the normal fracture part NF and considering just shear fracture IFF2 (a *macro-scopic SF*) leads to the M-C curve in *Fig.7-1.*

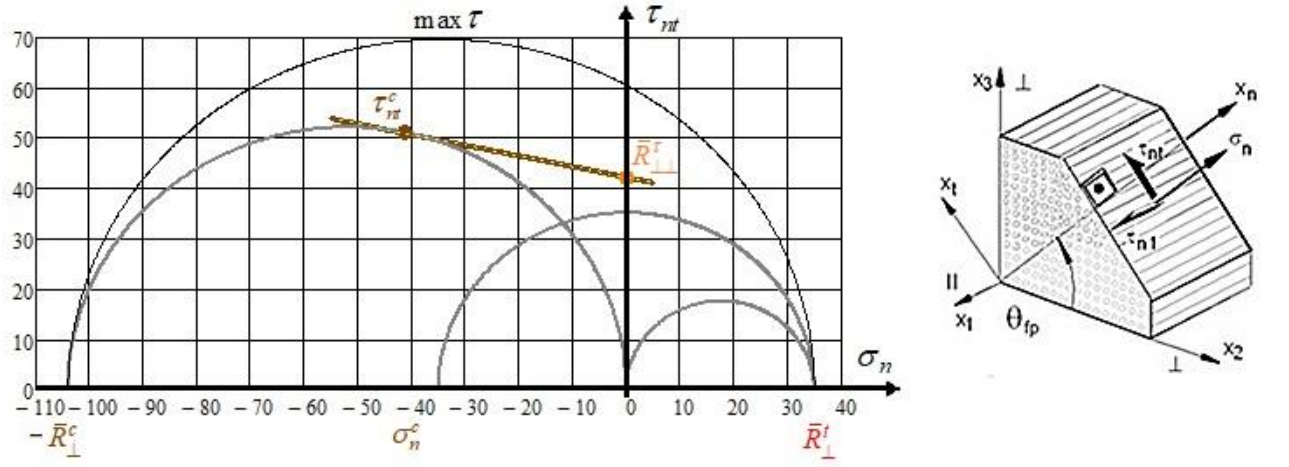

Fig. 7-1: Mohr shear curves τ_{nt} (σ_n) with its special points and the four Mohr half-circles, see Annex 1

$\bar{R}^t_{\perp} = 35\text{MPa},\ \bar{R}^c_{\perp} = 104\ \text{MPa},\ \Theta^c_{fp}{}^\circ = 51°,\ \bar{R}_{\perp\perp} = 42\ \text{MPa},\ \sigma_n{}^c = -41.3\ \text{MPa},\ \tau_{nt}{}^c = 50.9\ \text{MPa},$

$C = C^c_{fp} = \cos(2 \cdot \Theta^c_{fp}{}^\circ \cdot \pi / 180°),\ \mu_{\perp\perp} = -\tan\rho = -C^c_{fp} / S^c_{fp} = -C^c_{fp} / \sqrt{1 - C^{c\,2}_{fp}} \cong -C^c_{fp} = 0.21,$

$a_{\perp\perp} = 0.26,\ b_{\perp\perp} = a_{\perp\perp} + 1,\ \tan\phi \equiv \tan\rho$

Above curve is an extrapolation from the compressive strength point – keeping the fracture angle measure $C = C^c_{fp}$ constant. It depicts the touch point and the 'linear' Cohesive Strength point $\bar{R}^{\tau}_{\perp\perp}$ at $\sigma_n = 0$, located in the mode's transition zone. For a better orientation the four Mohr half-circles are included in *Fig.7-1*. Both the shear curves 'Linear Mohr-Coulomb' and the simple 'FMC-based equation' above – due to the definition of the friction value – are linear and equal and lie on top of another, viewing the 'brown' curve.

Touch point coordinates $\tau_{nt}{}^c, \sigma_n{}^c$:

From the transformation equations the values of the point coordinates are to determine:

$$c = \cos(\Theta^c_{fp}) = \cos(\Theta^c_{fp}{}^\circ \cdot \pi / 180^\circ)$$

$$\sigma_n = c^2 \cdot \sigma_2, \quad \tau_{nt} = -s \cdot c \cdot \sigma_2 \text{ and } \Theta^c_{fp}{}^\circ = 51°,\ \bar{R}^c_{\perp} = 104\ \text{MPa}$$

$$\sigma_n{}^c = \cos(\Theta^c_{fp})^2 \cdot (-\bar{R}^c_{\perp}) = -41.3\ \text{MPa}, \quad \tau_{nt}{}^c = -\sin(\Theta^c_{fp}) \cdot \cos(\Theta^c_{fp}) \cdot (-\bar{R}^c_{\perp}) = 50.9\ \text{MPa}.$$

Cohesive shear strength $\bar{R}^{\tau}$ (isotropic material) $\rightarrow \bar{R}_{\perp\perp}$ (transversely-isotropic UD)***:***

The next figure provides the different terms when using Mohr-Coulomb in Mechanical Engineering and in Civil engineering (*construction, being older due to geo-applications*). In construction compressive stresses were used as positive stresses and thus depicted in the graph blow *(right side of Fig.7-2*).

The Mohr-Coulomb failure criterion $\tau_n = c + \tan\phi \cdot \sigma_n$ is basically used in civil engineering, especially for soil investigations considering dams and geo-structures. Its two characteristic parameters are the cohesive strength of the material $\bar{R}_{\perp\perp} = \tau_{nt}{}^c + \mu \cdot \sigma_n{}^c$ and the friction angle. Therein $\tau_{nt}{}^c$ is the maximum shear stress the soil can take without failure under a normal compressive stress $\sigma_n{}^c$.

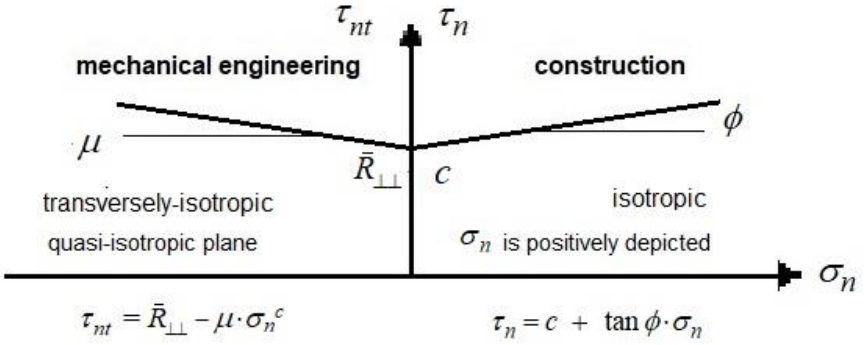

Fig. 7-2: Visualization of the isotropic linear Mohr-Coulomb SFC in construction (right) and mechanical engineering (left). Isotropic cohesion $c \equiv \bar{R}^{\tau}$ becomes $\bar{R}_{\perp\perp}$ *transversely-isotropic (quasi-isotropic plane)*

7.2 Action Plane Resistance $\bar{R}_{\perp\perp}{}^{A}$ and so-called Cohesive shear Strength $\bar{R}_{\perp\perp}$

The different approaches deliver different cohesive strengths:

* From Linear Mohr-Coulomb approach: $\bar{R}_{\perp\perp} = \tau_{nt}{}^{c} + \mu \cdot \sigma_n{}^{c} \quad \Rightarrow \bar{R}_{\perp\perp} = 42$ MPa.

* From the IFF2 equation, extrapolated: $\tau_{nt}(\sigma_n,\ C_{fp}{}^{c})\colon\ \bar{R}_{\perp\perp} = \tau_{nt}(\sigma_n = 0) = 42$ MPa.

* In *Annex1* a more realistic IFF2 mode and a non-linear τ_{nt}-curve will be derived.

Puck cites for the action plane resistance " $\bar{R}^{A}_{\perp\perp} \neq \bar{R}_{\perp\perp}$ ", and gave the formula $\bar{R}^{A}_{\perp\perp} = 0.5 \cdot \bar{R}^{c}_{\perp} / \left(1 + p^{c}_{\perp\perp}\right)$ with $0.25 < p_{\perp\perp}{}^{c} > 0.30$ for CFRP. Inserting these properties gives $\bar{R}^{A}_{\perp\perp} = 0.5 \cdot 104 / (1 + 0.275) = 41$ MPa as a value extrapolated from the compressive domain. On the other hand follows for

$$\tau_{nt}(\sigma_n = 0) \quad \Rightarrow \left(\frac{\tau_{nt}}{\bar{R}^{A}_{\perp\perp} - p_{\perp\perp}{}^{c} \cdot \sigma_n}\right)^2 + \left(\frac{\tau_{n\ell}}{\bar{R}^{A}_{\perp\parallel} - p_{\perp\parallel}{}^{c} \cdot \sigma_n}\right)^2 = 1, \quad [Puc96, p.143]$$

$$\left(\frac{\tau_{nt}}{\bar{R}^{A}_{\perp\perp} - p_{\perp\perp}{}^{c} \cdot 0}\right)^2 = 1 \ \rightarrow\ \tau_{nt} = \bar{R}^{A}_{\perp\perp}, \text{ which symbolically corresponds to } \bar{R}_{\perp\perp}$$

and which also corresponds to *Fig.6-2*, where $R^{A}_{\perp\perp}$ is found in the horizontal cross-section of Puck's Master failure body. It is the chosen Mohr model-linked quantity. Therefore for Cuntze, $\bar{R}_{\perp\perp}$ was just used as a 'model-necessary' strength parameter and not a physical strength. It vanished in the development of Puck's SFC.

Final note on shear stress τ–caused failure: For $\bar{R}_{\perp\perp}$ as well as for $\bar{R}_{\perp\parallel}$ the fracture failure basically comes from tensile stress-caused micro-mechanical stress component of the macro-scopic shear stress. The engineering view is however macro-mechanically, neglecting that shear loading always means a stressing by two stresses of opposite sign. Hence, cohesive strength is the result of joint failure danger. This shall be little more explained:

- Brittle UD material:

$R_{\perp\perp}$: 2 macro-scopic fracture modes are activated, NF and SF. Fracture primarily comes from the tensile stress component of $\tau_{\perp\perp}$, which means NF dominates

$R_{\perp\parallel}$: 1 macro-scopic fracture mode SF is activated, SF. However, 2 micro-scopic fracture modes are activated NF and SF and NF again dominates.

- Ductile isotropic material: Only 1 macro-scopic failure mode is activated, shear yielding SY, 45° shear angle ($R^t_{02} = R^c_{02}$).

Principally to be inserted into the SFCs of above three originators Tsai-Wu, Hashin and Puck is the transverse shear strength $\bar{R}_{\perp\perp}$, which represents the. $\tau_{23}^{\text{failure}}$-value. However, assuming a sixth strength in $\{\bar{R}\} = (\bar{R}^t_{\parallel}, \bar{R}^c_{\parallel}, \bar{R}^t_{\perp}, \bar{R}^c_{\perp}, \bar{R}_{\perp\parallel};\ \bar{R}_{\perp\perp})^{\mathrm{T}}$ contradicts to material symmetry which seems to demand for UD materials a 'generic' number of 5.

7.3 Non-linear Mohr-Coulomb curve, Pre-view for Annex 1

Viewing *Fig.7-3*, indicator $Eff^{\perp\sigma}$, the transversely-isotropic cohesive strength $\bar{R}_{\perp\perp}$ belongs to the transition zone of the normal fracture mode domain IFF1 and therefore not alone to the shear fracture mode domain IFF2. One cannot extrapolate from a compressive strength point.

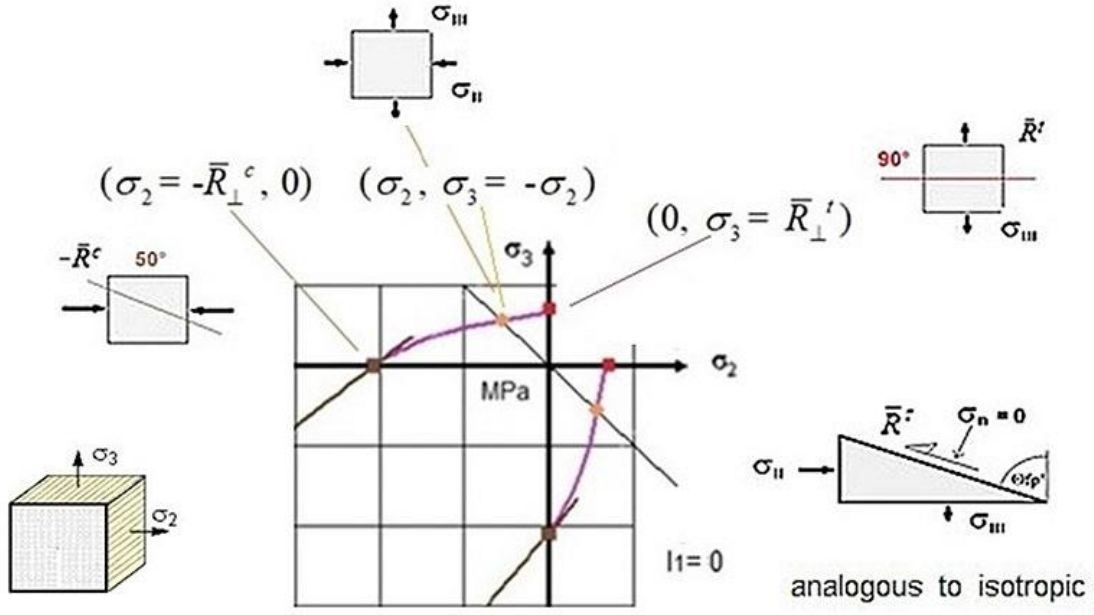

Fig. 7-3, Quasi-isotropic plane: (upper) Stress states belonging to the distinct points. (below) Linear Mohr-Coulomb *curve with a crossing point on the curve* $\sigma_3 = -\sigma_2$

Considering a non-constant $C(\sigma_n)$ leads to a non-linear M-C curve. This curve will be determined in Annex1 regarding both the modes. It is accompanied by a novel effortful derivation (*Table A1-1*) and finally the computation of $C(\sigma_n)$, (firstly performed in [*Cun22*,§7.2]), using addition theorems for a simplified working.

8 SFC-Application and Material Data Input

8.1 Comments on SFC Validity Limits

Before any application of the UD-FCs some comments shall be presented on their applicability, mainly given for UD material and especially on Cuntze's FMC-based ones:

- In case of discontinuities such as notches with steep stress decays only a *toughness + characteristic length-based energy balance condition* may form a sufficient set of two fracture conditions*[Leg02]*
- When applying test data from 'isolated lamina' test specimens (*like tensile coupons*) to an embedded lamina of a laminate one should consider that a coupon test delivers tests results of 'weakest link' type. An embedded or even an only one-sided constrained lamina, however, possesses redundant behavior
- A SFC usually describes only a one-fold occurrence of a mode or of a failure mechanism, respectively! A multiple occurrence of a mode, such as for $\sigma_I = \sigma_{II}$ or for $\sigma_2 = \sigma_{3,}$ is to be mapped by an additional term in the interaction equation *Eff* = 1
- Each failure stress state represents one point on the surface *Eff* = 100% of the failure body. This is valid for 1D- (*these represent the strength values*), for 2D- and for 3D-stress states. In the case of a multiaxial compressive stress state the load ability increases, however the (technical) strength does not increase but the risk to fracture becomes smaller, indicated by *Eff* which then becomes lower than 100 % !
- Each failure mechanism is affected by an associated typical state of stress. The failure mechanism with the highest material stressing effort will dominate the UD failure.
- The mode effort has to become zero if the mode driving stress is zero
- Not design-driving stresses of a mode might increase or decrease the material stressing effort *Eff* , which is basically sized by the design driving Eff^{mode}. This influence is considered in the equivalent mode stress

- ✓ Cuntze's SFC does not use the strength quantity $\bar{R}_{\perp\perp}$, it just employs measurable strengths
- ✓ The 5 strength and 2 friction parameters can be measured and therefore fulfil a basic design verification requirement: Strength properties shall be statistically-based, material friction properties μ are so-called physical quantities which shall be average (typical) values in order to best meet the optimum being the maximum expectation value of 50% probability
- ✓ The FFs are special fiber strain failure equations to capture filament fracture under bi-axial compression
- ✓ When mapping, then $\bar{R}$ must be used, because the average behavior is required
- ✓ Only *Eff* = 100% is equal to the SFC *F* = 1.

A reminder for the numeric procedure:

Determination of material Stressing Effort $Eff \neq 1$: $Eff = [\Sigma\,(Eff^{\text{modes}})^m]^{m-1}$,

Determination of failure curve, body $Eff = 1$: $1 = \Sigma\,(Eff^{\text{modes}})^m$.

8.2 Enabling an Automatic Insertion of 3D stress states into the FMC-based SFCs

When automatically inserting the FEA stress output $\{\sigma\}=(\sigma_1,\sigma_2,\sigma_3,\tau_{23},\tau_{13},\tau_{12})^T$ into all 5 effort equations some efforts may become negative which mechanically means zero *Eff*. In order to make an automatic use of the FMC-based fracture SFCs also in a 3D state of stresses possible and to avoid complicate queries in the computer program some specific procedures are to consider:

(1) FF, IFF: By the automatic insertion of a 3D state of stress physically incorrect negative efforts and negative equivalent stresses may occur. Then a value of 0 shall replace the negative value. A negative

$\sigma_{eq}^{\perp\tau}$ may occur in the case of a combination of a high friction parameter $a_{\perp\perp}$ with a certain state of bi-axial stressing. These are bypassed by using absolute values

FF: $Eff^{\|\sigma} = (\varepsilon_1 + |\varepsilon_1|) \cdot E_{\|} / (2 \cdot \bar{R}_{\|}^{t})$, $Eff^{\|\tau} = (-\varepsilon_1 + |\varepsilon_1|) \cdot E_{\|} / (2 \cdot \bar{R}_{\|}^{c})$, and

IFF: $\sigma_{eq}^{\perp\sigma} = (+\sigma_{eq}^{\perp\sigma} + |\sigma_{eq}^{\perp\sigma}|)/2$, $\sigma_{eq}^{\perp\tau} = (-\sigma_{eq}^{\perp\tau} + |\sigma_{eq}^{\perp\tau}|)/2$

or formalistically by taking the Macauly brackets (≡ Föppl symbols {}). They describe a discontinuous function and are defined here by $\{Eff^{mode}\} = \begin{cases} 0, & Eff^{mode} < 0 \\ Eff^{mode}, & Eff^{mode} \geq 0 \end{cases}$.

Numerical Use of the Equation of the fracture body:

$$Eff^{m} = (\{Eff^{\|\sigma}\})^{m} + (\{Eff^{\|\tau}\})^{m} + (\{Eff^{\perp\sigma}\})^{m} + (\{Eff^{\perp\|}\})^{m} + (\{Eff^{\perp\tau}\})^{m}$$

Deleting the woven brackets the total efforts reads:

$$Eff = \sqrt[m]{(Eff^{\|\sigma})^{m} + (Eff^{\|\tau})^{m} + (Eff^{\perp\sigma})^{m} + (Eff^{\perp\|})^{m} + (Eff^{\perp\tau})^{m}}$$

however, in Mathcad to be formulated for achieving a solution as

$$Eff = [(Eff^{\|\sigma})^{m} + (Eff^{\|\tau})^{m} + (Eff^{\perp\sigma})^{m} + (Eff^{\perp\|})^{m} + (Eff^{\perp\tau})^{m}]^{m^{-1}}.$$

(**2) IFF1, IFF2**: A problem is originated by the fact that a shear stress τ_{23} can be composed of a normal tensile stress and a normal compressive stress (mind: *only a shear stress can be substituted by (shear) stress components!)* which affects two failure modes but just one is significant in the case of the actual, brittle behaving UD material. Naturally in case of a brittle behaving material a tensile driving effort $Eff^{\perp\sigma}$ is caused together with a compressive effort $Eff^{\perp\tau}$. The compressive effort incorporates a smaller additional failure danger due to $R^t < R^c$. This is simply outlined via the principal stresses in the quasi-isotropic UD domain where a transformation into the two principal stresses is performed

$$\sigma_2^{pr} = 0.5 \cdot (\sigma_2 + \sigma_3) + \sqrt{(0.5 \cdot (\sigma_2 - \sigma_3))^2 + {\tau_{23}}^2}, \quad \sigma_3^{pr} = 0.5 \cdot (\sigma_2 + \sigma_3) - \sqrt{(0.5 \cdot (\sigma_2 - \sigma_3))^2 + {\tau_{23}}^2}.$$

setting $\sigma_I : 0$, if $\sigma_I \geq 0$, σ_I otherwise and $\sigma_{II} : 0$, if $\sigma_{II} \geq 0$, σ_{II} otherwise.

Then it holds for the more problematic IFF2

$$Eff^{\perp\tau} = [\ b_{\perp\perp} \cdot \sqrt{{\sigma_I}^2 - 2 \cdot \sigma_I \cdot \sigma_{II} + {\sigma_{II}}^2 + 4 \cdot 0^2} + a_{\perp\perp} \cdot (\sigma_I + \sigma_{II})\ ]\ /\ \bar{R}_{\perp}^{c}.$$

$Eff^{\perp\tau} = 1$ delivers for $\sigma_2 (\sigma_3)$ two roots and therefore two branches as can be seen in the presented *Fig.7-3* (being WWFE-II, TC 5, [*Cun12*]), for instance.

8.3 Test Data Set

As available UD material data sets are rare the provided WWFE properties are added in *Table 8-1*. For the friction value the same value could be inserted in Design Dimensioning for all materials, namely $\mu_{\perp\|} = 0.2$. As polymeric matrix applied is Epoxy EP.

Note:

Guided from another specific investigation Cuntze could sort out, that the high-performance carbon fibers, due to the graphitization-caused stiffness size - and thereby CFRP - could be divided into the three stiffness groups: Standard PAN-CFRP, UHM PAN-CFRP and mPitch-CFRP. This variety has an essential impact on the UD behavior and its wide applications.

Table 8-1: Test data sets provided in the WWFE

Fibre type	IM7	T300	A-S	S2-glass	E-Glass
Matrix	**8551-7**	**PR-319**	**Epoxy1**	**Epoxy2**	**MY750**
Fibre volume fraction V_f (%)	60	60	60	60	60
Longitudinal modulus E_1 (GPa)	*165**	*129*	*140**	*52*	*45.6*
Transverse modulus E_2 (GPa)	*8.4*	*5.6+*	*10*	*19*	*16.2*
Through-thickness modulus E_3 (GPa)	8.4	5.6+	10	19	16.2
In-plane shear modulus G_{12} (GPa)	*5.6**	*1.33+*	*6**	*6.7**	*5.83**
Transverse shear modulus G_{13} (GPa)	5.6*	1.33+	6*	6.7*	5.83*
Through-thickness shear modulus G_{23} (GPa)	2.8	1.86	3.35	6.7	5.7
Major Poisson's ratio υ_{12}	*0.34*	*0.32*	*0.3*	*0.3*	*0.28*
Major transverse Poisson's ratio υ_{13}	0.34	0.32	0.3	0.3	0.28
Through-thickness Poisson's ratio υ_{23}	*0.5*	*0.5*	*0.49*	*0.42*	*0.4*
Longitudinal tensile strength X_T (MPa)	*2560*	*1378*	*1990*	*1700*	*1280*
Longitudinal compressive strength X_C (MPa)	*1590*	*950*	*1500*	*1150*	*800*
Transverse tensile strength Y_T (MPa)	*73*	*40*	*38*	*63*	*40*
Transverse compressive strength Y_C (MPa)	*185***	*125***	*150***	*180***	*145***
Through-thickness tensile strength Z_T (MPa)	63	40	38	50	40
Through-thickness compressive strength Z_C (MPa)	185**	125**	150**	180**	145**
In-plane shear strength S_{12} (MPa)	*90***	*97***	*70***	*72***	*73***
Transverse shear strength S_{13} (MPa)	90**	97**	70**	72**	73**
Through-thickness shear strength S_{23} (MPa)	57	45	50	40	50
Longitudinal tensile failure strain ε_{1T} (%)	*1.55*	*1.07*	*1.42*	*3.27*	*2.81*
Longitudinal compressive failure strain ε_{1C} (%)	*1.1*	*0.74*	*1.2*	*2.21*	*1.75*
Transverse tensile failure strain ε_{2T} (%)	*0.87*	*0.43*	*0.38*	*0.33*	*0.246*
Transverse compressive failure strain ε_{2C} (%)	*3.2*	*2.8*	*1.6*	*1.5*	*1.2*
Transverse tensile failure strain ε_{3T} (%)	0.76	0.43	0.38	0.263	0.25
Through-thickness compressive failure strain ε_{3C} (%)	3.2	2.8	1.6	1.5	1.2
In-plane shear failure strain γ_{12u} (%)	*5*	*8.6*	*3.5*	*4*	*4*
Transverse shear failure strain γ_{13u} (%)	5	8.6	3.5	4	4
Through-thickness shear failure strain γ_{23u} (%)	2.1	1.5	1.5	0.59	0.88
Longitudinal thermal coefficient α_1 (10^{-6}/°C)	-1	-1	-1	8.6	8.6
Transverse thermal coefficient α_2 (10^{-6}/°C)	18	26	26	26.4	26.4
Through-thickness thermal coefficient α_3 (10^{-6}/°C)	18	26	26	26.4	26.4
Energy release rates G_{Ic}, G_{IIc} ($J/m^2 = 1N/m$)	200				240, 1500
mixed (fracture mechanics) mode to be assumed					
Stress free temperature (°C)	177	120	120	120	120
Test Case	TC10,11,12	TC2,3,4	TC7	TC6	TC1,5,8,9

* Initial modulus. ** Nonlinear behaviour and stress strain curves and data points are provided

\+ These values are considered to be low, compared with typical data for the same material published somewhere else or quoted by the manufacturers. We have not attempted to change them in order to facilitate a comparison with test data in Part B.

9 Conclusions and Findings

The natural differences of the depicted four 3D-SFCs can become really obvious in the 3D stress case, only!

Characteristics of the four investigated Strength Failure Criteria

A comparison of SFCs requires 3D-mappings and not just 2D ones! *Table 9-1* tries to shortly cite the basic differences together with some Pros (*for*) & Cons (*contra*).

Table 9-1: Characteristics including Pros (+) and Cons (-) of the four 3D SFCs

	Cu	T-W	Ha	Pu
fully 'global' basis with full stress interaction		*yes*		
fully 'modal' basis	*yes*			*yes*
identification of the driving IFF mode	*+, 3*		*+, 2*	*+, 3*
use of measurable material quantities, only	*yes*			*(yes)*
direct use of friction values, beside strengths	*+*			
use of the strength quantity $\bar{R}^{A}_{\perp\perp} \neq \bar{R}_{\perp\perp}$ (cohesive strength)	*no*	*yes*	*yes*	*(yes)*
strengths values, friction values by the approach	*5, 2*	*6, no*	*6, no*	*6, 2*
3D interaction of all 5 modes (2FF +3IFF)	*+, direct*		*?*	*+, additionally*
Interaction of the 3 IFF modes (Mohr model)				*yes*

Due to the present computer power the calculation effort is practically not a problem anymore.

Comments on SFC applicability limits

Principally, a SFC is a necessary but not a sufficient condition to predict failure *[Leg02,Wei15],* a fracture mechanics-based energy condition may be to fulfill, too. Even in plain (*smooth*) stress regions a SFC may be not sufficient for the prediction of 'onset of fracture', i.e. the in-situ lateral strength in an embedded lamina. Example: thick layers fail earlier than thin ones under the same 2D stress state, see the early work of [*Fla82*], because the flaw-induced micro-damage has a lower effect. Due to being strain-controlled, the material flaws in a *thin* lamina cannot grow freely up to micro-crack size in the thickness direction (*this is sometimes called 'thin layer effect'*), because the neighboring laminas act as micro-crack-stoppers. Considering fracture mechanics, the strain energy release rate G_{Ic} (*energy, dissipated during the fracture process of a newly created fracture surface area),* responsible for the development of damage in the 90° plies from flaws into micro-cracks and larger cracks, increases with increasing ply thickness. Therefore, the actual absolute thickness of a lamina in a laminate is a driving parameter for initiation or onset of micro-cracks. Investigations on the more expensive but better performing thin layer laminates are present works.

Conclusions on FMC-based Design

The more than 50 year's old Tsai-Wu 'global' SFC shall not to be assessed here, just conclusions on the author's half that old FMC-based 'modal' SFC set shall be listed:

- The FMC is a material symmetry-driven, invariant-linked basis to optimally generate SFCs like 'Mises', who was the author's inspiring invariant idol, about 1993,
- The FMC-based criteria are provided for brittle materials. These can be defined in the case of isotropic materials by $R^c / R^t > 3$ and for UD materials by $R^c_{\perp} / R^t_{\perp} > \approx 2$, because these materials usually suffer from more flaws than isotropic ones

- The invariant-based 3D-SFC set (*transfer between coordinate systems is automatically given by using invariants)* and is physically-based due to the choice of solid-behavior associated invariants together with material-symmetry. If the material element experiences effects like a volume change, a shape change and friction, then, a successful demonstration of the advantageous use of the 'physics-based' invariants can be given because the applied invariants are linked to these effects
- FMC-based 'modal' SFCs are simple but describe physics of each separately mapped failure mechanism of different material families pretty well, [*Cun22,Cun17*]. They deliver a combined formulation of independent modal failure modes, without facing the shortcomings of 'global' SFC formulations, which mathematically combine *in-dependent* failure modes
- The determination of model parameters is to perform by mapping test data in each pure failure domain, and of the interaction exponent *m* by mapping the transition zone between modes. A good guess is $m = 2.6$ for all mode transition domains and all material families isotropic, transversely-isotropic and orthotropic
- The experience of the author proves: Similarly behaving materials possess the same shape of a fracture body and the same failure function *F* can be used, or *Eff* respectively
  - The use of the entity *Eff* excellently supports 'understanding the multi-axial strength capacity of materials'. 3D-compression stress states have a higher bearing capacity, but the value of *Eff* nevertheless remains at 100%. This has nothing to do with an increase of a (uniaxial) technical strength *R* which is the result of a standard-fixed, welcomed common agreement that offers the chance to compare material properties! Test experience with isotropic materials recommend to transfer these findings to the quasi-isotropic plane of the UD-material, $\sigma_3(\sigma_2)$
- The size of each Eff^{mode} informs the designing engineer about the failure importance of a mode
- Clear equivalent stresses can be calculated for the presented modal SFCs. In this context, one should remember: Unfortunately in general, equivalent stresses are differently defined in 'global' SFCs which causes confusion and does not give a hint which mode is the critical one for a probably necessary redesign
- A usual SFC just describes a 1-fold occurring failure mode or mechanism! A multi-fold occurrence of the same failure mode with its joint probabilistic failure effect must be additionally considered in each formulated 'modal' SFC or 'global' SFC. *Question: Which of the popular SFCs takes care of this effect?*
- Effective lamina strengths depend on ply-'thinness' and stress rate. Beyond IFF the embedded ply, strain-controlled by the vicinity, still contributes to the strength and stiffness capacity
- Switching between material families generally improves material understanding.

In the context of conclusions one must always keep in mind:

"Test results can be far away from the reality like an inaccurate theoretical model. Theory creates a model of the reality, one experiment shows one realization of the reality".

REFERENCES

[Awa78] Awaji H and Sato S: *A Statistical Theory for the Fracture of Brittle Solids under Multiaxial Stresses.* Int. J. of Fracture, 14 (1978), R 13-16

[Boe87] Boehler J P : *Introduction to the invariant formulation of anisotropic constitutive equations*. 1987. In: Boehler J.P. (Ed.) *Applications of Tensor Functions in Solid Mechanics*. CISM Course no.292. Springer-Verlag. In addition a personal note from J. Boehler (1985) on UD invariants which were later applied by the author in his FMC

[Chr98] Christensen R M: *The Numbers of Elastic Properties and Failure Parameters for Fiber Composites*. Transactions of the ASME, Vol. 120 (1998), 110-113

[Cun04] Cuntze R: *The Predictive Capability of Failure Mode Concept-based Strength Criteria for Multidirectional Laminates*. Part B, Composites Science and Technology 63 (2004), 487-516

[Cun06] Cuntze R: *Failure Conditions for Isotropic Materials, Unidirectional Composites, Woven Fabrics - their Visualization and Links*. https://www.ndt.net › cdcm2006 › papers › cuntze, PDF

[Cun12] Cuntze R: *The predictive capability of Failure Mode Concept-based Strength Conditions for Laminates composed of UD Laminas under Static Tri-axial Stress States*. WWFE-II, Part A, Journal of Composite Materials 46 (2012), 2563-2594

[Cun13] Cuntze R: *Comparison between Experimental and Theoretical Results using Cuntze's Failure Mode Concept model for Composites under Tri-axial Loadings – Part B of the WWFE-II*. Journal of Composite Materials", Vol.47 (2013), 893-924

[Cun17] Cuntze R: *Fracture Failure Bodies of Porous Concrete (foam-like), Normal Concrete, Ultra-High-Performance-Concrete and of the Lamella - generated on basis of Cuntze's Failure-Mode-Concept (FMC*). NWC2017, June 11-14, NAFEMS, Stockholm

[Cun19] Cuntze R: *Technical terms for composite components in civil engineering and mechanical engineering*. Fachbegriffe mit Erklärung und Definition. In: Fachbegriffe für Kompositbauteile – Technical terms for composite parts. 171 pages, Springer Vieweg, Wiesbaden (2019)

[Cun22] Cuntze T: *Life-Work Cuntze - a compilation.* > 750 pages, Draft December 2022, permanent downloading address from January 2023 on: Carbon Connected | Prof. Ralf Cuntze (carbon-connected.de)

[Cun23] Cuntze R: *Design of Composites using Failure-Mode-Concept-based tools - from Failure Model Validation to Design Verification*. Mechanics of Composite Materials, Vol. 59, No. 2, May, 2023, pp. 263-282

[Fla82] Flaggs D L and Kural, MH: *Experimental Determination of the In Situ Transverse Lamina Strength in Graphite Epoxy Laminates*. J. Comp. Mat. Vol 16 (1982), 103-116

[Har93b] Hart-Smith L J: *An Inherent Fallacy in Composite Interaction Failure Curves*. Designers Corner, Composites 24 (1993), 523-524 [Has80] Hashin Z: *Failure Criteria for Unidirectional Fiber Composites*. J. of Appl. Mech. 47 (1980), 329-334

[Has80] Hashin Z: *Failure Criteria for Unidirectional Fiber Composites*. J. of Appl. Mech. 47 (1980), 329-334

[Hin02] Hinton M J , Kaddour A S and P.D. Soden P D: *A comparison of the predictive capabilities of current failure theories for composite laminates, judged against experimental* ***evidence*** (it would have been very nice). Composites Science and Technology 2002 (62), 1725-97

[HSB] (luftfahrttechnisches) Handbuch für Strukturberechnung (German aerospace handbook). Edited by the industrial committee (*working group*!) IASB = IndustrieAusschuss für StrukturBerechnung

[Huy02] Huybrechts D, Cuntze R, Druwen S and Lutz G.: *VDI-Richtlinie 2014, Blatt3, Berechnungen*. SAMPE 2002

[Kad13] Kaddour A S and Hinton M: *Maturity of 3D failure criteria for fiber-reinforced composites: Comparison between theories and experiments*. Part B of WWFE-II, J. Compos. Mater. 47 (6-7) (2013) 925–966

[Kap22] Kappel E: *Unique Manufacturing Opportunity*. Chapter 3 in [Tsa22]

[Kap23] Kappel E and Cuntze R: *Designing Laminates with In-plane 2D-Strength Design 'Master' Sheets applying the Tsai-Wu UD Strength Fracture Criterion and Cuntze's*. (in progress)

[Kno03] Knops M.: *Sukzessives Bruchgeschehen in Faserverbundlaminaten*. Diss. 2003. Aachen, Institut für Kunststoffverarbeitung

[Kno07] Knops M: *The Puck theory of failure in fiber polymer laminates: Fundamentals, verification, and applications*. Springer-Verlag, Berlin Heidelberg New York, 2007

[Leg 02] Leguillon D: *Strength or Toughness? –A criterion for crack onset at a notch*. Europ. J. of Mechanics A/Solids 21 (2002), 61 – 72 end. Ist. D. sci. Lett., Cl. Mat. Nat.18, 705-714 (1885

[Lut06] Lutz G: *The Puck theory of failure in laminates in the context of the new guideline VDI 2014, Part 3*. NDT.net https://www.ndt.net › cdcm2006 › papers › lutzii, PDF

[Lut13] Lutz G: *Highlights of the updated version of Part 3 of VDI Guideline (Development of Fibre-Reinforced Plastics components, Analysis*. htpps://www.ndt.net/?id=4169

[Pet15] Petersen E, Cuntze R and Huehne C: *Experimental Determination of Material Parameters in Cuntze's Failure-Mode-Concept-based UD Strength Failure Conditions*. Composite Science and Technology 134, (2016), 12-25

[Puc96] Puck A: *Festigkeitsanalyse von Faser-Matrix-Laminaten - Modelle für die Praxis*: München, Carl Hanser Verlag, 1996

[Puc02b] Puck A, Knops M and Kopp J: *Guidelines for the determination of the parameters in Puck's action plane strength criterion*. Comp. Science and Technology 62 (3) (2002) 371–378

[Puc02] Puck A and Schuermann H: *Failure Analysis of FRP Laminates by Means of Physically based Phenomenological Models*. Composites Science and Technology 62 (2002), 1633-1662

[Tsa71] Tsai S W and Wu E M: *A General Theory of Strength for An-isotropic Materials*. Journal Comp. Materials 5 (1971), 58-80

[Tsa22] Tsai S W: *DOUBLE-DOUBLE –a New Perspective in the Manufacture and Design of Composites*. Department of Aeronautics & Astronautics, Stanford University. 2022 by Composites Design Group

[VDI97] Cuntze R et al. (R. Cuntze (*project leader*), R. Deska, B. Szelinski, R. Jeltsch-Fricker, S. Meckbach, D. Huybrechts, J. Kopp, L. Kroll, S. Gollwitzer and R. Rackwitz): *Neue Bruchkriterien und Festigkeitsnachweise für unidirektionalen Faserkunststoffverbund unter mehrachsiger Beanspruchung – Modellbildung und Experimente* VDI Progress Reports Series 5 Vol.506, VDI-Verlag, Düsseldorf, 1997, 250 pages, (book is in *German*). (New fracture criteria - Hashin-Puck action plane criteria - and Strength Design Verifications' for Uni-directional FRPs subjected to Multi-axial States of Stress – Model development and experiments)

[VDI06] VDI 2014, *German Guideline, Sheet 3, Development of Fibre-Reinforced Plastic Components, vVDI06Analysis*. Beuth-Verlag, 2006 (in German and English, Cuntze author was convenor, editor and co-author

[Wei15] Weißgräber P, Leguillon D and Becker W: *A Review of Finite Fracture Mechanics: crack initiation at singular and non-singular stress raisers*. Arch. Appl. Mech. DOI 10.1007/s00419-015-1091-7, Springer-Verlag Berlin Heidelberg 2015

** Permanent download address: https://www.carbon-connected.de/Group/Prof.Ralf.Cuntze

Acknowledgement:

The contents of this elaboration base on the author's non-funded Failure Mode Concept.
Nevertheless some supporters shall be not forgotten:
* Further many thanks to his former colleague Bernd Szelinski for checking the manuscript as a potential user and giving valuable MathCad-application hints
* The author is very grateful to Dr. Erik Kappel for excellent comments especially regarding the Tsai-Wu criterion.
* ??

"It's one thing to have an idea, here Cuntze's FMC–based UD strength criteria set, but it's another to make it fly."

Annex 1 Derivation of $\tau_{nt}(\sigma_n)$ and of $\Theta_{fp}(\sigma_n)$ from a mapped test fracture curve $\sigma_3(\sigma_2)$

A1.1: Accuracy Problem of the envelope in the transition zone IFF2(SF)-IFF1(NF)

In this subchapter the cohesion strength $\bar{R}_{\perp\perp}$, activated by $\tau_{\perp\perp}$, in the quasi-isotropic plane of the UD material is envisaged. This quantity is located in the transition zone of the two modes IFF1 and IFF2. With isotropic materials the author learned that a transformation from UD lamina stresses into the desired formulations in Mohr stresses τ_{nt}, σ_n must be also possible. Thereby a closer look at $\bar{R}_{\perp\perp}$ and at the Mohr envelope $\tau_{nt}(\sigma_n)$ or M-C curve, respectively, as mode interaction curve will be possible as well.

The invariant-based formulation for IFF2 is a relatively simple engineering approach. It is mathematically homogeneous, which simply means that $|F| = Eff$. A practical approach can be always 'just' a compromise. Here, it is (*similar to isotropic concrete materials, investigated multi-axially compression test-based by the author in [Cun22])* a UD compromise 'on the safe Reserve Factor side'. This means: The engineering approach of above $Eff^{\perp\tau}$ (SF) is not problematic for Design Verification, because $Eff = 1$ delivers conservative *RF*-values in the transition zones, since the curve runs more internally due to the generally minimum choice of the interaction exponent *m*.

Focus here is the derivation of $\tau_{nt}(\sigma_n)$ and of $\Theta_{fp}(\sigma_n)$ from a measured fracture curve $\sigma_3(\sigma_2)$ still displayed in *Fig.7-3* and its course in the 2nd quadrant of $\sigma_3(\sigma_2)$ which represents an identical basis of the M-C curve $\tau_{nt}(\sigma_n)$. In <u>*Table A1-1*</u> all relations, necessary for the transformation are compiled and formulas for the searched entities τ_{nt}, σ_n, $\Theta_{fp}°$ are presented. After transformation of the UD lamina (layer) stresses σ_2, σ_3, τ_{23} in the quasi-isotropic plane into the principal stresses σ^{pr} (*index pr means principal*), the shear stress τ_{23} vanishes. Therefore, with no loss of generality σ^{pr} can be simpler written in the further text, back again as plain letter σ, but thinking they might be principal stresses. The transformation of the lamina stresses into Mohr stresses more practically works via addition theorems such as $C(\Theta_{fp}°) = c^2\text{-}s^2$, being the fracture angle measure.

As the author still found with isotropic materials, the interaction considering magenta curve (thinly-marked) in <u>*Fig.A1-1*</u> cannot accurately map the course of test data. The **bold**-marked curve is physically more accurate and to model.

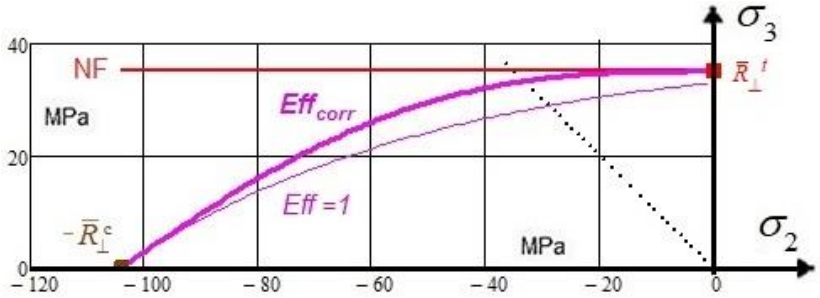

Fig.A1-1: Interaction curve $\sigma_3^{\text{fracture}}(\sigma_2)$ *from Eff = 1. Numerical example stems from a measurement of the fracture plane angle* $\Theta_{fp}°$ *in [VDI97].*

$$Eff = [(Eff^{\perp\sigma})^m + (Eff^{\perp\tau})^m]^{m-1}$$

$$\text{IFF1: } Eff^{\perp\sigma} = [(\sigma_2 + \sigma_3) + \sqrt{\sigma_2^2 - 2\sigma_2 \cdot \sigma_3 + \sigma_3^2}] / 2\bar{R}_{\perp}^{t},$$

$$\text{IFF2: } Eff^{\perp\tau} = [a_{\perp\perp} \cdot (\sigma_2 + \sigma_3) + b_{\perp\perp}\sqrt{\sigma_2^2 - 2\sigma_2\sigma_3 + \sigma_3^2}] / \bar{R}_{\perp}^{c}.$$

Table A1-1: Derivation of $\tau_{nt}(\sigma_n)$, $\Theta_{fp}°$ *from a measured fracture curve* $\sigma_3(\sigma_2)$

$SF:\ Eff^{\perp\tau} = [a_{\perp\perp}\cdot(I_2) + b_{\perp\perp}\cdot\sqrt{I_4}]\ /\ \bar{R}_{\perp}^{c} = 1$

$= [a_{\perp\perp}\cdot(\sigma_2{}^{pr}+\sigma_3{}^{pr}) + b_{\perp\perp}\cdot\sqrt{(\sigma_2{}^{pr}-\sigma_3{}^{pr})^2+0^2}]\ /\ \bar{R}_{\perp}^{c} = 1$ (lamina stresses)

$\equiv [a_{\perp\perp}\cdot(\sigma_n+\sigma_t) + b_{\perp\perp}\cdot\sqrt{(\sigma_n-\sigma_t)^2+4\tau_{nt}{}^2}]\ /\ \bar{R}_{\perp}^{c} = 1$ (in Mohr stresses)

$NF:\ Eff^{\perp\sigma} = (\sigma_2{}^{pr}+\sigma_3{}^{pr}) + \sqrt{(\sigma_2{}^{pr}-\sigma_3{}^{pr})^2+0^2}]\ /\ 2\cdot\bar{R}_{\perp}^{t} = 1$

$\equiv [(\sigma_n+\sigma_t) + \sqrt{(\sigma_n-\sigma_t)^2+4\tau_{nt}{}^2}]\ /\ 2\cdot\bar{R}_{\perp}^{t} = 1.$

Known: $\sigma_2{}^{pr}$, $\sigma_3{}^{pr}$. Searched is: σ_n, τ_{nt}, Θ_{fp} with $C = \cos(2\cdot\Theta_{fp}°\cdot\pi/180°)$

Two quantities are known and one quantity is to determine.

Use of addition theorems, $\sigma_\lambda = 0$. For lamina stresses ^{pr} now dropped for simplification

$\sigma_n-\sigma_t = c^2\cdot(\sigma_2-\sigma_3) - s^2\cdot(\sigma_2-\sigma_3) = C\cdot(\sigma_2-\sigma_3),\ \ S = \sqrt{1-C^2}$

$\sigma_t = \sigma_n - C\cdot(\sigma_2-\sigma_3),\ C = c^2-s^2 = 2c^2-1 = 1-2s^2,$

$\sigma_n+\sigma_t = \sigma_2+\sigma_3,\ \ \tau_{nt} = -0.5\cdot S\cdot(\sigma_2-\sigma_3) = -0.5\cdot\sqrt{1-C^2}\cdot(\sigma_2-\sigma_3)$

Fracture (interaction) equation ≡ mathematical equation of the fracture body

$Eff = [(Eff^{NF})^m + (Eff^{SF})^m]^{m^{-1}}$ *or* computationally simpler

$(Eff^{NF})^m + (Eff^{SF})^m = 1 = 100\%$ total effort.

Differentiation of structural stresses-linked Mohr stresses delivers

$\frac{d\tau_{nt}}{d\sigma_n} = \frac{(s^2-c^2)\cdot(\sigma_2-\sigma_3)}{-2\cdot s\cdot c\cdot(\sigma_2-\sigma_3)} = \frac{C}{S}$, valid *uni* - and *bi* - *axia*l (like isotropic!)

Missing equation from differentiation of the interaction equation (σ_t to insert before)

$\{[(\sigma_n+\sigma_n-C\cdot(\sigma_2-\sigma_3)) + \sqrt{(\sigma_n-\sigma_n-C\cdot(\sigma_2-\sigma_3))^2+4\tau_{nt}{}^2}]\ /\ 2\cdot\bar{R}_{\perp}^{t}\}^m +$

$+\{[a_{\perp\perp}\cdot(\sigma_n+\sigma_n-C\cdot(\sigma_2-\sigma_3)) +$

$+ b_{\perp\perp}\cdot\sqrt{(\sigma_n-\sigma_n-C\cdot(\sigma_2-\sigma_3))^2+4\tau_{nt}{}^2}]\ /\ \bar{R}_{\perp}^{c}\}^m = 1.$

$d[(Eff^{NF})^m + (Eff^{SF})^m]/d\sigma_n =$

$m\cdot\{2\sigma_n - C\cdot(\sigma_2-\sigma_3) + \sqrt{(C\cdot(\sigma_2-\sigma_3))^2+4\tau_{nt}{}^2}]/2\bar{R}_{\perp}{}^{t}\}^{m-1}/\bar{R}_{\perp}{}^{t} +$

$+2a_{\perp\perp}\cdot m\cdot\{a_{\perp\perp}(2\sigma_n - C\cdot(\sigma_2-\sigma_3)) + b_{\perp\perp}\sqrt{(C\cdot(\sigma_2-\sigma_3))^2+4\tau_{nt}{}^2}]\ /\ \bar{R}_{\perp}{}^{c}\}^{m-1}/\bar{R}_{\perp}{}^{c},$

$d[(Eff^{NF})^m + (Eff^{SF})^m]/d\tau_{nt} =$

$\frac{2m\cdot\tau_{nt}\cdot\{2\sigma_n - C\cdot(\sigma_2-\sigma_3) + \sqrt{(C\cdot(\sigma_2-\sigma_3))^2+4\tau_{nt}{}^2}]/2\bar{R}_{\perp}{}^{t}\}^{m-1}}{\bar{R}_{\perp}{}^{t}\cdot\sqrt{(C\cdot(\sigma_2-\sigma_3))^2+4\tau_{nt}{}^2}} +$

$+4b_{\perp\perp}\cdot m\cdot\{a_{\perp\perp}(2\sigma_n - C\cdot(\sigma_2-\sigma_3)) + b_{\perp\perp}\sqrt{(C\cdot(\sigma_2-\sigma_3))^2+4\tau_{nt}{}^2}]\ /\ \bar{R}_{\perp}{}^{c}\}^{m-1}/\bar{R}_{\perp}{}^{c}.$

Equating the two equations and replacing Mohr stresses by structural stresses

via $\sigma_n = (C+1)\cdot0.5\cdot\sigma_2 + (1-C)\cdot0.5\cdot\sigma_3,\ \ \tau_{nt} = -0.5\cdot\sqrt{1-C^2}\cdot(\sigma_2-\sigma_3)$

yields an equation for the fracture angle measure C, m vanishes

$\frac{C(\sigma_2,\sigma_3)}{\sqrt{1-C^2}} = -[\frac{m\cdot A}{\bar{R}_{\perp}{}^{t}} + \frac{2\cdot a_{\perp\perp}\cdot m\cdot B}{\bar{R}_{\perp}{}^{c}}]/[\frac{2\cdot m\cdot A}{\bar{R}_{\perp}{}^{t}\sqrt{(\cdot\sigma_2-\sigma_3)^2}} + \frac{4\cdot b_{\perp\perp}\cdot m\cdot B\cdot\tau_{nt}}{\bar{R}_{\perp}{}^{c}\sqrt{(\cdot\sigma_2-\sigma_3)^2}}]$

$A = [\frac{\sigma_2+\sigma_3+\sqrt{(\sigma_2-\sigma_3)^2}}{2\cdot\bar{R}_{\perp}^{t}}]^{m-1},\ \ B = [\frac{a_{\perp\perp}\cdot(\sigma_2+\sigma_3)+b_{\perp\perp}\cdot\sqrt{(\sigma_2-\sigma_3)^2}}{\bar{R}_{\perp}^{c}}]^{m-1}$

and finally $\Theta_{fp}°$ and the Mohr stresses σ_n, τ_{nt}

$C = \cos(2\cdot\Theta_{fp}),\ \Theta_{fp} = 0.5\cdot\arccos C,\ \Theta_{fp}° = \Theta_{fp}\cdot 180°/\pi,$

$\sigma_n = (C+1)\cdot0.5\cdot\sigma_2 + (1-C)\cdot0.5\cdot\sigma_3,\ \ \tau_{nt} = -0.5\cdot\sqrt{1-C^2}\cdot(\sigma_2-\sigma_3).$

In more detail: *Fig A1-1* shows that with the IFF2-function the shear effort $Eff^{\perp\tau}$ cannot become zero in the M-C domain. This numerical behavior is a shortcoming in the transition zone of the 'simple' engineering FMC-based IFF2 approach. An accurate alteration of the fracture angle $\Theta_{fp}°$ and of the associated Mohr stresses τ_{nt}, σ_n is not to achieve with the mathematical course of the given 'engineering' IFF2 function or of $Eff^{\perp\tau}$, respectively. The mapping quality of the given IFF2 is not fully sufficient if the alteration of the fracture angle Θ_{fp} in the transition zone is to determine. This transition zone between a normal fracture mode domain NF and a shear fracture mode domain SF is ruled by interaction and corresponds to the bi-axially stressed M-C curve and therefore requires both the Eff-modes to be inserted into the interaction equation *Eff* = 1. Span of the investigated domain is: $(\sigma_2 = -\bar{R}_\perp^{\,c}, 0) \rightarrow (\sigma_2, \sigma_3 = -\sigma_2) \rightarrow (0, \sigma_3 = \bar{R}_\perp^{\,t})$.

In order to find an improvement it is essential to know how the pure mode efforts of the activated modes IFF1 and IFF2 change its influence along the σ_2-axis, which is depicted in <u>*Fig.A1.2*</u>. $Eff^{\perp\tau}$ firstly becomes zero at the equi-biaxial tensile 'strength' point $(\bar{R}_\perp^{\,tt}, \bar{R}_\perp^{\,tt}) < (\bar{R}_\perp^{\,t}, \bar{R}_\perp^{\,t})$. This zero point lies physically 'too late' for a more accurate revised local mode description.
An improvement is to achieve.

A1.2: Improvement of the IFF2 Criterion in the Transition Zone

The required entities τ_{nt} , σ_n , $\Theta_{fp}°$ only become accurate if a physically necessary correction of $Eff^{\perp\tau}$ is considered by using a correctively acting decay function f_{corr} . In order to implement f_{corr} one just has to replace $a_{\perp\perp}$ by $f_{corr} \cdot a_{\perp\perp}$ and $b_{\perp\perp}$ by $f_{corr} \cdot b_{\perp\perp}$. For a realistic transformation of the test curve, formulated in lamina stresses into a Mohr stress formulation, it is considered that $Eff^{\perp\tau}$ (SF) becomes physically zero when reaching the pure NF domain at $\sigma_3 = \bar{R}_\perp^{\,t}$ (see the course in <u>*Fig.A1-2*</u>):

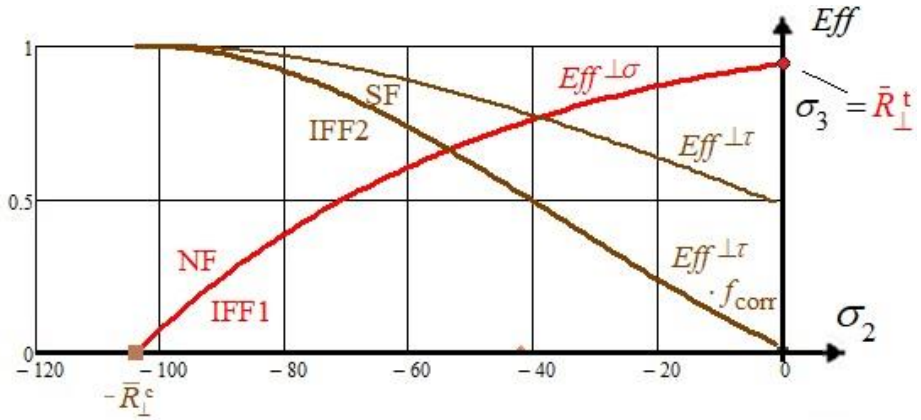

Fig.A1-2: Course of the two efforts $Eff^{\perp\sigma}$, $Eff^{\perp\tau}$ *composing the fracture stress curve Eff =1= 100%.*

$c_0 = 8.86 \cdot 10^{-5}$ *(corr is suffix for correction).*

$\bar{R}_\perp^{\,c} = 104 MPa$, $\bar{R}_\perp^{\,t} = 35$ MPa, $\Theta_{fp}° = 51°, C^c = -0.21 \leftrightarrow a_{\perp\perp} = 0.26$, $\mu_{\perp\perp} = 0.21$.

$f_{corr} = 1 + c_0 \cdot (\bar{R}_\perp^{\,c} + \sigma_2)^2$ with c_0 from inserting $(\sigma_2 = 0,\ \sigma_3 = \bar{R}_\perp^{\,t})$

IFF1: $Eff^{\perp\sigma} = [(\sigma_2 + \sigma_3) + \sqrt{\sigma_2^{\,2} - 2\sigma_2 \cdot \sigma_3 + \sigma_3^{\,2}}\,] / 2\bar{R}_\perp^{\,t}$,

IFF2: $Eff^{\perp\tau} = [a_{\perp\perp} \cdot f_{corr} \cdot (\sigma_2 + \sigma_3) + b_{\perp\perp} \cdot f_{corr} \sqrt{\sigma_2^{\,2} - 2\sigma_2\sigma_3 + \sigma_3^{\,2}}\,] / \bar{R}_\perp^{\,c}$.

Similar to the isotropic case the bi-axial stress-ruled M-C curve is oppositely dominated by two modes, IFF2 (SF) with IFF1 (NF). Therefore, attention was paid to the interaction of both these modes in the transition zone in order to finally obtain an 'accurate' fracture angle $\Theta_{fp}°$, being the pre-condition to determine the envisaged two Mohr stresses τ_{nt}, σ_n with high fidelity.

The correction changes the formula for the determination of the fracture angle measure *C* in *Table A1-1* as follows:

$$\frac{C}{\sqrt{1-C^2}} = -\left[\frac{m\cdot A}{\bar{R}_{\perp}^{\,t}} + \frac{2\cdot a_{\perp\perp}\cdot f_{corr}\cdot m\cdot B}{\bar{R}_{\perp}^{\,c}}\right] / \left[\frac{2\cdot m\cdot A}{\bar{R}_{\perp}^{\,t}\sqrt{(\cdot\sigma_2-\sigma_3)^2}} + \frac{4\cdot b_{\perp\perp}\cdot f_{corr}\cdot m\cdot B\cdot \tau_{nt}}{\bar{R}_{\perp}^{\,c}\sqrt{(\cdot\sigma_2-\sigma_3)^2}}\right],$$

$$\mathrm{B} = \left[\frac{a_{\perp\perp}\cdot(\sigma_2+\sigma_3) + b_{\perp\perp}\cdot\sqrt{(\sigma_2-\sigma_3)^2}}{\bar{R}_{\perp}^{c}}\cdot f_{corr}\right]^{m-1} \quad \text{with} \quad f_{corr} = 1 + c_0\cdot(\bar{R}_{\perp}^{c} + \sigma_2)^2 \ .$$

Therewith the desired accurate, bi-axial fracture stress M-C-curve τ_{nt} (σ_n) could be derived.

A1.3: Relations for a Transformation from a Test Fracture Curve σ_3 (σ_2) to Mohr's τ_{nt} (σ_n)

The general stress state {σ} in the material point of the lamina has to be transformed around the 1-axis to the arbitrary Mohr stress state $\{\sigma^{\theta}\} = [T_{\sigma}(\theta)]\cdot\{\sigma\}$, a fibre-parallel plane, by applying Fig.A1-3, wherein *c*: = cos θ, *s* = sin θ and *n* is normal to the 'action plane' [*Cun22*] . Values of the Mohr-parameters depend on the approach, whether it is a linear or a parabolic one.

$$\begin{matrix}\\ \rightarrow\\ \\ \rightarrow\\ \rightarrow\end{matrix}\begin{bmatrix}\sigma_1\\ \sigma_n\\ \sigma_t\\ \tau_{nt}\\ \tau_{t1}\\ \tau_{n1}\end{bmatrix} = \left\{\sigma^{\theta}\right\} = \left[T_{\sigma}(\theta)\right]\{\sigma\} = \begin{bmatrix}1 & 0 & 0 & 0 & 0 & 0\\ 0 & c^2 & s^2 & 2sc & 0 & 0\\ 0 & s^2 & c^2 & -2sc & 0 & 0\\ 0 & -sc & +sc & c^2-s^2 & 0 & 0\\ 0 & 0 & 0 & 0 & c & -s\\ 0 & 0 & 0 & 0 & +s & c\end{bmatrix}\begin{bmatrix}\sigma_1\\ \sigma_2\\ \sigma_3\\ \tau_{23}\\ \tau_{31}\\ \tau_{21}\end{bmatrix}$$

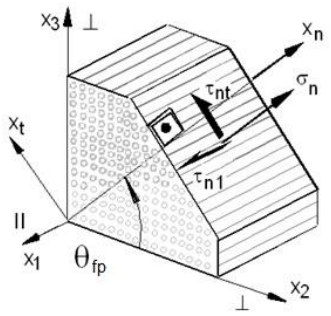

Fig. A1-3: Visualization of the transformation of lamina stresses into associated Mohr stresses. $\theta = \Theta_{fp}$ denotes the angle of the anti-clockwise transformation from the (1, 2, 3)-COS to the (1, n, t)-CoS

According to

$$\sigma_n^A(\theta) = c^2\cdot\sigma_2 + s^2\cdot\sigma_3 + 2\cdot s\cdot c\cdot\tau_{23},\ \tau_{n1}^A(\theta) = c\cdot\tau_{21} + s\cdot\tau_{31}\ ,\ \tau_{nt}^A(\theta) = -s\cdot c\cdot(\sigma_2-\sigma_3) + (c^2-s^2)\cdot\tau_{23}$$

the transformed stresses $\sigma_n(\theta)$, $\sigma_t(\theta)$, $\tau_{nt}(\theta)$ or 'Action Plane' Stresses, *Fig.A1-3, right,* in the turned CoS depend on (σ_2, σ_3, τ_{23}) only, whereas τ_{t1}, τ_{n1} is linked to (τ_{31}, τ_{21}). They are acting in the potentially physical (fracture) failure 'plane' and are decisive for fracture. In case of normal stress-induced fracture (NF) σ_n will be responsible for fracture and in case of shear stress-induced fracture τ_{nt} will be the fracture dominating one. The Mohr stress τ_{t1} has no impact but has to be considered in the derivations of the *Eff*-functions until it vanishes during the later transformation process.
Fracture plane will become that 'action plane' where *Eff*(σ(θ)) will reach the value 1 = 100% at maximum failure loading and by that where the material reserve factor f_{RF} will become a minimum.

Finally *Fig.A1-4* was obtained, presenting after an effortful MathCad programming and numerical computations as basic information:

- IFF2-IFF1- interacted fracture curve (*thin, original IFF2. From the simple approach, that does not consider* $\bar{R}_{\perp}^{tt}$ *, the curve cannot run through* $\bar{R}_{\perp}^{t}$)
- IFF2-IFF1- interacted fracture curve *(upper, bold, IFF2 decay function corrected, which better maps the course of measured fracture stress data)* and the desired
- **Course** of the fracture plane angle $\Theta_{fp}°/2$.

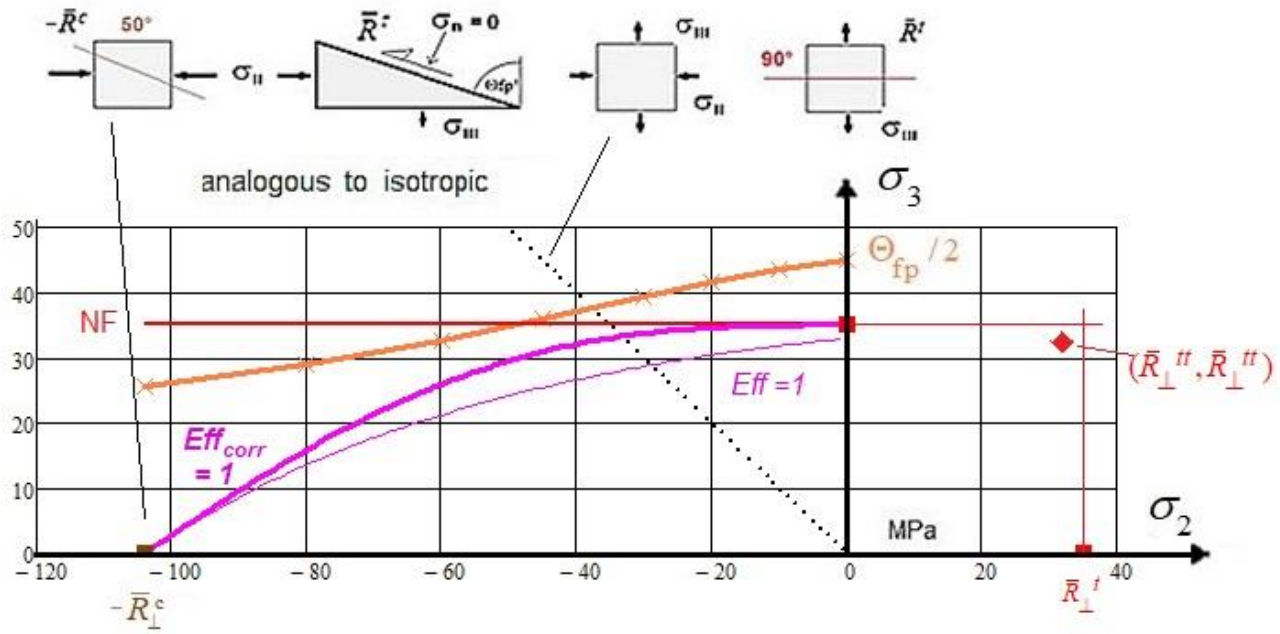

Fig. A1-4: Failure stress curve $\sigma_2(\sigma_3)$ *with alteration of fracture angle* $\Theta_{fp}°$ *in the transition zone.*

A1.4: Application of the improved function f_d *for an improved M-C curve*

The interaction curve (magenta) can be dedicated to the basic Mohr-Coulomb curve which runs from the compression strength point till the tensile strength point $\sigma_3 = \bar{R}_{\perp}^{t}$, see *Fig.A1-4* and *Fig.A1-5*.

In order to find all relationships in one diagram the Mohr stresses are also inserted as functions of the lamina stresses σ_2 (σ_3) and not of σ_n alone, which is the usual diagram form. *Fig.A1-5* includes the development of the fracture plane angle as function of the lamina stress σ_2 .

Fig.A1-5 presents all MathCad-computed Mohr entities providing:

- A straight Linear Mohr-Coulomb curve (*extrapolation*)
- IFF2-determined Mohr-Coulomb fracture curve (*IFF2-extrapolation = linear Mohr*)
- The course of the fracture plane angle $\Theta_{fp}°/2$ *(bold, decay function corrected) and*
- The full IFF2-IFF1-interacted Mohr-Coulomb fracture curve *(bold, decay function-corrected)*

The definition of the cohesive (shear) strength is $(\tau_{nt} = \bar{R}_{\perp\perp},\ \sigma_n = 0)$. Searching $\bar{R}_{\perp\perp}(C)$, a MathCad-computation, using a loop in order to continuously determine the alternating fracture plane measure C with the associate fracture angle $\Theta_{fp}°$, unfortunately did not lead to realistic values. Therefore, distinct points $(-\sigma_2, \sigma_3)$ from the measured bi-axial failure curve have been inserted into the same C-function and realistic fracture angles could be obtained then, which fully map the transition zone from 51° at the compressive strength point up to 90° at the tensile strength point.

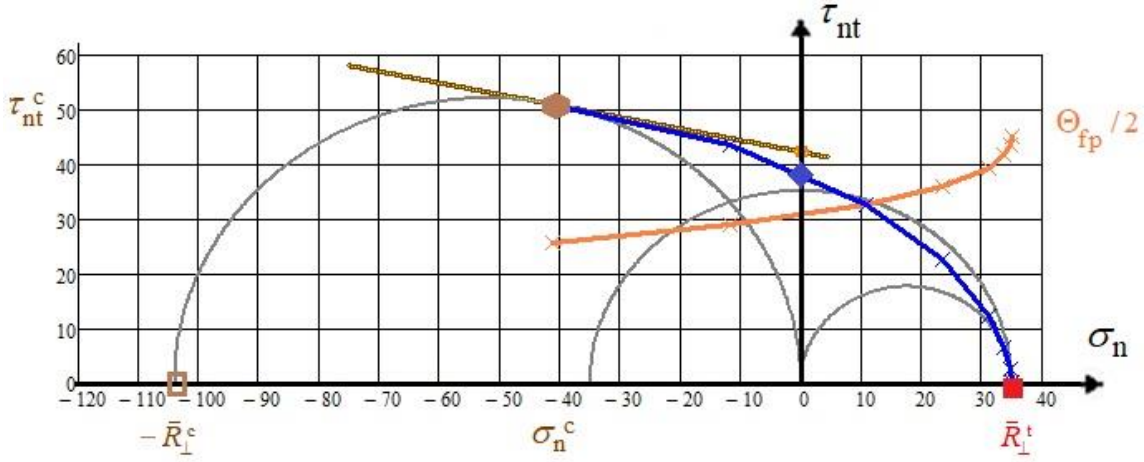

Fig.A1-5: Joint display of the UD failure curve in Mohr stresses (above) with ***fracture angle increase*** $\Theta_{fp}°$ *when approaching* $\bar{R}^t_\perp$ *and in lamina stresses (below).* ***Linear M-C*** curve. $(\bar{R}_{\perp\perp}, \sigma_n = 0)$

$\bar{R}^t_\perp = 35$ MPa, $\bar{R}^c_\perp = 104$ MPa, $\Theta^c_{fp}° = 51°$, $C = -0.21, \mu_{\perp\perp} \cong 0.21$, $\tau^c_{nt} = 50.9$ MPa, $\sigma^c_n = -41.3$ MPa, (2 modes)

* Linear extrapolation: $\bar{R}_{\perp\perp} = 42$ MPa, C= -0. 21, $\Theta_{fp}° = \Theta^c_{fp}° = 51°$, $\sigma_2 = -52$ MPa, $\sigma_3 = 34$ MPa

* Improved by f_{corr}: $\bar{R}_{\perp\perp} = 37.5$ MPa, C= -0.59, $\Theta_{fp}° = 63°$, $\sigma_2 = -73$ MPa, $\sigma_3 = 19$ MPa.

(Ductile isotropic, for comparison, single yield stress τ_{yield}: $\Theta_{fp}° = 45°$, $\sigma_2 = -\tau_{yield}$, $\sigma_3 = \tau_{yield}$ (1 mode).

Using the Mohr stress-Layer stress relations $\sigma_n = 0.5 \cdot \left[\sigma_2 \cdot (C+1) + \sigma_3 \cdot (1-C)\right]$, $\tau_{nt} = -0.5 \cdot (1-C)^2 \cdot (\sigma_2 - \sigma_3)$.

The interpretation of *Fig.A1-5* leads to the following conclusions:

- The general macro-mechanical IFF2 approach cannot offer a full accuracy of the realistically predicted Mohr-Coulomb curve. Just the *physically-based* decay function correction delivers the desired fidelity
- A SFC in lamina stresses can be transferred into a Mohr-Coulomb version
- The course of the fracture plane angle $\Theta_{fp}°$ can be determined, too
- Below the figure an interesting comparison of failure angles is depicted
- The idea of the FMC that IFF1 and IFF2 commonly add its *Eff* portions, which lead to the result that $\Theta_{fp}°$ is in the sixty degrees ° at the cohesive strength point $\bar{R}_{\perp\perp}$, with a degree value being the higher the higher the strength ratio $\bar{R}^c_\perp / \bar{R}^t_\perp$ is.
-

Analogous to the saying " *If something becomes a fact it is no science anymore*"
now here the "*Cohesive strength* $\bar{R}_{\perp\perp}$ *is no mystery anymore*".

Annex 2 Replacing fictitious Model Parameters $a_{\perp\perp}, a_{\perp\parallel}$ by measurable Friction Values μ

A2.1: Relation of Friction parameter $a_{\perp\perp}$ to Fracture angle $\Theta_{fp}{}^{c}$ and Friction value $\mu_{\perp\perp}$

The measurement of a realistic fracture angle is practically not possible, just the determination of the friction curve parameter $a_{\perp\perp}(\mu_{\perp\perp})$ by mapping the course of test data points is a practical approach. Then, from the mapped test curve the relationship curve parameter $a_{\perp\perp}$ to friction value $\mu_{\perp\perp}$ and to the fracture angle $\Theta_{fp}°$ can be derived according to the formulas in *Table A2-1*. This is to perform in the compressive strength point $\bar{R}_{\perp}{}^{c}$.

Basic assumption is the *brittle-fracture hypothesis* which goes back to O. Mohr's "*The strength of a material is determined by the Mohr stresses on the fracture plane".* This means for the Linear Mohr-Coulomb (M-C) formulation $\tau_{nt} = \bar{R}_{\perp\perp} - \mu_{\perp\perp} \cdot \sigma_n$ which includes the friction value $\mu_{\perp\perp}$ being an intrinsic property of the UD material. If IFF occurs in a parallel-to-fiber plane of the UD lamina, the components of the failure stress vector are the normal Mohr stress σ_n and the two Mohr shear stresses τ_{nt} and τ_{n1}. The shear stress τ_{tl} and the normal stress σ_t will have no influence and this is to be proven in the derivation. The Mohr stress τ_{n1} belongs to IFF3 and is not of interest, here.

Table A2-1: Relationships for the determination of the friction curve parameter $a_{\perp\perp}(\mu_{\perp\perp})$

IFF2: $F_{\perp}^{\tau} = [a_{\perp\perp} \cdot (\sigma_2 + \sigma_3) + b_{\perp\perp} \cdot \sqrt{(\sigma_2 - \sigma_3)^2 + 4\tau_{23}{}^2}\,] \,/\, \bar{R}_{\perp}^{c} = 1$, in Mohr stresses, after inserting $\bar{R}_{\perp}{}^{c}$

$= [a_{\perp\perp} \cdot (\sigma_n + \sigma_t) + b_{\perp\perp} \cdot \sqrt{(\sigma_n - \sigma_t)^2 + 4\tau_{nt}{}^2}\,] \,/\, \bar{R}_{\perp}^{c} = 1$, $a_{\perp\perp} = b_{\perp\perp} - 1$ is friction parameter

$$\frac{dF}{d\sigma_n} \cdot \bar{R}_{\perp}^{c} = a_{\perp\perp} + b_{\perp\perp} \cdot (\sigma_n - \sigma_t) / \sqrt{(\sigma_n - \sigma_t)^2 + 4\tau_{nt}{}^2}, \quad \frac{dF}{d\tau_{nt}} \cdot \bar{R}_{\perp}^{c} = 4 \cdot b_{\perp\perp} \cdot \tau_{nt} / \sqrt{(\sigma_n - \sigma_t)^2 + 4\tau_{nt}{}^2}$$

$$\frac{d\tau_{nt}}{d\sigma_n} = -\frac{dF}{d\sigma_n} / \frac{dF}{d\tau_{nt}} = -[\frac{b_{\perp\perp} \cdot (\sigma_n - \sigma_t) + (b_{\perp\perp} - 1) \cdot \sqrt{(\sigma_n - \sigma_t)^2 + 4\tau_{nt}{}^2}}{4 \cdot b_{\perp\perp} \cdot \tau_{nt}}]$$, minus implicit derivation

Stress σ_t has no influence, as Mohr assumed! Failure responsible due to Mohr

are just τ_{nt} with σ_n ! $\sigma_n - \sigma_t = C \cdot \sigma_2$, $S = \sqrt{1 - C^2}$

$$\frac{d\tau_{nt}}{d\sigma_n} = -\mu_{\perp\perp} = \frac{C}{S} = -[\frac{b_{\perp\perp} \cdot (\sigma_n - \sigma_t) + (b_{\perp\perp} - 1) \cdot \sqrt{(\sigma_n - \sigma_t)^2 + 4\tau_{nt}{}^2}}{4 \cdot b_{\perp\perp} \cdot \tau_{nt}}] =$$

$$= -[\frac{b_{\perp\perp} \cdot (C \cdot \sigma_2) + (b_{\perp\perp} - 1) \cdot \sqrt{(C \cdot \sigma_2)^2 + 4 \cdot (-0.5 \cdot S \cdot \sigma_2)^2}}{4 \cdot b_{\perp\perp} \cdot (-0.5 \cdot S \cdot \sigma_2)}]$$

$$C = -[\frac{b_{\perp\perp} \cdot (C \cdot \sigma_2) + (b_{\perp\perp} - 1) \cdot \sqrt{(C \cdot \sigma_2)^2 + 4 \cdot (-0.5 \cdot \sigma_2)^2 \cdot (1 - C^2)}}{4 \cdot b_{\perp\perp} \cdot (-0.5 \cdot \sigma_2)}]$$; $C \rightarrow C_{fp}{}^{c}$ inserting strength $\bar{R}_{\perp}{}^{c}$

$$\rightarrow C_{fp}{}^{c} = -[\frac{b_{\perp\perp} \cdot C_{fp}{}^{c} \cdot (-\bar{R}_{\perp}{}^{c}) + (b_{\perp\perp} - 1) \cdot \sqrt{C_{fp}{}^{c2} \cdot (-\bar{R}_{\perp}{}^{c})^2 + 4 \cdot (-0.5 \cdot (-\bar{R}_{\perp}{}^{c}))^2 \cdot (1 - C_{fp}{}^{c2})}}{4 \cdot b_{\perp\perp} \cdot (-0.5 \cdot (-\bar{R}_{\perp}{}^{c}))}]$$

Resolving : $b_{\perp\perp} = \frac{1}{C_{fp}{}^{c} + 1} \cong \frac{1}{1 - \mu_{\perp\perp}}$, $a_{\perp\perp} \cong \frac{\mu_{\perp\perp}}{1 - \mu_{\perp\perp}}$, $\mu_{\perp\perp} = -\frac{C}{S} = -\frac{C_{fp}{}^{c}}{S_{fp}{}^{c}} \cong -C_{fp}{}^{c}$ (if it is small value).

Assuming $\Theta_{fp}^{c}° = 51°$: *Example* $C_{fp}^{c} = \cos(\frac{2 \cdot \Theta_{fp}^{c}°}{180°} \cdot \pi) = -0.21$, $\mu_{\perp\perp} = 0.21 \cong -C_{fp}^{c}$, $a_{\perp\perp} = 0.26$.

The transformation of the IFF2 SFC in lamina stresses into Mohr stresses works via the addition theorems in *Table A.2-1*.

There are a lot of lessons learned LL, during the transformation procedure**:**

- *The Linear Mohr-Coulomb model can be employed to obtain a sufficiently good relationship for the determination of the friction value μ in the compressive strength point* $\sigma_2 = -\bar{R}_{\perp}^{c}$.
- *Establishing the relationship* $a_{\perp\perp}(\mu_{\perp\perp})$ *it is assumed that the tangent of the FMC-curve has the same value as that of the straight Linear Mohr envelope curve* $\tau_{nt}(\sigma_n)$ *in the touch point with Mohr's circle, see Fig.A2-1*
- σ_1 *is not relevant. The shear stress* τ_{23} *can be assumed zero because it would anyway vanish after a principal stress transformation. No reduction of generality is caused*
- *The stress* σ_t *has no influence! It is not representative such as Mohr supposes. Failure responsible are* τ_{nt} *and* σ_n, *only. But mind in the differentiation process: the Mohr stress* $\sigma_{\mathbf{t}}$ *cannot be simply set zero at the beginning of the derivations, it must be considered due to its relation to* σ_n,
- *Above derivation proves that, if really desired, the fracture plane angle* $\Theta_{fp}{}^{c}$ *of an UD-material could be also determined from an invariant-based SFC*
- *Viewing Fig.A2-1, it is obvious that the cohesive strength* $\bar{R}_{\perp\perp}$ at $\sigma_n = 0$ *belongs to the transition zone of the normal fracture mode domain IFF1 and therefore not alone to the shear fracture mode domain IFF2. Hence, one cannot accurately extrapolate from the compressive strength point.*

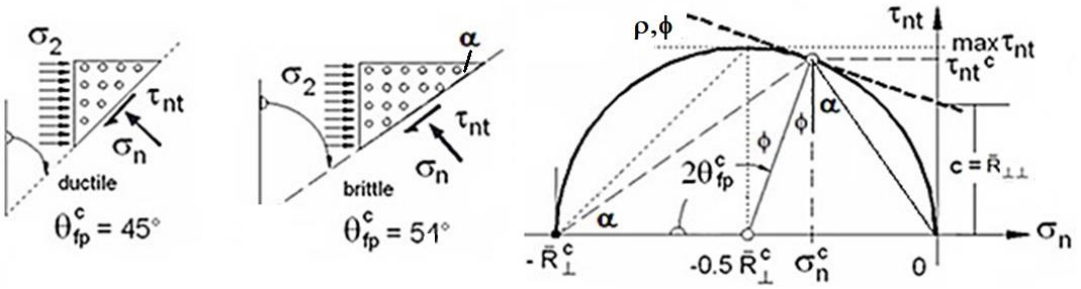

Fig.A2-1: Shear fracture plane angle in the touch point and 'linear' Mohr-Coulomb friction curve. The touch point is defined by $(\sigma_n^c, \tau_{nt}^c)$ *and linked to* $\bar{R}_{\perp}{}^{c}$

A2.3: Relation of Friction parameter Friction value $a_{\perp\parallel}(\mu_{\perp\parallel})$

The same procedure is analogously to perform for the mode IFF3, see *Table A2-2*.

Table A2-2: Relationships for the determination of friction curve parameter $a_{\perp\parallel}(\mu_{\perp\parallel})$

$$F_{\perp\parallel} = \frac{I_3^2}{\bar{R}_{\perp\parallel}^{\ 4}} + b_{\perp\parallel} \cdot \frac{I_2 \cdot I_3 - I_5}{\bar{R}_{\perp\parallel}^{\ 3}} = 1 \quad \text{with} \quad I_{23-5} = 2 \cdot \sigma_2 \cdot \tau_{21}^2 + 2 \cdot \sigma_3 \cdot \tau_{31}^2 + 4 \cdot \tau_{23}\tau_{31}\tau_{21},$$

$$I_2 = \sigma_2 + \sigma_3 \ , \ I_3 = \tau_{21}^2 + \tau_{31}^2, \ I_5 = (\sigma_2 - \sigma_3) \cdot (\tau_{31}^2 - \tau_{21}^2) - 4 \cdot \tau_{23}\tau_{31}\tau_{21}.$$

The transfer to a Mohr-shaped SFC is directly possible because the fracture plane is already known (parallel to the fibre direction) via $(\tau_{n1},\ \sigma_n) \equiv (\tau_{21},\ \sigma_2)$, $|\tau_{21}| = \bar{R}_{\perp\parallel} - \mu_{\perp\parallel} \cdot \sigma_2$

* FMC: $\frac{\tau_{21}^4}{\bar{R}_{\perp\parallel}^{\ 4}} + a_{\perp\parallel} \cdot \frac{2 \cdot \sigma_2 \cdot \tau_{21}^2}{\bar{R}_{\perp\parallel}^{\ 3}} = \frac{\tau_{nt}^2}{\bar{R}_{\perp\parallel}^{\ 4}} + a_{\perp\parallel} \cdot \frac{2 \cdot \sigma_n \cdot \tau_{nt}^2}{\bar{R}_{\perp\parallel}^{\ 3}} = 1 \ \rightarrow \sigma_n = \frac{\bar{R}_{\perp\parallel}^{\ 3} \cdot \left(\tau_{21}^4 / \bar{R}_{\perp\parallel}^{\ 4} - 1\right)}{2 \cdot \tau_{nt}^2 \cdot a_{\perp\parallel}}$

$\frac{d\tau_{n1}}{d\sigma_n} \rightarrow$ simpler to perform is $\frac{d\sigma_n}{d\tau_{n1}} = \frac{2 \cdot \tau_{21}}{\bar{R}_{\perp\parallel}^{\ 3} \cdot a_{\perp\parallel}} - \frac{\bar{R}_{\perp\parallel}^{\ 3} \cdot \left(\tau_{21}^4 / \bar{R}_{\perp\parallel}^{\ 4} - 1\right)}{\tau_{21}^3 \cdot a_{\perp\parallel}}$

* Simple linear Mohr: $\tau_{n1} = \bar{R}_{\perp\parallel} - \mu_{\perp\parallel} \cdot \sigma_n \quad \rightarrow \quad \sigma_n = \frac{\bar{R}_{\perp\parallel} - \tau_{21}}{\mu_{\perp\parallel}}$

$$\frac{d\sigma_n}{d\tau_{nt}} = \frac{-1}{\mu_{\perp\parallel}} \ .$$

In the strength point $\tau_{n1} = \bar{R}_{\perp\parallel}$ an equal slope exists and then equating delivers

$$\frac{2 \cdot \tau_{21}}{\bar{R}_{\perp\parallel}^{\ 3} \cdot b_{\perp\parallel}} - \frac{\bar{R}_{\perp\parallel}^{\ 3} \cdot \left(\tau_{21}^4 / \bar{R}_{\perp\parallel}^{\ 4} - 1\right)}{\tau_{21}^3 \cdot a_{\perp\parallel}} = \frac{-1}{\mu_{\perp\parallel}} \quad \rightarrow \quad a_{\perp\parallel} = \frac{\mu_{\perp\parallel} \cdot \left(\bar{R}_{\perp\parallel}^{\ 4} + \tau_{21}^4\right)}{\tau_{21}^3 \cdot a_{\perp\parallel}} \quad \Rightarrow a_{\perp\parallel} = 2 \cdot \mu_{\perp\parallel}.$$

A good guess for $\mu_{\perp\parallel}$ is sufficient for application.

A2-3: Evaluation of friction values $\mu_{\perp\perp}$, $\mu_{\perp\parallel}$ from test results

The determination of curve parameters *a(μ)* and thereby also of *μ* can be performed differently:

1. One strength value with one multi-axial failure stress point on the respective pure mode curves, usually applying a linear Mohr friction envelope (*sufficient*, *see Fig. A2-2 below, it requires some fitting to optimally map the course*)
2. More sophisticated fitting optimization process of the test data course in the respective pure domain (*min error square*) in 'pure' failure mode domains
3. If a Tension/Compression-Torsion test rig is not available: 1 point on the pure mode Iff2-curve plus one in the transition zone IFF2-IFF1, see *Fig.A2-3*
4. For $\mu_{\perp\perp}$, in addition: Derivation from fracture angle measurements Θ_{fp}^{c}° [*VDI97]*, facing a pretty high scatter.

The formulas for the friction values read:

- $\mu_{\perp\parallel}$:

  Linear Mohr envelope: $\mu_{\perp\parallel} \cong (\tau_{21}{}^{fr} - \bar{R}_{\perp\parallel}) / \sigma_2{}^{fr}$ from tension-compression/torsion test machine with tube test specimens, evaluating at least two curve points or if sufficient tests from curve fitting .

- $\mu_{\perp\perp}$:

  * From bi-axial compression test in order to compute the friction value from evaluating $\mu_{\perp\perp} = (R_{\perp}^{c} + \sigma_3^{fr}) / \sigma_2^{fr}$. However, the danger to buckle is to face

* If the test machine only allows a $\mu_{\perp\perp}$-test in the transition zone of the modes, *Fig.A2-3*, then, the estimation from strength point $(\sigma_3^{c\,fr}, \sigma_2^{t\,fr})$ demands for a qualified stress interaction-mapping SFC. For the evaluation the interaction equation has to be employed, shown by the following MathCad procedure:

Mathcad implicite calculation: *Vorgabe* $\mu_{\perp\perp} := 0.1$ (estimation)

$$\left(\left[(\sigma_2+\sigma_3) + \sqrt{(\sigma_2-\sigma_3)^2+0}\,\right] / 2\bar{R}_{\perp}^{t}\right)^m + \left(\left[\left(\frac{\mu_{\perp\perp}}{1-\mu_{\perp\perp}}\right)\cdot(\sigma_2+\sigma_3) + \frac{1}{1-\mu_{\perp\perp}}\sqrt{(\sigma_2-\sigma_3)^2+4\tau_{23}{}^2}\,\right] / \bar{R}_{\perp}^{c}\right)^m = 1 = Eff = 100\% \; .$$

Search *Suchen* $(\mu_{\perp\perp})$.

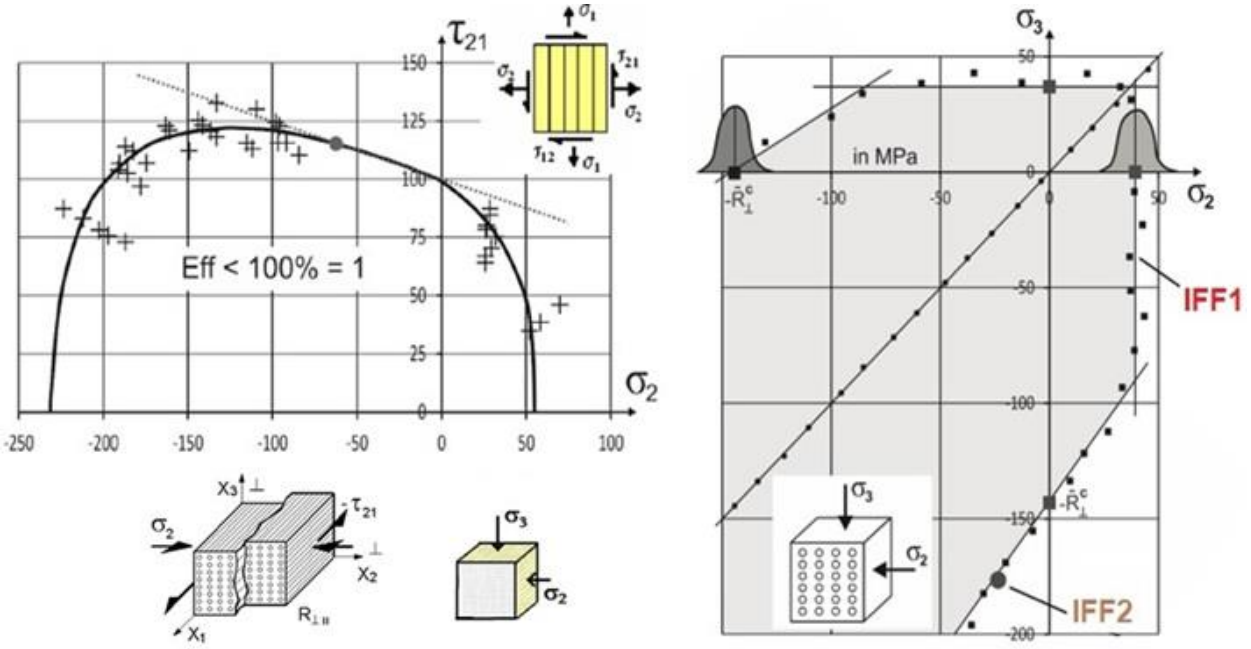

Fig.A2-2: Determination of the friction values $\mu_{\perp\perp}$, $\mu_{\perp||}$

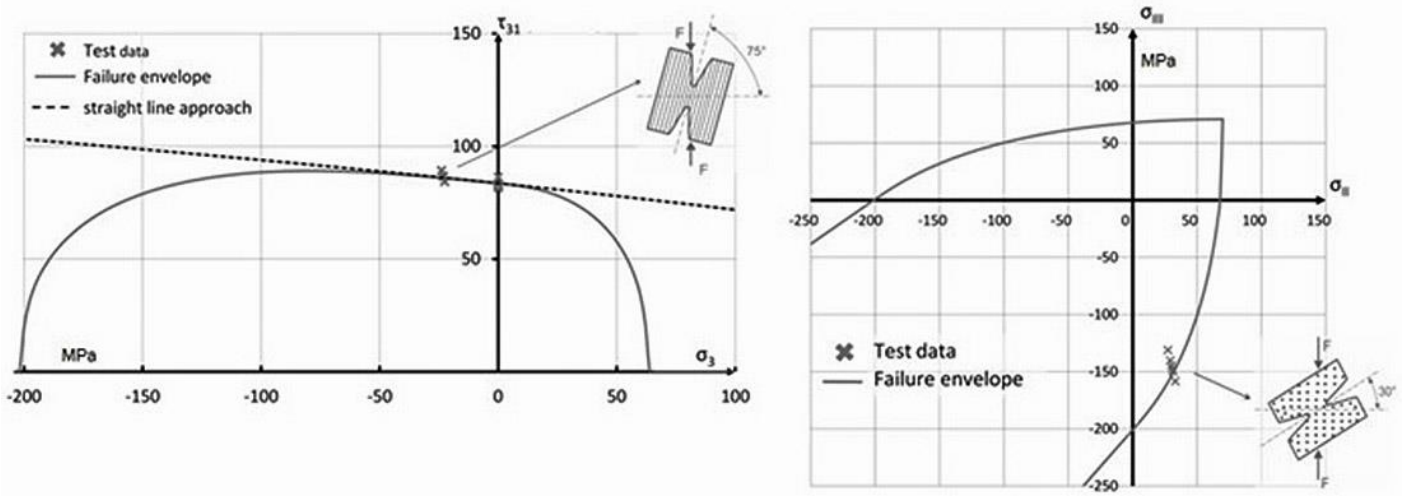

Fig.A2-3: ARCAN tests performed on distinct stress paths. UD prepreg [*Pet15*]

Annex 3 Proportional Loading Concept marking the In-plane-Difference of *Eff* to |*F*|

The Failure-Mode-Concept is dedicated to brittle materials whereas 'Mises' (Hencky-v.Mises-Huber, a modal SFC, shortly termed Mises) describes the yield behavior of ductile materials. Both the failure conditions shall be used to enlighten the difference between the absolute value of a failure function *F* and material stressing effort *Eff* of both the SFCs.

The difference is very essential in the elastic domain and thereby for Design Verification, where – *caused by the load-multiplying design safety factor j* – most of the structural components with its critical locations are to be strength-assessed.

Basis of this assessment is the usual agreement to apply the so-called Proportional Stressing (*usually termed loading, which is only equal if linear*), where all stress states alter proportionally. At first for the well-known homogeneous Mises –SFC, using $\sigma = R \cdot Eff$:

Mises' Yield Condition for ductile materials $\bar{R}_{0.2}{}^{t} \cong \bar{R}_{0.2}{}^{c} = \bar{R}_{0.2}$

$$F^{Mises} = \frac{\sqrt{3J_2}}{\bar{R}_{0.2}} = 1 \quad \leftrightarrow \quad \frac{\sqrt{3J_2}}{\bar{R}_{0.2} \cdot Eff} = 1 \quad \rightarrow \quad Eff^{Mises} = \frac{\sqrt{3J_2}}{\bar{R}_{0.2}} = \frac{\sigma_{eq}^{Mises}}{\bar{R}_{0.2}} \ .$$

Employing now the mathematically non-homogeneous Tsai-Wu-SFC 2D-Tsai-Wu, failure function *F* and |*F*| read:

$$F = \frac{\sigma_1^{\,2}}{\bar{R}_{||}^{\,t} \cdot \bar{R}_{||}^{\,c}} + \sigma_1 \cdot \left(\frac{1}{\bar{R}_{||}^{\,t}} - \frac{1}{\bar{R}_{||}^{\,c}}\right) + 2 \cdot \frac{F_{12}}{\sqrt{\bar{R}_{||}^{\,t} \cdot \bar{R}_{||}^{\,c} \cdot \bar{R}_{\perp}^{\,t} \cdot \bar{R}_{\perp}^{\,c}}} \cdot \sigma_1 \cdot \sigma_2 + \frac{\sigma_2^{\,2}}{\bar{R}_{\perp}^{\,t} \cdot \bar{R}_{\perp}^{\,c}} + \sigma_2 \cdot \left(\frac{1}{\bar{R}_{\perp}^{\,t}} - \frac{1}{\bar{R}_{\perp}^{\,c}}\right) + \frac{\tau_{12}^{\,2}}{\bar{R}_{\perp||}^{\,2}} = 1$$

$$\rightarrow \quad |F| = \frac{\sigma_1^{\,2}}{\bar{R}_{||}^{\,t} \cdot \bar{R}_{||}^{\,c}} + \sigma_1 \cdot \left(\frac{1}{\bar{R}_{||}^{\,t}} - \frac{1}{\bar{R}_{||}^{\,c}}\right) + 2 \cdot \frac{F_{12}}{\sqrt{\bar{R}_{||}^{\,t} \cdot \bar{R}_{||}^{\,c} \cdot \bar{R}_{\perp}^{\,t} \cdot \bar{R}_{\perp}^{\,c}}} \cdot \sigma_1 \cdot \sigma_2 + \frac{\sigma_2^{\,2}}{\bar{R}_{\perp}^{\,t} \cdot \bar{R}_{\perp}^{\,c}} + \sigma_2 \cdot \left(\frac{1}{\bar{R}_{\perp}^{\,t}} - \frac{1}{\bar{R}_{\perp}^{\,c}}\right) + \frac{\tau_{12}^{\,2}}{\bar{R}_{\perp||}^{\,2}} \ .$$

As next, the 2D-Tsai-Wu SFC will be formulated in the 'global' *Eff which is obviously different to* |*F*| :

$$\frac{\sigma_1^{\,2} / Eff^{\,2}}{\bar{R}_{||}^{\,t} \cdot \bar{R}_{||}^{\,c}} + \sigma_1 \cdot \left(\frac{1}{\bar{R}_{||}^{\,t}} - \frac{1}{\bar{R}_{||}^{\,c}}\right) / Eff + \frac{2F_{12}}{\sqrt{\bar{R}_{||}^{\,t} \cdot \bar{R}_{||}^{\,c} \cdot \bar{R}_{\perp}^{\,t} \cdot \bar{R}_{\perp}^{\,c}}} \cdot \sigma_1 \cdot \sigma_2 / Eff^{\,2} + \frac{\sigma_2^{\,2} / Eff^{\,2}}{\bar{R}_{\perp}^{\,t} \cdot \bar{R}_{\perp}^{\,c}} + \sigma_2 \cdot \left(\frac{1}{\bar{R}_{\perp}^{\,t}} - \frac{1}{\bar{R}_{\perp}^{\,c}}\right) / Eff + \frac{\tau_{12}^{\,2} / Eff^{\,2}}{\bar{R}_{\perp||}^{\,2}} = 1$$

Resolving for *Eff* makes a direct 2D-comparison in *Effs* of Tsai-Wu and Cuntze possible.

LL:

- *In the case of a* linear (*mathematically homogeneous*) *equation* $Eff \equiv F$.
- *FI does not correspond to Eff if the functional parts of F possess different power*.

Of interest is not only the failure envelope ($F = Eff = 1 = 100\%$) but in design analysis the values for stress states below fracture. A numerical example shall outline the differences one will face when using |*F*| as Failure Index *FI*. Just a distinct 2D-stress state will be analyzed:

$$(\sigma_1, \sigma_2, \sigma_3, \tau_{23}, \tau_{31}, \tau_{21})^{\mathrm{T}} \rightarrow \{\sigma\} = (\sigma_1, \sigma_2, 0, 0, 0, \tau_{21})^{\mathrm{T}} \mathrm{MPa},$$

$$\{\bar{R}\} = (\bar{R}_{||}^{t}, \bar{R}_{||}^{c}, \bar{R}_{\perp}^{t}, \bar{R}_{\perp}^{c}, \bar{R}_{\perp||})^{\mathrm{T}} = (2500, 1500, 35, 104, 75)^{\mathrm{T}} \mathrm{MPa},$$

$$\sigma_1 = 100 \ \mathrm{MPa}, \quad \tau_{21} = 5 \ \mathrm{MPa}, \quad m = 2.6, \quad F_{12} = -0.5.$$

For the desired comparison Cuntze's SFC are given as

$$\{\bar{R}\} = (\bar{R}_{||}^{t}, \bar{R}_{||}^{c}, \bar{R}_{\perp}^{t}, \bar{R}_{\perp}^{c}, \bar{R}_{\perp||})^{T} = (2500,1500,35,104,75)^{T}\text{MPa},\ \ \mu_{\perp||} = 0.2.$$

$$Eff = [(Eff^{||\sigma})^{m} + (Eff^{||\tau})^{m} + (Eff^{\perp\sigma})^{m} + (Eff^{\perp||})^{m} + (Eff^{\perp\tau})^{m}]^{m-1} \text{ with the mode portions}$$

$$Eff^{||\sigma} = \frac{(\sigma_1 + |\sigma_1|)}{2 \cdot R_{||}^{t}},\ Eff^{||\tau} = \frac{(-\sigma_1 + |\sigma_1|)}{2 \cdot R_{||}^{c}},\ Eff^{\perp\sigma} = \frac{\sigma_2 - |\sigma_2|}{2 \cdot \bar{R}_{\perp}^{t}},\ Eff^{\perp\tau} = \frac{-\sigma_2 + |\sigma_2|}{2 \cdot \bar{R}_{\perp}^{c}},\ Eff^{\perp||} = \frac{|\tau_{21}|}{\bar{R}_{\perp||} - \mu_{\perp||} \cdot \sigma_2}.$$

Fig.A3-1 presents three curves: (1) *FI* = |*F*|, (2) Tsai-Wu, *Eff*-transformed with proportional stressing (*corresponds to his so-called strength ratio R, a name which is unfortunately for a long timel fixed for 'Strength Ratio' R meaning compressive strength divided by tensile strength and for the 'Stress* Ratio*'* R as ratio $\min\sigma / \max\sigma$ *in fatigue*), and (3) Cuntze's SFC used as *Eff*-formulation.

Fig.A3-1 documents that for this stress state Tsai's so-called strength ratio, corresponding to *Eff*, runs on the same curve in the plot, below. The example further depicts the difference of *FI* and *Eff* .

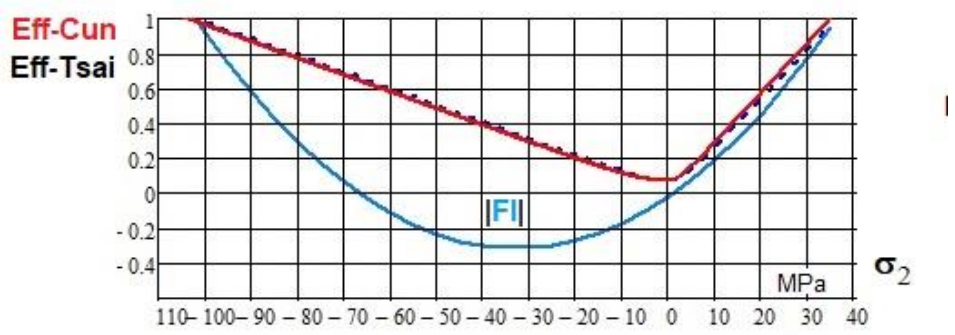

Fig.A3-1: Comparison of the course of the Effs of Tsai-Wu and Cuntze and difference to |FI|

And for a relatively high negative stress σ_1 *Fig.A3-2* outlines an increase of the differences.

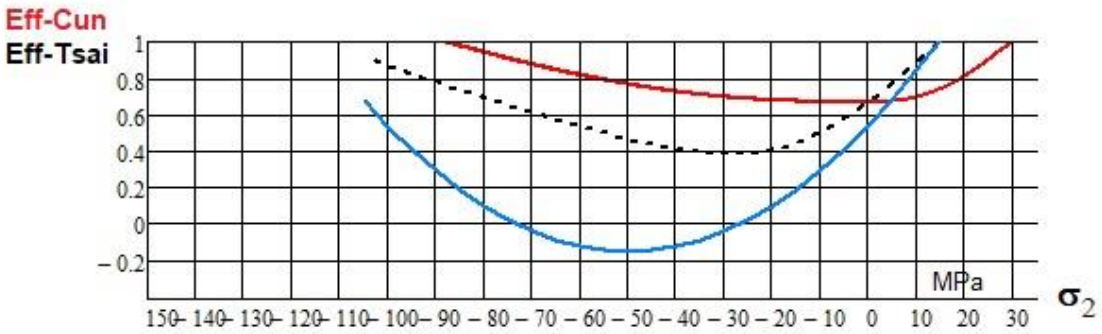

Fig.A3-2: Comparison of the course of the Effs of Tsai-Wu and Cuntze and difference to |FI| for a high fiber-parallel stress $\sigma_1 \cong V_f \cdot \sigma_f$

$$\{\sigma\} = (\sigma_1, \sigma_2, 0, 0, 0, \tau_{21})^{T}\text{MPa},\ \ \{\bar{R}\} = (2500,1500,35,104,75)^{T}\text{MPa},$$

$$\sigma_1 = -1000\ \text{MPa},\ \ \tau_{21} = 5\text{MPa},\ m = 2.6,\ F_{12} = -0.5 \text{ and } \mu_{\perp||} = 0.2.$$

In the figure collection of *Fig.A3-3* , for the properties given at the top of the plot, three detailed computation procedures have been executed. The reader is asked to draw his conclusions.

$Rpt := 2500 \quad Rpc := 1500 \quad Rst := 35 \quad Rsc := 104 \quad Rsp := 75 \quad \mu := 0.2$ average values $\sigma1 := 100 \quad \tau21 := 5$ $mint := 2.6$ $F12 := -0.5$

$$Eff(\sigma2) := \left[\left(\frac{\sigma1 + |\sigma1|}{2Rpt} \right)^{mint} + \left(\frac{-\sigma1 + |\sigma1|}{2Rpc} \right)^{mint} + \left(\frac{\sigma2 + |\sigma2|}{2Rst} \right)^{mint} + \left(\frac{-\sigma2 + |\sigma2|}{2Rsc} \right)^{mint} + \left[\frac{|\tau21|}{Rsp - \mu \cdot (\sigma2)} \right]^{mint} \right]^{-mint^{-1}}$$

Vorgabe $Eff := 0.05$

$$1 = \frac{\sigma1^2}{Rpt \cdot Rpc \cdot Eff^2} + \frac{\sigma1}{Eff} \cdot \left(\frac{1}{Rpt} - \frac{1}{Rpc} \right) + 2 \cdot \left(\frac{F12}{\sqrt{Rpt \cdot Rpc \cdot Rst \cdot Rsc}} \right) \cdot \frac{\sigma1 \cdot \sigma2}{Eff^2} + \frac{\sigma2^2}{Rst \cdot Rsc \cdot Eff^2} + \frac{\sigma2}{Eff} \cdot \left(\frac{1}{Rst} - \frac{1}{Rsc} \right) + \frac{\tau21^2}{Rsp^2 \cdot Eff^2}$$

$f(\sigma2) := Suchen(Eff) \quad j := 1..Rsc + Rst \quad \sigma2_j := j - Rsc \quad Eff_j := f(\sigma2_j)$

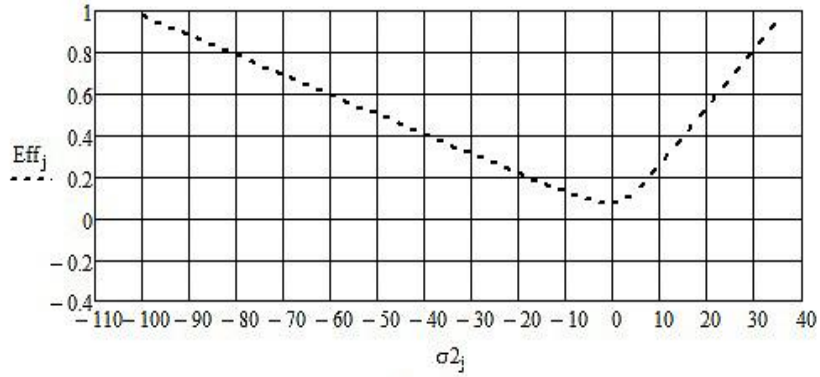

$j := 0..n \quad A := -105 \quad E := 35 \quad Ink_j := \frac{(E - A)}{n} \quad \sigma2_j := A + j \cdot Ink_j$

$$FI_j := \frac{\sigma1^2}{Rpt \cdot Rpc} + \sigma1 \cdot \left(\frac{1}{Rpt} - \frac{1}{Rpc} \right) + 2 \cdot \frac{F12}{\sqrt{Rpt \cdot Rpc \cdot Rst \cdot Rsc}} \cdot \sigma1 \cdot \sigma2_j + \frac{(\sigma2_j)^2}{Rst \cdot Rsc} + \sigma2_j \cdot \left(\frac{1}{Rst} - \frac{1}{Rsc} \right) + \frac{\tau21^2}{Rsp^2}$$

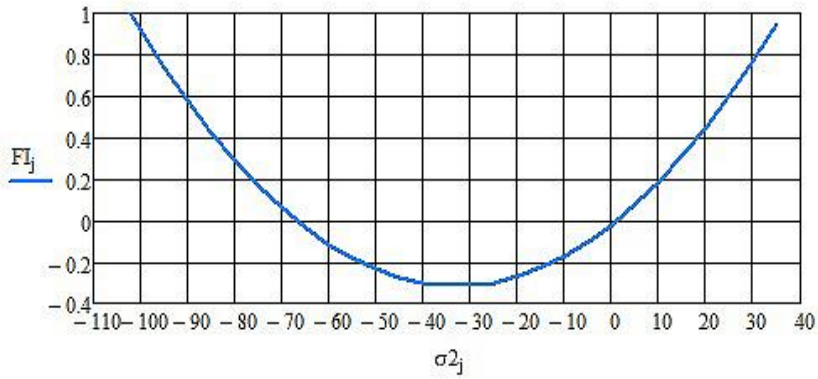

Fig.A3-3: Detailed MathCad 15 computation procedures for three applications

Note on the generally accepted Standard Procedure "Proportional Stressing Concept":

It is mandatory that the chosen *F*- or *Eff*-formulation does become zero with a vanishing failure driving stress, see the Mohr model for in-plane shear below. This is not given for the Mohr-SFC

$$\tau_{21} = \bar{R}_{\perp\|} - \mu_{\perp\|}\cdot\sigma_2 \;\rightarrow\; \frac{\tau_{21}}{Eff} = \bar{R}_{\perp\|} - \mu_{\perp\|}\cdot\frac{\sigma_2}{Eff} \;\Rightarrow\; Eff = \left(\tau_{21} + \mu_{\perp\|}\cdot\sigma_2\right)/\bar{R}_{\perp\|}.$$

But for just dividing the basic failure driving shear stress, this becomes fulfilled by

$$Eff = \tau_{21}/(\bar{R}_{\perp\|} - \mu_{\perp\|}\cdot\sigma_2).$$

In the context above, see *Annex 4*.

Annex 4: Influence of Compression Stress States on Compressive Strength Capacity (IFF2)

On the surface of the fracture failure body the material stressing effort *Eff* is 100%. Located on the (failure) surface of a fracture body are the uniaxial failure stress points, termed technical strengths, equi-biaxial 'strengths' and all other 2D and 3D failure stress state points. Investigated shall be now the influence of Compression Stress States on IFF2 Strength Capacity (CFRP). Thereby, a 'Deign driving stress concept' is compared with the standard 'Proportional stressing concept'. And, the difference between a proportionally-stressing derived *Eff* and a driving stress-derived *Eff* is intentionally outlined. The two concepts invite for discussion. ⊥ = s

$$Eff2 := \frac{(\sigma2 + \sigma3)\cdot ass + \sqrt{(\sigma2 - \sigma3)^2}\cdot bss}{Rsc} \quad\rightarrow\quad Eff2 := \frac{bs\cdot\sqrt{0.25(\sigma2 - \sigma3)^2}}{Rsc - as\cdot(\sigma2 + \sigma3)}.$$

Stress States			Eff in %	Eff in %
	σ_2	σ_3	proportional	driving stress
1D	0	$-R_\perp^c$	100	100
2D	$-0.5\,R_\perp^c$	$-R_\perp^c$	24	45
	$-R_\perp^c$	$-R_\perp^c$	-52	0
⊥ = s			$a_{\perp\perp} = 0.26$, $a_{\perp\perp} = a_{\perp\perp} + 1$	as = 0.26, bs = 2.52

Conclusions:

1. In the quasi-isotropic plane of a dense UD-material multiaxial compression lowers *Eff* as with isotropic materials (120°-symmetry, [*Cun23*] or bi-axial compression causes no fracture, *Eff* < 0.
2. 2D compression generates a tensile stress because the fibers withstand axial straining. This stress from the constraint situation is usually easily captured by the fiber, on top of the loading stress with $\sigma_1 = \sigma_\|$
3. Using a 'failure driving stress concept' will lead to higher *Eff*s. Has this concept ever been discussed? Anyway, if the driving stress becomes zero a 'modal' SFC should also become zero
4. Multi-axial failure stresses, higher than the uni-axial strengths, have nothing to do with an increase of strength. In the case of multi-axial compression stress states of dense brittle materials the strength is not increased but the risk of shear fracture becomes smaller indicated by a smaller *Eff* value, see the Table above
5. In the strain hardening and softening domains of a material the material stressing effort *Eff* keeps 100% !